OUKA
The University of Osaka
Institutional Knowledge Archive

Title	A Comprehensive Source Contribution Assessment of PM2.5 in Thailand Using Chemical Transport Model
Author(s)	Chantaraprachoom, Nanthapong
Citation	大阪大学, 2026, 博士論文
Version Type	VoR
URL	https://doi.org/10.18910/105461
rights	
Note	

The University of Osaka Institutional Knowledge Archive : OUKA

https://ir.library.osaka-u.ac.jp/

The University of Osaka

大阪大学
THE UNIVERSITY OF OSAKA

Doctoral Dissertation

A Comprehensive Source Contribution Assessment of $PM_{2.5}$ in Thailand Using Chemical Transport Model

CHANTARAPRACHOOM NANTHAPONG

Division of Sustainable Energy and Environmental Engineering
Graduate School of Engineering
The University of Osaka

January 2026

Supervisor

Prof. Dr. Hikari SHIMADERA
Engineering for Assessing the Sustainable Environment
Division of Sustainable Energy and Environmental Engineering
The University of Osaka

Committee Members

Prof. Dr. Michihiko IKE
Bio-Environmetal Engineering
Division of Sustainable Energy and Environmental Engineering
The University of Osaka

Assoc. Prof. Dr. Takashi MACHIMURA
Green Engineering for Global Environment
Division of Sustainable Energy and Environmental Engineering
The University of Osaka

Acknowledgments

Foremost, I extend my deepest gratitude to my supervisor, **Professor Hikari SHIMADERA**. His guidance throughout my academic journey has been invaluable. I am particularly thankful for his profound understanding and unwavering support during periods when I was not in a fully performative condition. I also acknowledge **Professor Akira KONDO** for accepting me into this laboratory and for ensuring a supportive environment for conducting research during the initial phase of my studies. My appreciation is further extended to **Associate Professor Katsushige URANISHI** for his thorough and valuable review of my manuscript before submission. I also recognize **Assistant Professor Tomohito MATSUO** for his support during my tenure in the laboratory.

I am also indebted to my Master's supervisor, **Professor Tatsuhide HAMASAKI**, for his essential recommendation to this lab and for consistently providing thoughtful counsel on both academic pursuits and personal life matters.

A special acknowledgment goes to **Ms. Hisae MARUOKA**, Administrative Assistant at the Shimadera lab. I cannot adequately express my gratitude for having such a caring and supportive person, who could also communicate in my native language. Indeed, my time in the lab would have been much more difficult without her assistance. Moreover, I am grateful to my lab mates for creating a warm and supportive atmosphere. I am particularly indebted to **Daichi MOCHIZUKI** for his instruction in the fundamentals of air quality modeling and for setting me on the optimal research trajectory.

Financial support was generously provided by the **SGH Foundation**. I gratefully acknowledge this scholarship and the opportunity it afforded to network with many remarkable individuals who subsequently became cherished companions.

Beyond the laboratory, I extend my appreciation to all the clubs and circles I attended during my time at the University of Osaka, including but not limited to **Keion ROCK, A-tune, and Chomromthai DD**, for enriching my final phase of academic life. Furthermore, I thank the **Thai Students' Association in Japan under the Royal Patronage** for providing a valuable platform to practice leadership skills and cultivate invaluable friendships along the way.

My deepest and most profound gratitude is reserved for **my parents**. Their unconditional love provided a constant source of stability and strength. I remain eternally grateful for their sacrifices and dedication. Thank you to all **my friends**, both back home and those I met in Japan. We shared drinks, smiles, laughter, tears, and pains. Their unwavering presence and support meant I did not have to seek external mental health support.

Last of all, I acknowledge **myself** for believing in my own strength and holding on during the darkest period of my life. This doctoral study is proof that I can push through anything and succeed.

Achievements

Journal Publications

- **Chantaraprachoom, N.**, Mochizuki, D., Shimadera, H., Luong, M., Matsuo, T., & Kondo, A. (2023). Impact assessment of biomass burning in Southeast Asia to 2019 annual average $PM_{2.5}$ concentration in Thailand using atmospheric chemical transport model. *E3S Web of Conferences*, *379*.

- **Chantaraprachoom, N.**, Shimadera, H., Uranishi, K., Mui, L. V., Matsuo, T., & Kondo, A. (2024). A Nation-by-Nation Assessment of the Contribution of Southeast Asian Open Biomass Burning to $PM_{2.5}$ in Thailand Using the Community Multiscale Air Quality-Integrated Source Apportionment Method Model. *Atmosphere*, *15*(11), 1358.

- **Chantaraprachoom, N.**, Uranishi, K., Matsuo, T., & Shimadera, H. (2025). Comprehensive Source Apportionment and Sensitivity Analyses of $PM_{2.5}$ and Its Species Over Thailand Using the WRF-CMAQ Model. *Environmental Advances* (under review).

- Le, H. Q., Pham, T. T. P., Le, T. M., Bui, M. Q., Nguyen, T. Q., **Chantaraprachoom, N.**, Uranishi, K., Matsuo, T., Kondo, A., & Shimadera, H. (2025). Chemical Composition and Source apportionment of $PM_{2.5}$ in Hanoi, Vietnam: A Comparison of PMF and CMAQ-ISAM Approaches. *Environmental Advances* (under review).

Academic Conferences

- **Chantaraprachoom, N.**, Mochizuki, D., Shimadera, H., Luong, M., Matsuo, T., & Kondo, A. (2023). "Impact Assessment of Biomass Burning in Southeast Asia to 2019 Annual Average $PM_{2.5}$ Concentration in Thailand Using Atmospheric Chemical Transport Model." Presented at the *13th International Conference on Future Environment and Energy*, Tokyo, Japan, January 2023.

- **Chantaraprachoom, N.**, Mochizuki, D., Shimadera, H., Luong, M., Matsuo, T., & Kondo, A. (2023). "The Impact of Biomass Burning in Southeast Asia on Thailand $PM_{2.5}$ Concentration: A Nation-by-nation Assessment Using WRF-CMAQ Air Quality Model." Presented at the *2023 International Conference on CMAS-Asia-Pacific*, Saitama, Japan, July 2023.

Abstract

Fine particulate matter ($PM_{2.5}$) pollution constitutes a persistent environmental and public health challenge across Thailand. Understanding source contributions is essential for effective policy development. This dissertation utilized the WRF-CMAQ chemical transport model to perform a comprehensive assessment of $PM_{2.5}$ sources across Thailand's key receptor areas. Two distinct approaches were employed: the Brute Force Method (BFM), which quantifies $PM_{2.5}$ sensitivity to emission perturbations via multiple comparative simulations, and the Integrated Source Apportionment Method (ISAM), which estimates direct contribution of emissions using tagged tracers within a single simulation. The research established three core objectives: (1) to quantify the overall contribution of open biomass burning (OBB) in Southeast Asia to $PM_{2.5}$ level; (2) to conduct a detailed nation-by-nation source apportionment of OBB using ISAM; and (3) to perform a sector-by-sector source apportionment and sensitivity analysis of seven domestic anthropogenic sectors. The research background and methodology are detailed in Chapters 1 and 2, respectively.

Chapter 3 presented an assessment of contribution from OBB to $PM_{2.5}$ levels in 2019, using the BFM. In the Northern province of Chiang Mai, OBB accounted for 49.1% of the annual average $PM_{2.5}$ concentration, peaking at 70.7% during the intense burning season in April. Conversely, the contribution in the Bangkok Metropolitan Region (BMR) was substantially lower, at 13.1%, with a seasonal peak of 35.5% in March.

Building upon these findings, Chapter 4 applied the ISAM to conduct a detailed, nation-by-nation source apportionment of OBB emissions from Thailand and neighboring countries. The results revealed that transboundary transport contributes more to $PM_{2.5}$ than domestic burning in the Upper Northern Region. During the peak burning period (Mar–Apr), OBB contributions reached up to 61.9% in the West Upper Northern sub-region, with Myanmar being the single largest source at 31.5%. While OBB did not contribute significantly to $PM_{2.5}$ in the BMR on an annual basis, during peak months, the contribution from transboundary OBB increased substantially, reaching up to 27.0%.

Finally, Chapter 5 provided a comprehensive assessment of domestic emission sectors across four receptor regions: the Upper Northern Region, the BMR, Khon Kaen, and Saraburi. The dual approach of utilizing both ISAM and BFM is essential for optimizing control strategies, especially for secondary $PM_{2.5}$ where non-linear atmospheric chemistry leads to differences between a source's direct contribution and its future reduction potential. This analysis established that the "Other" sector, encompassing long-range transboundary and natural emissions, was the dominant contributor across all sites, peaking at 62.7% in the Upper Northern Region. Domestic source profiles were highly localized: OBB was the largest domestic source in the Upper Northern Region, while the industrial, residential, and road transport

sectors dominated the urban and industrial areas, with the industrial sector in Saraburi contributing as much as 29.5%. The sensitivity analysis on secondary inorganic aerosols revealed that Thai atmosphere is in an ammonia-rich regime, justifying the need for policies that control acidic precursors (SO_2 and SO_x) over NH_3 emissions.

In conclusion, $PM_{2.5}$ sources in Thailand are highly regional. Effective mitigation strategies require both targeted domestic emission controls and international collaboration to effectively address both local and transboundary pollution.

Contents

Acknowledgments iii

Achievements iv

Abstract v

Contents vii

List of Tables x

List of Figures xii

List of Abbreviations xv

I Introduction 1

1 Introduction 2

1.1 Particulate matter 2.5 ($PM_{2.5}$) . . . 2

1.1.1 Physical and chemical characteristics of $PM_{2.5}$ . . . 2

1.1.2 Impacts of $PM_{2.5}$ on health and the environments . . . 4

1.2 $PM_{2.5}$ pollution in Thailand . . . 6

1.2.1 The Upper Northern Region . . . 7

1.2.2 The Bangkok Metropolitan Region . . . 8

1.2.3 Khon Kaen . . . 9

1.2.4 Saraburi . . . 9

1.3 $PM_{2.5}$ source contribution assessment in Thailand . . . 10

1.4 Research gaps and research objectives . . . 10

1.4.1 Research gaps . . . 10

1.4.2 Research objectives . . . 11

1.5 Scope of study . . . 12

II Methodology 14

2 Methodology 15

2.1 Chemical transport model . . . 15

2.1.1 WRF meteorological model . . . 15

2.1.2 CMAQ chemical transport model . . . 17

2.2 Methods for source contribution assessment . . . 20

2.2.1 Sensitivity analysis . . . 20

2.2.2 Source apportionment 21

III Contribution Assessment of Open Biomass Burning in Southeast Asia to $PM_{2.5}$ in Thailand 23

3 Contribution Assessment of Open Biomass Burning in Southeast Asia to $PM_{2.5}$ in Thailand 24
3.1 Introduction 24
3.2 Methodology 25
3.2.1 Study area 25
3.2.2 Simulation setup 26
3.2.3 Emission inventories 27
3.2.4 Observation data and model evaluation 29
3.3 Results and discussions 30
3.3.1 Model performance 30
3.3.2 Contribution from open biomass burning 31
3.4 Conclusion 33

IV A Nation-by-Nation Contribution Assessment of Southeast Asian Open Biomass Burning to $PM_{2.5}$ in Thailand 34

4 A Nation-by-Nation Assessment of the Contribution of Southeast Asian Open Biomass Burning to $PM_{2.5}$ in Thailand 35
4.1 Introduction 35
4.2 Methodology 36
4.2.1 Study area 36
4.2.2 Model configuration 37
4.2.3 Source apportionment 39
4.2.4 Observation data and model evaluation 39
4.3 Results and discussions 40
4.3.1 Model performance 40
4.3.2 Nation-by-nation contribution assessment 42
4.4 Conclusion 46

V Source Apportionment and Sensitivity Analyses of $PM_{2.5}$ and Its Species Over Thailand 48

5 Source Apportionment and Sensitivity Analyses of $PM_{2.5}$ and Its Species Over Thailand 49
5.1 Introduction 49

5.2 Methodology . . . 49
5.2.1 Study area . . . 49
5.2.2 Model configuration . . . 51
5.2.3 Simulation setup . . . 52
5.2.4 Observation data and model evaluation . . . 53
5.3 Results and discussions . . . 54
5.3.1 Model performance . . . 54
5.3.2 Source apportionment and sensitivities of Total $PM_{2.5}$ . . . 57
5.3.3 Source apportionment and sensitivities of $PM_{2.5}$ species . . . 63
5.3.4 Implications for air pollution mitigation policies . . . 68
5.4 Conclusion . . . 69

VI Conclusions and Recommendations 70

6 Conclusions and Recommendations 71
6.1 Conclusions . . . 71
6.2 Limitations and recommendations . . . 72

Appendices 75

A Sector-by-Sector Source Apportionment and Sensitivity Analyses Results 75

Bibliography 83

List of Tables

Table 1 Model configuration settings used for the **WRF** and **CMAQ** models. 28
Table 2 Summary of Emission Inventories Used in the CMAQ Model. 29

Table 3 Statistical metrics for the evaluation of the CMAQ model's performance. Monthly mean values were used for calculation. 42

Table 4 List of selected $PM_{2.5}$ receptor areas in this study, categorized by region. 50
Table 5 Emission sectors for source apportionment and sensitivities in this study 52
Table 6 Comparison of model performance metrics (R, NMB, NME) for simulated quarterly mean $PM_{2.5}$ concentrations against the benchmark criteria from Emery et al. (2017) [208]. 55

Table A.1 Comparison of source contributions to Total $PM_{2.5}$ in each target receptor area. The values are shown as concentration in $\mu g/m^3$ with the percentage contribution in parentheses. For each cell, the top value represents the ISAM result (**bold**) and the bottom value represents the BFM result (*italic*). 76
Table A.2 Comparison of source contributions to $PM_{2.5}$ EC in each target receptor area. The values are shown as concentration in $\mu g/m^3$ with the percentage contribution in parentheses. For each cell, the top value represents the ISAM result (**bold**) and the bottom value represents the BFM result (*italic*). 77
Table A.3 Comparison of source contributions to $PM_{2.5}$ POC in each target receptor area. The values are shown as concentration in $\mu g/m^3$ with the percentage contribution in parentheses. For each cell, the top value represents the ISAM result (**bold**) and the bottom value represents the BFM result (*italic*). 78
Table A.4 Comparison of source contributions to $PM_{2.5}$ NH_4^+ in each target receptor area. The values are shown as concentration in $\mu g/m^3$ with the percentage contribution in parentheses. For each cell, the top value represents the ISAM result (**bold**) and the bottom value represents the BFM result (*italic*). 79
Table A.5 Comparison of source contributions to $PM_{2.5}$ NO_3^- in each target receptor area. The values are shown as concentration in $\mu g/m^3$ with the percentage contribution in parentheses. For each cell, the top value represents the ISAM result (**bold**) and the bottom value represents the BFM result (*italic*). 80

Table A.6 Comparison of source contributions to $PM_{2.5}$ SO_4^{2-} in each target receptor area. The values are shown as concentration in $\mu g/m^3$ with the percentage contribution in parentheses. For each cell, the top value represents the ISAM result (**bold**) and the bottom value represents the BFM result (*italic*). 81
Table A.7 Source contributions from BFM to SOA in each target receptor area. The values are shown as concentration in $\mu g/m^3$ with the percentage contribution in parentheses. 82

List of Figures

Figure 1 Size comparisons for $PM_{2.5}$ and PM_{10} (Source: US EPA [19]). 3
Figure 2 Number of days in 2023 with air quality exceeding national standards in each province of Thailand (Source: PCD [60]). 7
Figure 3 Regions of Thailand. (Source: Martin et al. [71] 8

Figure 4 WRF modeling framework (Source: Skamarock et al. [126]). 17
Figure 5 WPS schematic diagram (Source: Skamarock et al. [126]). 17
Figure 6 Overview of science process in CMAQ model (Source: United States Environmental Protection Agency (US EPA) [130]). 19
Figure 7 CMAQ modeling framework (Source: United States Environmental Protection Agency (US EPA) [130]). 20
Figure 8 ISAM flow chart (Source: Kwok et al. [125]). 22

Figure 9 Modeling domain. The locations of monitoring stations (used for model evaluation) and receptor sites (used for contribution analysis) are marked by colored circles. 26
Figure 10 Average $PM_{2.5}$ emission intensities in the modeling domain: **(a)** Total $PM_{2.5}$ emissions from all sources and **(b)** $PM_{2.5}$ emissions solely from open biomass burning. 30
Figure 11 Comparison of the simulated (CMAQ) and observed $PM_{2.5}$ concentrations at selected ground-based monitoring stations 31
Figure 12 Comparison of observed (black line) and simulated (red line) monthly mean $PM_{2.5}$ concentrations at the target receptor sites. Red bars indicate the contribution from open biomass burning: (**a**) Bangkok and (**b**) Chiang Mai. 31
Figure 13 Spatial distribution of simulated $PM_{2.5}$ concentrations: **(a)** annual mean from base case and **(b)** annual mean from open biomass burning (base-OBB0). 32

Figure 14 Study area: (**a**) Modeling domain. The locations of EANET monitoring stations used in the model evaluation are marked with red circles. (**b**) Target source countries. (**c**) Upper Northern Region of Thailand. The locations of PCD monitoring stations used in the model evaluation are shown in purple circles. (**d**) Bangkok Metropolitan Region, with the locations of PCD monitoring stations marked with green circles. 36
Figure 15 Average $PM_{2.5}$ emission intensities in the modeling domain: (**a**) emissions from open biomass burning and (**b**) emissions from other sources. 38

Figure 16 Time series of the observed (black line) and simulated (red line) monthly mean $PM_{2.5}$ concentrations in each target receptor area, with whiskers representing the range between minimum and maximum values: (**a**) BMR, (**b**) WUN, (**c**) CUN, and (**d**) EUN. 41
Figure 17 Comparison of the simulated and observed $PM_{2.5}$ concentrations: (**a**) EANET stations and (**b**) PCD stations. 41
Figure 18 Spatial distribution of simulated $PM_{2.5}$ concentrations: (**a**) annual mean and (**b**) mean during the intensive burning period (March–April). 43
Figure 19 Average annual contribution of $PM_{2.5}$ concentrations due to OBB in each target source country: (**a**) Thailand, (**b**) Laos, (**c**) Myanmar, (**d**) Cambodia, (**e**) Vietnam, and (**f**) other countries. 44
Figure 20 Spatial distribution of $PM_{2.5}$ from OBB in each target source country during March–April: (**a**) Thailand, (**b**) Laos, (**c**) Myanmar, (**d**) Cambodia, (**e**) Vietnam, and (**f**) other countries. 44
Figure 21 Annual nation-by-nation contributions from OBB to the $PM_{2.5}$ concentrations in each target receptor area: (**a**) BMR, (**b**) WUN, (**c**) CUN, and (**d**) EUN. 45
Figure 22 Nation-by-nation contributions from OBB to $PM_{2.5}$ concentrations from March to April in each target receptor area: (**a**) BMR, (**b**) WUN, (**c**) CUN, and (**d**) EUN. 45

Figure 23 Study area. The locations of monitoring stations used in the model evaluation are marked with circles. (**a**) Upper Northern Region (**b**) BMR 50
Figure 24 Modeling domains 51
Figure 25 Density scatter plots of simulated versus observed hourly $PM_{2.5}$ concentrations for each quarter of 2019: Q1 (Jan-Mar), Q2 (Apr-Jun), Q3 (Jul-Sep), Q4 (Oct-Dec). 55
Figure 26 Comparison of observed (black line) and simulated (red line) monthly mean $PM_{2.5}$ concentrations at the target receptor sites. Whiskers indicate the monthly minimum-maximum range: (**a**) Bangkok, (**b**) Samut Prakan, (**c**) Samut Sakhon, (**d**) Pathum Thani, (**e**) Chiang Rai, (**f**) Chiang Mai, (**g**) Lampang, (**h**) Phrae, (**i**) Mae Hong Son, (**j**) Nan, (**k**) Tak, (**l**) Khon Kaen, (**m**) Saraburi - Na Phra Lan, and (**n**) Saraburi - Mueang. 56
Figure 27 Spatial distribution of annual mean $PM_{2.5}$ contributions from domestic emission sectors in Thailand as estimated by ISAM: (**a**) Open Biomass Burning, (**b**) Residential, (**c**) Industrial, (**d**) Power Generation, (**e**) Road Transport, (**f**) Other Transport, and (**g**) Other Anthropogenic Sources. 57
Figure 28 Spatial distribution of annual mean $PM_{2.5}$ contributions from other sources (including transboundary transport and natural emissions) in Thailand as estimated by ISAM. 58

Figure 29 Source apportionment derived by ISAM and sensitivities derived by BFM of the simulated $PM_{2.5}$ and its species concentrations to all emission sectors in each target receptor area. Thick black lines denotes the simulated concentrations 59
Figure 30 Source sensitivities to secondary organic aerosol (SOA) concentrations, derived by BFM in each target receptor region. Thick black lines indicate the simulated baseline concentrations. 60

List of Abbreviations

ASOA Anthropogenic Secondary Organic Aerosols

BFM Brute Force Method

BMR Bangkok Metropolitan Region

BSOA Biogenic Secondary Organic Aerosols

BVOC Biogenic Volatile Organic Compound

CMAQ Community Multiscale Air Quality

CMB Chemical Mass Balance

CTM Chemical Transport Model

CUN Central Upper Northern

EANET Acid Deposition Monitoring Network in East Asia

EC Elemental Carbon

ERA5 ECMWF Reanalysis version 5

EUN East Upper Northern

FINN Fire Inventory from NCAR

GEOS Goddard Earth Observing System

GFAS Global Fire Assimilation System

GFED Global Fire Emissions Database

GMTED Global Multi-Resolution Terrain Elevation Data

HTAP Task Force for Hemispheric Transport of Air Pollution

ISAM Integrated Source Apportionment Method

MCIP Meteorology–Chemistry Interface Processor

MEGAN Model of Emissions of Gases and Aerosols from Nature

MODIS Moderate Resolution Imaging Spectroradiometer

NCAR National Center for Atmospheric Research

NCEP National Centers for Environmental Prediction

NOAA National Oceanic and Atmospheric Administration

NMB Normalized Mean Bias

NME Normalized Mean Error

NMVOC Non-Methane Volatile Organic Compound

OBB Open Biomass Burning

PBL Planetary Boundary Layer

PCA Principal Component Analysis

PCD Pollution Control Department

POC Primary Organic Carbon

PM Particulate matter

$PM_{2.5}$ Particulate matter with a diameter smaller than 2.5 μm

PM_{10} Particulate matter with a diameter smaller than 10 μm

PMF Positive Matrix Factorization

PPM Piecewise Parabolic Method

PSCF Potential Source Contribution Function

RADM Regional Acid Deposition Model

REAS Regional Emission Inventory in Asia

RRTMG Rapid Radiative Transfer Model for General Circulation Models

SAPRC State Air Pollution Research Center

SIA Secondary Inorganic Aerosols

SOA Secondary Organic Aerosols

SOC Secondary Organic Carbon

USEPA United States Environmental Protection Agency

VOC Volatile Organic Compound

WACCM Whole Atmosphere Community Climate Model

WHO World Health Organization

WRF Weather Research and Forecasting

WUN West Upper Northern

Chapter 1

Introduction

Introduction 1

1.1 Particulate matter 2.5 ($PM_{2.5}$)

Air pollution is defined as the atmospheric contamination by chemical, physical, or biological agents at concentrations exceeding natural background levels, which results in the degradation of ambient air quality [1, 2, 3]. This issue is recognized globally as one of the most significant environmental challenges facing humanity today. While the industrial revolution brought about substantial progress in technology and society, it also initiated an era defined by the extensive release of harmful air pollutants [4, 5]. In the modern era, rapid urbanization and industrialization have intensified this issue worldwide [3, 6, 7]. Consequently, air pollution has become a primary public health hazard, posing significant threats to human health [1, 8, 9] and contributing to an estimated nine million premature deaths annually. In addition, it also affect ecosystems [10, 11], and the climate [1, 12].

Among various pollutants, fine particulate matter with an aerodynamic diameter less than 2.5 μm ($PM_{2.5}$) is recognized as a major concern [13, 14]. According to estimates based on the 2018 and 2020 data [15], 7.3 billion people, or 94% of the global population, are exposed to $PM_{2.5}$ levels exceeding the World Health Organization (WHO)'s guideline of 5 $\mu g/m^3$ [16]. Given the severity and pervasive nature of this public health challenge, $PM_{2.5}$ pollution serves as the central focus of this dissertation. The following subsections detail the foundational understanding of $PM_{2.5}$, including its definition, key characteristics, and impacts to human health and the environments.

1.1.1 Physical and chemical characteristics of $PM_{2.5}$

Particulate matter (PM) refers to a complex mixture of tiny solid particles and liquid droplets suspended in the air. These particles can be emitted directly from a source or formed through chemical reactions in the atmosphere [17, 18]. While some, such as dust or smoke, are large enough to be visible, others are microscopic [19]. For health and regulatory purposes, PM is categorized by its aerodynamic diameter. PM_{10} (coarse particles) refers to inhalable particles with a diameter of 10 micrometers or less. $PM_{2.5}$ (fine particles) refers to particles with a diameter of 2.5 micrometers or less. These particles are microscopic and invisible to the naked eye. Figure 1 illustrates their small scale in comparison to a human hair and a grain of sand. Due to their significantly smaller size, $PM_{2.5}$ particles pose a greater health risk than PM_{10} as they can bypass the body's defenses, lodge deep within the lungs, and even penetrate the bloodstream, leading to serious health complications [20, 21, 22].

Based on their formation mechanism, $PM_{2.5}$ particles are classified as either

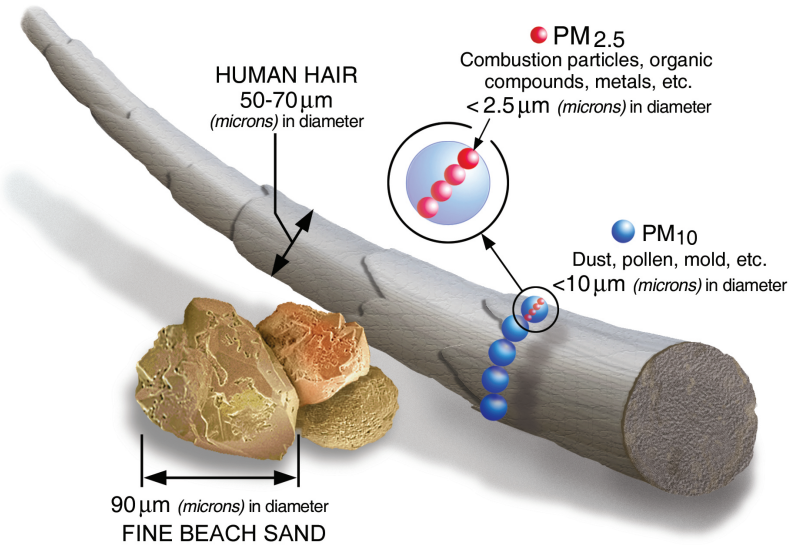

Figure 1: Size comparisons for $PM_{2.5}$ and PM_{10} (Source: US EPA [19]).

primary or secondary [18, 23]. Primary $PM_{2.5}$ is emitted directly into the atmosphere from a source. Examples include soot from diesel engines, ash from biomass burning, or dust from construction sites. In contrast, secondary $PM_{2.5}$ is not emitted directly. Instead, it forms in the atmosphere through complex gas-to-particle conversion processes. These processes involve the chemical reactions of precursor gases such as sulfur dioxide (SO_2), nitrogen oxides (NO_x), ammonia (NH_3), and volatile organic compounds (VOCs).

Chemically, $PM_{2.5}$ is not a single pollutant but a complex, heterogeneous mixture whose composition varies significantly by location and season. Its components can be clearly categorized by their formation pathway. Primary $PM_{2.5}$ components, which are emitted directly, consist mainly of carbonaceous aerosols, crustal material, and sea salts [18]. The primary carbonaceous aerosols are elemental carbon (EC) and primary organic carbon (POC). EC, also known as black carbon or soot, is a primary particle resulting from the incomplete combustion of fossil fuels (e.g., from diesel engines) and biomass (e.g., from forest fires or agricultural burning) [18, 24, 25]. POC is also emitted together with EC from these combustion sources. The relative ratio of EC and POC in primary emissions is highly dependent on the fuel type and combustion conditions [18, 25, 26, 27, 28, 29]. In addition, POC is also released from biogenic sources like pollen and fungi [25, 30, 31]. Crustal materials, the other major primary component, are comprised of mineral dust, soil, and road dust suspended by wind [18].

Secondary $PM_{2.5}$ components are formed in the atmosphere through chemical reactions and consist of Secondary Inorganic Aerosols (SIAs) and Secondary Organic Aerosols (SOAs), depending on their precursor gases [18, 32]. SIAs are a dominant component and are composed primarily of sulfate (SO_4^{2-}), nitrate (NO_3^-), and ammonium (NH_4^+) [32, 33]. These form from the atmospheric oxidation of precursor gases: sulfate from sulfur dioxide (SO_2), mainly from power generation

and industrial facilities; nitrate from nitrogen oxides (NO_x), mainly from vehicle exhaust and power plants; and ammonium from ammonia (NH_3), overwhelmingly from agricultural activities. The formation of SIA is governed by a thermodynamic equilibrium in which gaseous NH_3 neutralizes acidic sulfate and nitrate aerosols [32, 34]. This process follows a preferential pathway. First, sulfuric acid (H_2SO_4), which is formed from the oxidation of SO_2, is a low-volatility acid that is preferentially neutralized by NH_3 to form stable ammonium sulfate (NH_2SO_4). Any NH_3 that remains is then available to react with nitric acid (HNO_3), which is formed from the oxidation of NO_x. This second reaction forms the more volatile and thermally unstable ammonium nitrate (NH_4NO_3). Because the availability of precursors from one sector can fundamentally alter the chemical pathways for precursors from another, the entire system is highly non-linear [34].

Unlike the inorganic ions that compose SIAs, SOAs consist of secondary organic carbon (SOC) formed from the atmospheric oxidation of various VOCs [35, 36, 37, 38]. Depending on their precursors, SOAs are further classified as Anthropogenic SOAs (ASOAs) from human-made sources, or Biogenic SOAs (BSOAs) from natural sources. ASOAs originate from anthropogenic VOCs, such as those from vehicle exhaust and industrial solvents. BSOAs are formed from biogenic VOCs (BVOCs) emitted by vegetation, primarily isoprene and monoterpenes, which are a dominant source on a global scale. The oxidation of all these VOCs contributes to the formation of SOA.

1.1.2 Impacts of $PM_{2.5}$ on health and the environments

The adverse effects of $PM_{2.5}$ on human health are widely documented. Due to their minute size, these fine particles can bypass the respiratory tract's primary natural defense mechanisms, such as nasal hairs and mucus linings, which typically trap larger particles. This allows them to deeply penetrate within the pulmonary alveoli and subsequently translocate directly into the bloodstream [20, 21, 22]. Once in the bloodstream, $PM_{2.5}$ functions as a systemic irritant that induces widespread inflammation and oxidative stress. This fundamental pathway is a contributing factor to the development and worsening of a range of serious health conditions, particularly respiratory and cardiovascular diseases such as asthma, bronchitis, reduced lung function, heart disease, and strokes [39, 40, 41]. This constitutes a staggering global health crisis. In 2019 alone, long-term exposure to ambient $PM_{2.5}$ was estimated to be responsible for 4.14 million deaths worldwide, making it one of the leading environmental risk factors for mortality [42].

Beyond its well-known health effects, $PM_{2.5}$ pollution poses a significant threat to global ecology, with research indicating that all ecosystem types are vulnerable [43]. In terrestrial systems, these impacts are clearly seen in both soil and vegetation. PM negatively affects soil quality. PM deposition directly influence nutrient cycling, especially that of nitrogen, by affecting rhizosphere bacteria and fungi. While additional nitrogen may initially alleviate deficiencies and stimulate growth in certain forest ecosystems, chronic deposition eventually leads to nitrogen saturation, where inputs exceed the biological uptake capacity of plants and microorganisms. This state triggers a cascade of negative effects, including

increased nitrate leaching, the disruption of mycorrhizal fungal communities essential for nutrient acquisition, and imbalances in foliar nutrient ratios. These physiological disruptions are further exacerbated as the deposition of various PM classes dramatically alters soil pH, governing the availability of alkaline cations and mobilizing phytotoxic aluminum. This shift in soil chemistry ultimately impairs metabolic functions and suppresses cambial growth, resulting in significantly reduced plant growth [44]. On a cellular level, PM detrimentally affects plants by disrupting both their physical structure and internal processes. Morphological effects include alterations to leaf area, leaf count, stomatal structure, and overall growth, while biochemical functions like pigment and enzyme levels are also disrupted [45, 46]. These micro-level disruptions scale up to significant agricultural consequences. High particulate pollution, which creates regional haze over major crop-growing regions, can reduce solar irradiance by 28–49%. This loss of sunlight directly depresses the optimal yields of essential crops, leading to estimated reductions in total rice and wheat production [47].

The impacts are equally profound in aquatic environments, where $PM_{2.5}$ pollutants accumulate through wet and dry deposition [48, 49]. A primary ecological effect is the acidification of water bodies [50]. Common $PM_2.5$ components like anthropogenic sulfate and nitrate aerosols, formed from SO_2 and NO_x emissions, cause acid rain and lower the pH of lakes and streams [46, 50]. This acidification, in turn, negatively impacts the species diversity and richness of freshwater communities [43, 50]. Beyond acidification, the pollutants are directly toxic to aquatic wildlife. High $PM_2.5$ concentrations and associated acidity (pH 5.0), for instance, significantly decrease the movement of freshwater snails, while more severe acidification (pH 3.5) can cause high mortality in the same species [46, 50]. Other aquatic invertebrates also suffer physical, physiological, and molecular harm, leading to developmental problems and multi-organ toxicity [51]. This pollution also fundamentally alters core ecosystem processes. Leaf litter breakdown, a critical function for energy flow in streams, slows significantly with increased $PM_2.5$ concentration and associated acidity [46].

Air pollution also inflicts direct harm on a wide range of animals and disrupts critical ecosystem services. Avian species are particularly vulnerable due to their highly efficient respiratory systems, which make them more susceptible than mammals to high concentrations of reactive gases and aerosols [43]. Exposure to SO_2, aerosols, and smoke has been linked to respiratory distress, immunosuppression, and impaired reproductive success in birds, which may in turn reduce population density and species diversity [43]. The health impacts extend to domestic animals as well, with $PM_{2.5}$ reported to be related to an increase in veterinary visits for house cats and dogs [52]. Beyond direct harm to animals, $PM_{2.5}$ threatens essential processes like pollination, which is a vital service for plant reproduction. Particulate matter adheres to the body hairs of pollinators like bees and is ingested through contaminated pollen and honey. This poses a serious risk to pollinator health and compromises the pollination service itself [53].

Furthermore, $PM_{2.5}$ is also a key agent in forcing changes within the global climate system. This influence stems from the complex ways aerosol particles interact directly with solar radiation. Depending on their chemical composition, for

instance, elemental carbon (black carbon), a major component of $PM_{2.5}$, is highly absorptive while sulfates and nitrates are highly reflective. As a result, they can either absorb solar energy, which warms the atmosphere, or scatter it back to space, which induces a surface cooling effect [54, 55]. This alteration of the planet's radiative balance disrupts atmospheric temperature dynamics. Furthermore, these particles have powerful indirect impacts, acting as the points around which cloud droplets form. Changes in aerosol concentrations can thus alter cloud properties, such as their brightness and lifespan, leading to cascading effects on atmospheric circulation and regional precipitation patterns [56, 57, 58]. However, it is important to note that, according to the IPCC Assessment Reports [59], aerosols represent the largest source of uncertainty in global radiative forcing estimates. Unlike well-mixed greenhouse gases, these particles exhibit high spatial and temporal variability. Their complex interactions with clouds result in a wide range of uncertainty regarding their net impact on the global warming potential.

1.2 $PM_{2.5}$ pollution in Thailand

Thailand has long confronted severe air pollution issues. Figure 2 depicts the number of days in 2023 in which the daily mean levels of classic air pollutants exceeded the national standard, according to a report from the Pollution Control Department (PCD) [60]. $PM_{2.5}$ has been identified as the major air pollutant causing this issue. For the past decade, national annual mean $PM_{2.5}$ concentrations have consistently surpassed WHO guidelines by a factor of five, as reported by the PCD [60].

These elevated pollution levels have negatively affected public health and the national economy. Increased $PM_{2.5}$ concentrations are associated with higher rates of hospitalization and mortality in major cities [61, 62, 63, 64, 65]. The pollution has also contributed to a downturn in tourism [66, 67, 68]. The total socio-economic burden from $PM_{2.5}$ in 2012 was estimated at 1.19 billion USD [69]. Furthermore, projections indicate that without additional interventions beyond current policies, this damage could escalate significantly. The nation might face 12.5 billion USD in annual health-related costs and 170,000 premature deaths each year [70].

Thailand is commonly divided into six regions as illustrated in Figure 3. The severity of $PM_{2.5}$ pollution is not consistent throughout the nation, as shown in Figure 2, The Northern and Central regions experience the most severe pollution, while some provinces in the Northeast are also significantly impacted. In contrast, the Southern and Eastern regions are less affected, likely due to their coastal proximity which facilitates better atmospheric dispersion. Furthermore, existing literature indicates that the dominant sources of $PM_{2.5}$ vary considerably by region. To investigate these complex, area-specific dynamics, this study will focus on four key regions.

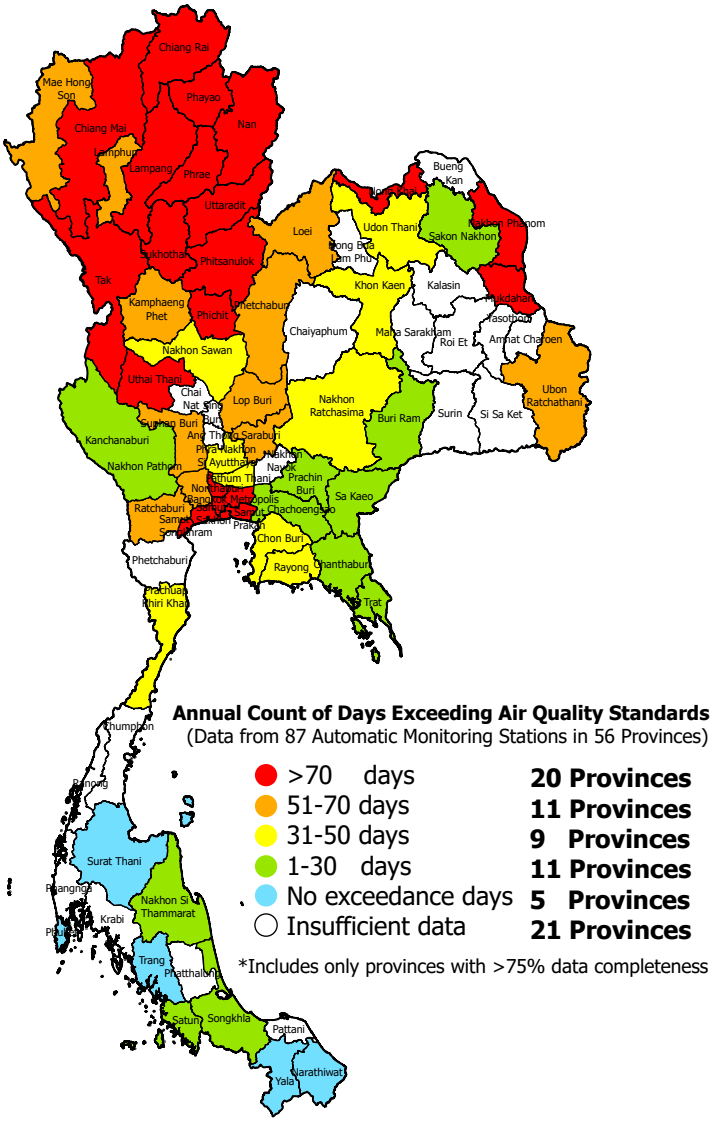

Figure 2: Number of days in 2023 with air quality exceeding national standards in each province of Thailand (Source: PCD [60]).

1.2.1 The Upper Northern Region

The Upper Northern Region of Thailand, encompassing nine provinces (Chiang Rai, Chiang Mai, Nan, Phayao, Phrae, Mae Hong Son, Lampang, Lamphun, and Uttaradit), is a critical area of interest due to its persistent challenge with high $PM_{2.5}$ levels. Geographically, the region is characterized by mountainous terrain and basin topography, which often trap air pollutants, making the area highly susceptible to severe air pollution episodes [72, 73]. According to the PCD report [60], seven of these nine provinces experienced $PM_{2.5}$ concentrations exceeding the national standard (15 $\mu g/m^3$) for more than 70 days annually, while the remaining two provinces registered exceedances for 51-70 days per year.

Previous research consistently identifies open biomass burning (OBB), originating both within Thailand and across its borders, as the principal source influencing



Figure 3: Regions of Thailand. (Source: Martin et al. [71]

$PM_{2.5}$ concentrations in the Upper Northern Region. This contribution is particularly pronounced during the dry season, which typically runs from January to April [74, 75, 76, 77, 78]. Although OBB affects the region's air quality throughout the year, emissions transported from neighboring countries are frequently found to surpass domestic sources [79, 80]. Nonetheless, local factors are also relevant. In major urban centers such as Chiang Mai, on-road vehicle emissions are also recognized as a substantial contributor alongside OBB, especially during non-burning periods [81, 82].

1.2.2 The Bangkok Metropolitan Region

The BMR comprises Thailand's capital, Bangkok, and the five neighboring provinces of Nonthaburi, Samut Prakan, Samut Sakhon, Pathum Thani, and Nakhon Pathom. As Thailand's most densely populated and economically significant area, the air quality in the BMR has a profound impact on public health and economic stability. Poor air quality poses a substantial threat to the large population residing and working in this vital region. A report by the PCD [60] indicated that four of

the six BMR provinces (Bangkok, Nonthaburi, Samut Prakan, and Samut Sakhon) experienced $PM_{2.5}$ concentrations above the national standard for more than 70 days. The remaining two provinces (Nakhon Pathom and Pathum Thani) recorded fewer exceedance days, ranging from 51-70 days and 31-50 days, respectively.

While OBB typically contributes less significantly to $PM_{2.5}$ in the BMR compared to the Northern Region, its contribution substantially increases during the dry season, especially due to transboundary plumes from neighboring countries [83, 84]. Dominant source of $PM_{2.5}$ in the BMR is consistently reported as road transport throughout the year due to the high density of vehicles and frequent traffic congestion [74, 85, 86, 87, 88, 89].

1.2.3 Khon Kaen

The province of Khon Kaen was selected as the representative urban area for Thailand's Northeastern Region within this study. While not the largest city in terms of area or population in the region, Khon Kaen is recognized as one of the four principal urban centers, functioning as a vital administrative, economic, and educational hub in the Northeastern Region [90, 91].

This province has experienced notable air quality degradation, characterized by high ambient $PM_{2.5}$ concentrations in its urban areas. This situation is largely attributable to the effects of rapid urban development [92, 93]. Data published by the PCD indicated that Khon Kaen's $PM_{2.5}$ concentrations exceeded the national standard on more than 70 days throughout 2019 [94]. Although the frequency of exceedance days decreased to a range of 31–50 by 2023 [60], prior investigations have consistently established a link between $PM_{2.5}$ exposure in the province and considerable negative health impacts [92, 95, 96]. As for the source of the pollution, research suggests the primary contributors to this elevated pollution burden are a combination of emissions originating from OBB, road transportation, and residential activities such as cooking and waste burning [97].

1.2.4 Saraburi

Saraburi is one of the key industrial provinces in Thailand, located in the Central Region, roughly 100 km from Bangkok. This province faces persistent and severe air quality challenges. Its industrial significance is partly due to its rich limestone quarries, which have made the Na Phra Lan subdistrict, in particular, home to the country's largest cement production complex. This concentration of heavy industry, which involves quarrying, crushing, and high-temperature kiln operations, is a well-documented and significant source of local $PM_{2.5}$ pollution [60, 98, 99, 100]. As a direct consequence of these intensive industrial activities, the Na Phra Lan area has consistently registered the highest $PM_{2.5}$ levels in the nation for more than a decade, placing a significant public health burden on the local population [60]. Recognizing the severity and persistence of the problem, the province was officially declared a "Pollution Control Zone" in 2004. This legal designation was implemented specifically to mobilize targeted action plans, enforce stricter emissions standards, and allocate dedicated budgets to address the severe air pollution [98, 99].

1.3 $PM_{2.5}$ source contribution assessment in Thailand

The persistent issue of $PM_{2.5}$ pollution in Thailand highlights an urgent need for effective mitigation policies. The success of such policies depends on a clear and detailed understanding of the pollutant sources affecting each area [101, 102, 103, 104]. Source contribution quantification is typically achieved through either receptor modeling or source-oriented modeling. Receptor modeling represents a retrospective methodology, leveraging statistical analysis coupled with mass balance principles on collected ambient chemical data to identify the proportionate contributions from various emission sources [105]. Widely implemented examples of this statistical approach include Chemical Mass Balance (CMB), Principal Component Analysis (PCA), and Positive Matrix Factorization (PMF) [105, 106].

Numerous studies on air quality in Thailand have successfully utilized receptor modeling for source apportionment, including studies whose results are discussed in section 1.2 [74, 76, 82, 85, 88, 89, 99, 107, 108, 109, 110]. However, receptor approaches are inherently constrained by their foundational dependence on site-specific measurement data and fixed temporal periods. Furthermore, the specialized instrumentation required to gather the necessary high-resolution chemical data often restricts their broad application across large spatial and temporal domains [106, 111]. Given these limitations, particularly the limited access to advanced monitoring instruments across Thailand, simulation-based source-oriented models offer a superior alternative. This forward-modeling approach enables the quantitative assessment of source contributions at high spatial and temporal resolutions, making them a highly suitable methodological choice for regional air quality analysis [104, 106, 112].

1.4 Research gaps and research objectives

1.4.1 Research gaps

While several studies have utilized simulation-based source-oriented models to assess the source contribution of $PM_{2.5}$ in Thailand, they possess significant limitations in scope. Much of the existing research has focused either on a broad, national scale [113, 114] or, conversely, on specific and isolated provinces or on a specific time period [77, 79, 80, 86, 87, 115]. Crucially, there is a distinct lack of comprehensive research that simultaneously quantifies the contributions of all major domestic anthropogenic sectors and transboundary sources across these critical receptor regions.

Within this critical research gap, OBB is consistently reported as a major contributor to $PM_{2.5}$ pollution in Thailand, particularly in the Upper Northern Region. Its contribution is reported to substantially increase during the dry season, an intense period of burning activity that also significantly affects the air quality of the BMR. While there is a general consensus on the magnitude of OBB's influence, the precise, spatially and temporally resolved quantification of its

relative importance remains a critical and persistent ambiguity in the literature. Addressing this knowledge gap is essential for developing targeted and effective regional mitigation strategies.

A second critical ambiguity concerns the relative importance of overall domestic sources, including OBB, versus transboundary transport. Specifically, the contributions of individual neighboring countries to $PM_{2.5}$ levels in Thailand have not been thoroughly investigated. Quantifying these nation-specific contributions is vital because it moves beyond the generic classification of transboundary transport to identify the exact geographic origins of pollution. This level of detail provides a scientific basis for policymakers to engage in evidence-based diplomatic negotiations and coordinate regional cooperation through frameworks such as the ASEAN Agreement on Transboundary Haze Pollution [116]. Without understanding which specific neighbor contributes most to seasonal spikes, it remains challenging to implement collaborative mitigation measures that address the root causes of cross-border pollution.

Furthermore, other domestic anthropogenic sources such as the residential, industrial, and road transportation sectors are also deserving equally thorough investigation. While these sources are recognized as significant contributors to $PM_{2.5}$ in previous studies discussed in Section 1.2, detailed analyses of their specific impacts on Thailand's air quality remain sparse. A comprehensive study that quantifies their localized contributions across various receptor regions is essential for enabling policymakers to prioritize mitigation efforts. By determining the exact weight of each source, authorities can better allocate limited resources toward the most dominant pollution drivers and design cost-effective regulations that yield the greatest improvement in air quality.

Finally, current literature lacks a detailed analysis of the source contributions to specific $PM_{2.5}$ constituents in Thailand, including the primary carbonaceous aerosols, SOAs, and SIAs. Understanding the chemical composition of $PM_{2.5}$ from different sources is essential because the formation mechanisms of secondary species are highly complex and differ significantly from primary emissions. By distinguishing between these constituents, policymakers can better understand whether the pollution is driven by direct combustion or by atmospheric chemical reactions of precursor gases. This distinction is critical for making informed decisions on whether to focus regulations on primary particle reduction or the control of gaseous precursors like NO_x, SO_2, and VOCs, ultimately leading to more precise and effective air quality management.

1.4.2 Research objectives

The main objective of this dissertation is to provide a comprehensive assessment of the contributions from various major emission sources to ambient $PM_{2.5}$ levels across Thailand using chemical transport models (CTM). To fulfill this aim, the following three specific objectives were established:

1. To quantify the overall contribution of OBB within Southeast Asia to $PM_{2.5}$ concentrations in the key receptor cities of Bangkok and Chiang Mai, utilizing

the Community Multiscale Air Quality (CMAQ) model in conjunction with the brute force method (BFM).

2. To assess the individual contributions of OBB emissions from Thailand, Laos, Myanmar, Cambodia, and Vietnam to $PM_{2.5}$ concentrations in the BMR and the Upper Northern Region, utilizing the CMAQ model coupled with the Integrated Source Apportionment Method (ISAM).

3. To evaluate the individual contributions of domestic emission sectors to total $PM_{2.5}$ concentrations and their chemical constituents across four critical receptor areas—the Upper Northern Region, the BMR, Khon Kaen, and Saraburi—by employing source sensitivity analysis via BFM and source apportionment via ISAM within the CMAQ modeling framework.

1.5 Scope of study

This dissertation is specifically conceived to provide a comprehensive, model-based quantification of emission source contributions to ambient $PM_{2.5}$ levels across Thailand's key receptor areas. The core methodological framework utilizes a CTM, specifically the WRF-CMAQ model, which must first be rigorously developed and validated to accurately reproduce the complex spatiotemporal distribution of $PM_{2.5}$ over both Thailand and the broader Asian region. Following this validation, the core analysis employs two complementary techniques: the ISAM for mass tracking and the BFM for source sensitivity analysis, which together allow for a precise assessment of source contribution. The scope of the research is executed through three distinct, progressively detailed objectives, each targeting critical pollution challenges in Thailand.

First, an initial assessment is conducted using the BFM to determine the overall contribution of OBB across Southeast Asia, including both domestic and transboundary sources, to annual and seasonal $PM_{2.5}$ concentrations in the primary urban centers of Bangkok and Chiang Mai.

Second, the analysis is refined using the ISAM in a detailed nation-by-nation source apportionment approach to individually quantify the transboundary impact of OBB from neighboring countries (specifically Myanmar, Laos, Cambodia, and Vietnam) as well as domestic OBB on $PM_{2.5}$ levels in the Upper Northern Region and the BMR. This specific objective is aimed to determine whether domestic or transboundary OBB contribute more to the pollution issue.

Lastly, to gain a comprehensive, detailed understanding of Thailand's source-receptor dynamics, a comprehensive source apportionment and sensitivity analysis using both ISAM and BFM is performed on seven domestic anthropogenic emission sectors: OBB, Residential (RES), Industrial (IND), Power Generation (POW), Road Transport (ROAD), Other Transport (OTT), and Other Anthropogenic (OTA) sources. This analysis is applied across four critical receptor regions: the Upper Northern Region, the BMR, Khon Kaen, and Saraburi. Importantly, all remaining unclassified contributions (including long-range transboundary

transport and natural emissions) are grouped and analyzed as the 'Other' (OTH) source category, ensuring all components of the $PM_{2.5}$ budget are accounted for.

The findings generated by this dissertation will serve as a robust, scientific evidence base for policymakers, enabling the design and implementation of highly effective, geographically tailored pollution mitigation policies that minimize the influence of the most dominant sources in each key receptor area.

Chapter II

Methodology

2 Methodology

2.1 Chemical transport model

A chemical transport model (CTM) is a computational tool that simulates the physical and chemical processes affecting air pollutants in the atmosphere [32, 117]. These models serve as powerful instruments for analyzing air quality. They are utilized to predict pollution episodes and to quantify the contributions of various emission sources. The outputs from these models provide critical information that facilitates easier decision-making for policymakers [117, 118, 119].

The CTMs widely employed for $PM_{2.5}$ research include the Weather Research and Forecasting (WRF) model coupled with the Community Multiscale Air Quality (CMAQ) model (hereafter WRF-CMAQ), the WRF model coupled with Chemistry (WRF-Chem), and the Goddard Earth Observing System coupled with Chemistry (GEOS-Chem) [120, 121]. In this dissertation, WRF-CMAQ was selected as the primary modeling framework for several strategic reasons. Inter-comparison studies show that predictive performance for $PM_{2.5}$ is generally comparable [120, 121, 122, 123]. However, their different framework setups provide distinct advantages based on the research objectives. GEOS-Chem is primarily a global model and often lacks the fine spatial resolution required for high-fidelity regional assessments in Southeast Asia [120]. Conversely, WRF-Chem offers 'online' coupling where meteorology and chemistry interact simultaneously but this integration demands significant computational resources. This burden becomes restrictive when conducting multiple sensitivity analyses and long-term simulations. In contrast, the 'offline' one-way coupling of WRF-CMAQ allows for efficient resource allocation and greater flexibility [121, 124]. Most crucially, CMAQ includes the built-in Integrated Source Apportionment Method (ISAM) [125] which is a specialized module for tracking multiple emission sectors and geographic regions. This capability was essential for the source contribution assessment conducted in this dissertation.

2.1.1 WRF meteorological model

WRF model is a modern state-of-the-science mesoscale numerical weather prediction system utilized for both meteorological research and operational forecasting. Its development in the late 1990s was a collaborative effort among several prominent U.S. agencies, including the National Center for Atmospheric Research (NCAR) and the National Oceanic and Atmospheric Administration (NOAA). The model is notable for its versatility, with applications spanning spatial scales from tens of meters to thousands of kilometers. It provides a computationally efficient platform for simulating real-world atmospheric conditions by integrating modern advancements in physics, numerics, and data assimilation. Consequently,

WRF has been widely adopted by national meteorological centers, such as the National Centers for Environmental Prediction (NCEP), as well as by universities and laboratories for real-time forecasting [126].

The WRF modeling framework is built around two distinct dynamical cores: the Advanced Research WRF (ARW) from NCAR [126] and the Nonhydrostatic Mesoscale Model (NMM) from NCEP [127]. These cores are mutually exclusive and cannot be used together, as they are based on different dynamic solvers, grid projections, vertical coordinate structures, and grid-staggering methods [128, 129]. It has been observed in operational comparisons that variations in forecast outcomes are often more attributable to the different physics packages associated with each core than to the foundational differences in the dynamical cores themselves [126]. Generally, the ARW core is favored for research applications, while the NMM core is primarily utilized for operational weather prediction [128, 129].

The underlying technical architecture of the two cores differs substantially [129]. The ARW core is a fully compressible, Eulerian nonhydrostatic model which also retains a hydrostatic option that can be selected at runtime. It employs an Arakawa C-grid staggering for its horizontal grid and utilizes a terrain-following hydrostatic-pressure vertical coordinate that allows for vertical grid stretching. In contrast, the NMM core originated as a fully compressible hydrostatic model for operational forecasting, which was later enhanced to include non-hydrostatic capabilities. This core uses an Arakawa E-grid staggering horizontally and is built on a mass-based, terrain-following hybrid (sigma-pressure) vertical coordinate. Furthermore, the physics packages commonly paired with each core are also different [129]. The ARW core is frequently implemented with the Kain-Fritsch convective scheme, the Asymmetric Convective Model (ACM2) for the planetary boundary layer (PBL), Dudhia and RRTM radiation schemes (shortwave and longwave, respectively), Thompson cloud microphysics, and the Pleim-Xiu (PX) land-surface model. Conversely, the NMM core is typically configured with the Betts-Miller-Janjic convection scheme, the Mellor-Yamada-Janjic PBL scheme, Lacis-Hansen and Fels-Schwartzkopf radiation schemes, Ferrier microphysics, and the NOAH land-surface model. In this study, WRF-ARW was utilized. For simplicity, it will be referred to as WRF from now on.

The WRF software framework, illustrated in Figure 4, initiates the process for a real-world simulation using the WRF Preprocessing System (WPS) [126]. Figure 5 provides a schematic diagram that details the programmatic components and data flow within the WPS, including how it supplies initial data to the ARW. This system comprises three primary components. First, geogrid defines the model domains and creates static files by interpolating terrestrial data, which includes fields such as soil texture category, land/water mask, vegetation greenness fraction, and terrain elevation. Second, ungrib decodes and extracts meteorological data from the standardized GRIB-formatted files provided by an external global model. Finally, metgrid horizontally interpolates these meteorological fields onto the simulation domains. The time-dependent, two-dimensional fields processed by metgrid include surface and sea-level pressure, multi-layer soil temperature and moisture, snow depth, skin temperature, and sea surface temperature. Once this preprocessing is complete, the real.exe program is executed to generate the model's

initial and boundary conditions, often applying four-dimensional data assimilation (FDDA). Finally, the wrf.exe program, the core numerical integration component, utilizes these conditions to compute the atmospheric state over time. This includes simulating key processes such as advection, cloud microphysics, radiative transfer, land-surface interactions, planetary boundary layer (PBL) dynamics, and cumulus parameterization [126].

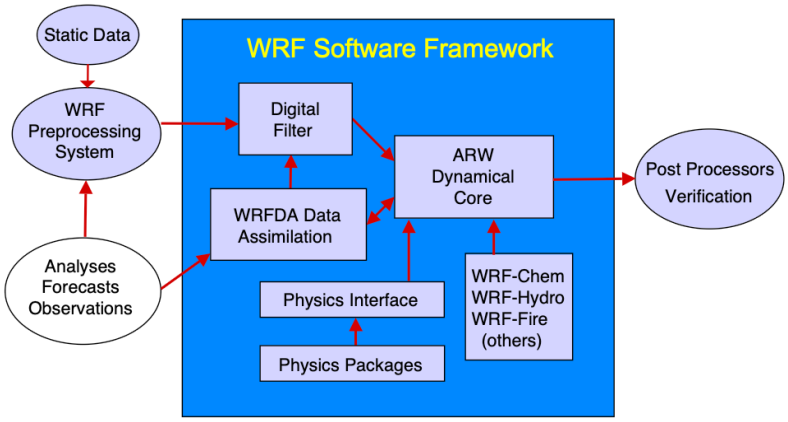

Figure 4: WRF modeling framework (Source: Skamarock et al. [126]).

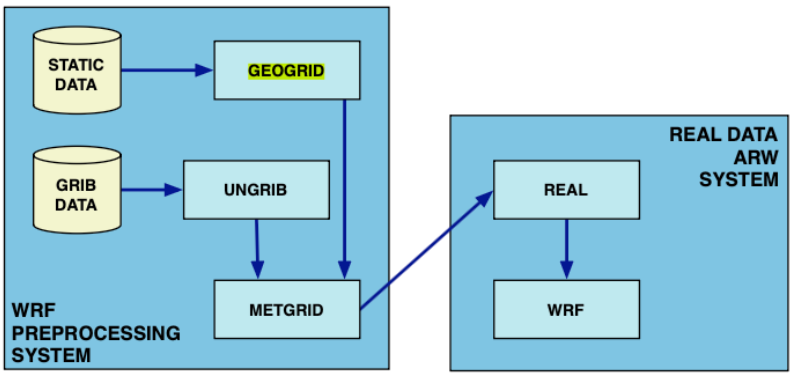

Figure 5: WPS schematic diagram (Source: Skamarock et al. [126]).

For the purposes of this dissertation, the meteorological fields generated by the WRF simulation, specifically wind speed, ambient temperature, relative humidity, PBL height, and precipitation, serve as the necessary inputs for the subsequent air quality calculations performed by the CMAQ model.

2.1.2 CMAQ chemical transport model

The CMAQ model, developed and continuously maintained by the United States Environmental Protection Agency (USEPA) Office of Research and Development, functions as the primary scientific tool for predicting atmospheric concentrations of a diverse range of key pollutants. These include ozone (O_3), particulate matter ($PM_{2.5}$), toxic compounds, and acid deposition [130, 131]. As an Eulerian-class

numerical air quality model, CMAQ is fundamentally rooted in first-principles science that simulates the complete life cycle of airborne gases and particles. It relies on the principle of mass conservation within a fixed three-dimensional grid to track pollutants from their initial emission to their ultimate fate via deposition. Designed for robust and comprehensive air quality assessment, the model produces technically sound estimates by integrating the latest advancements in atmospheric science with high-performance computing within a modular, open-source framework. At its core, CMAQ's primary objective is to solve all governing atmospheric processes simultaneously to produce dynamically consistent predictions. This "one-atmosphere" approach necessitates two principal categories of input data: accurate emission rates from all relevant sources and detailed meteorological information to drive the entire system.

The accurate simulation of atmospheric evolution necessitates the integration of mathematical representations of several crucial atmospheric phenomena, including pollutant transport, complex chemical transformation, and various removal processes. Pollutants emitted from a wide array of sources undergo transport throughout the modeling domain by atmospheric winds, where they are subject to continuous chemical production and loss. The governing atmospheric chemistry is described by a specific chemical mechanism, a comprehensive set of reactions selected by the user, which utilizes an extensive database of atmospheric reactions to predict the fate of hundreds of pollutants as they are carried downwind. As illustrated in Figure 6, the key chemical processes include photolysis, which provides the energy necessary for numerous chemical reactions. Predicting atmospheric evolution requires accurately accounting for the complex, interacting factors of light and chemistry. This involves solving the radiative transfer equation to accurately track the wavelength-dependent intensity of light through the atmosphere, factoring in extinction and scattering by clouds, aerosols, and gases. The results then determine the condition-dependent chemical products formed. Furthermore, Multiphase Chemistry is calculated using a semi-integrated approach that computes the net impacts of reactions occurring entirely in the gas phase (e.g., O_3 formation), entirely in the particle phase, or heterogeneously on particle surfaces or within liquid droplets. This heterogeneous chemistry is particularly critical during high PM episodes because the presence of a particle surface or liquid medium can significantly accelerate reactions. To maintain computational efficiency, the model incorporates various chemical mechanisms that utilize lumping strategies, where numerous related chemical compounds are grouped into "surrogates" to represent their collective mass and reactivity.

The CMAQ aerosol module handles Airborne Particle Microphysics by employing a moment-based algorithm from Binkowski and Roselle [132] to estimate size-dependent concentrations across three distinct particle size distributions: the Aitken, Accumulation, and Coarse modes. This comprehensive framework allows for the modeling of primary particles (e.g., soot, sea salt, soil fragments) emitted directly into the atmosphere. It also incorporates Secondary Particle Formation, a process where compounds formed in-situ through chemical reaction (such as sulfur dioxide (SO_2) oxidizing to form sulfuric acid (H_2SO_4)) condense onto pre-existing particles, as well as microphysical processes like mass transfer,

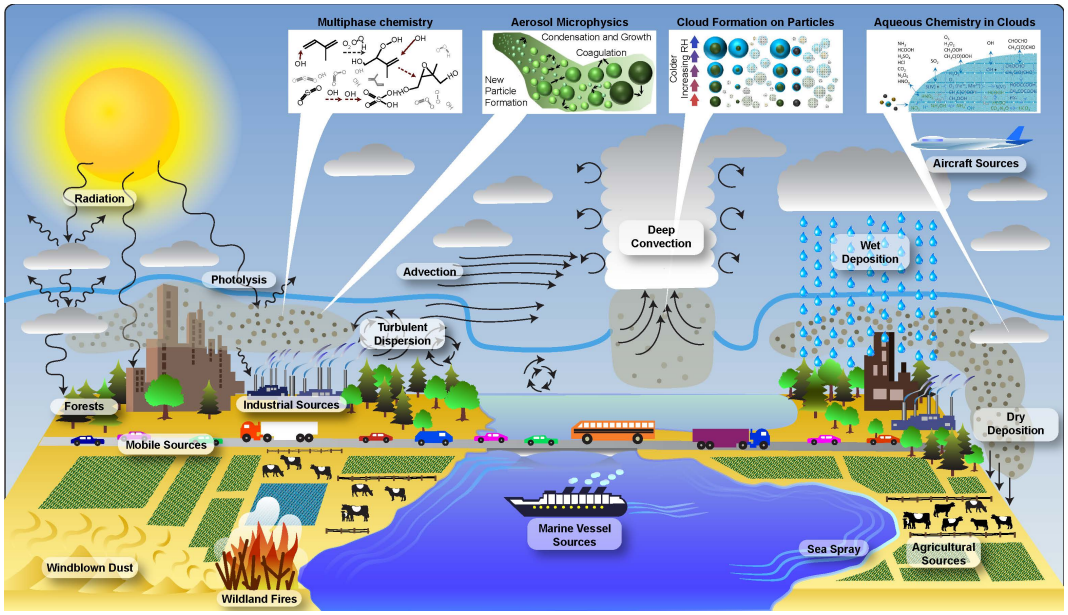

Figure 6: Overview of science process in CMAQ model (Source: United States Environmental Protection Agency (US EPA) [130]).

coagulation, and gravitational settling. Complementing these physical processes are the mechanisms for pollutant removal via air-surface exchange. This flux is defined by the concentration gradient between the atmosphere and the surface media. Dry deposition occurs when gases or particles impact a surface and are removed, driven by gravitational settling and turbulent wind patterns. Wet deposition is the removal of gases or aerosols by precipitation (rainout or washout), a process highly effective at removing $PM_{2.5}$. Clouds and fogs critically influence both processes by physically scavenging pollutants and chemically providing a liquid medium for reactions. Finally, Bidirectional Exchange is parameterized for key semivolatile pollutants, notably ammonia (NH_3). These compounds can either deposit to the surface or be re-emitted if the surface concentration is higher than the atmospheric concentration, which ultimately adds complexity to long-range transport predictions.

Figure 7 details the framework of the CMAQ model. The Chemistry-Transport Model (CCTM) serves as the core simulation engine, integrating inputs from several preprocessors to perform the full atmospheric simulation. Meteorological information, typically generated by the WRF model, must first be converted into the required netCDF-formatted input files via the Meteorology-Chemistry Interface Processor (MCIP). Additionally, the initial conditions processor (ICON) provides the concentrations of chemical species for the first time step across the entire domain, while the boundary conditions processor (BCON) defines the concentrations entering the domain from the lateral boundaries. Finally, the CCTM is fed comprehensive Emission Inputs that are categorized into five broad source types to accurately represent all inputs: Anthropogenic Sources, Biogenic and Natural Sources, Fire Sources, Wind-Blown Dust Sources, and Ocean and Sea Spray Sources.

In this dissertation, the CMAQ modeling system served as the primary numerical

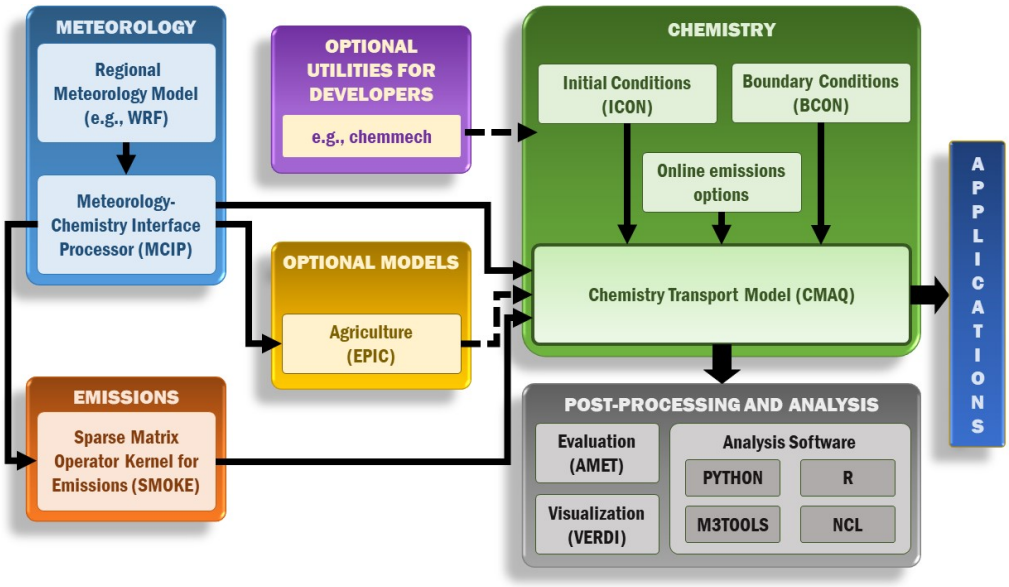

Figure 7: CMAQ modeling framework (Source: United States Environmental Protection Agency (US EPA) [130]).

engine to simulate the spatiotemporal variations of ambient $PM_{2.5}$ concentrations across the domain. The resultant simulated fields were subsequently utilized as the basis for the source contribution assessment. The detailed methodologies used are presented in the subsequent section.

2.2 Methods for source contribution assessment

Using the CMAQ model, the $PM_{2.5}$ source contribution in this dissertation was quantified using two distinct and complementary methodologies: sensitivity analysis, to assess how the atmosphere response to when emission source is perturbed, and source apportionment, to rigorously track the proportional mass contribution from specific sources to the total ambient concentration.

2.2.1 Sensitivity analysis

Sensitivity analysis measures how pollutant concentrations at receptors respond to perturbations at sources. The brute force method (BFM) is a widely adopted and computationally straightforward technique used for source sensitivity analysis in air quality modeling [101, 104, 112, 117]. Its core methodology is based on comparing a standard simulation run, termed the base case, against one or more perturbed simulations. In these perturbed runs, emissions from a specific source or region are systematically modified—either by applying a percentage reduction or by their complete removal (the "zero-out" method). The difference in pollutant concentration observed between the base case and the perturbed case then directly quantifies the environmental system's sensitivity to the emission change. This approach effectively quantifies the atmosphere's response to the emission alteration,

but it also intrinsically reveals the system's non-linear characteristics [112, 133]. As a result, the aggregated sensitivities from all individual source perturbations typically do not sum precisely to the total concentration found in the base case, a behavior commonly observed in the complex formation pathways of secondary aerosols.

Despite its diagnostic strengths, the BFM has significant practical drawbacks. The computational cost increases linearly with the number of perturbations required for comprehensive analysis. Moreover, the method's accuracy can be challenged when the resulting concentration differences between the base case and perturbed runs are small, as these subtle changes in pollutant levels may be strongly influenced by numerical errors inherent to the modeling system rather than reflecting genuine atmospheric sensitivity [101, 117].

2.2.2 Source apportionment

Source apportionment assumes clear mass continuity relationships exist between emissions and ambient concentrations. Its objective is to quantitatively determine the proportional contributions of specific emission sources or geographical areas to the total pollutant mass at a receptor location [101, 106, 117, 134]. Conceptually, the method decomposes the total simulated ambient pollutant mass (e.g., for this study, $PM_{2.5}$) the fractions attributable to different source categories or geographical regions [103].

For this dissertation, source apportionment was performed using the ISAM module integrated within the CMAQ model [125]. ISAM operates based on the tagged species method [103, 112], where emissions from designated source categories or regions are chemically 'tagged' as inert tracers. These tags are rigorously carried through the entire chemical transport simulation, tracking the mass contribution through complex atmospheric processes, including advection, diffusion, chemistry, and deposition. This continuous tracking mechanism allows for the precise quantification of each source's influence on $PM_{2.5}$ concentrations at every modeled grid cell and time step. Crucially, ISAM is configured to track contributions across all major atmospheric components, specifically distinguishing between background concentrations (from boundary and initial conditions) and contributions from predefined combinations of emission sectors and geographical regions. This tracking quantifies the resulting mass for both ambient and deposited primary $PM_{2.5}$ as well as secondarily formed inorganic $PM_{2.5}$ [125].

Figure 8 illustrates the computational flow of ISAM. The ISAM calculations strictly adhere to the standard CMAQ sequence of science processes, with each source tag being meticulously updated during every step [125]. The simulation sequence begins with transport processes, including vertical and horizontal advection (ZADV, HADV) and diffusion (VDIFF, HDIFF). Following transport, the model executes the cloud process (CLDPROC), then the gas-phase chemistry (CHEM) as defined by the adopted chemical mechanism, and finally, the aerosol process (AERO).

For primary particulate matter, the relationship between emissions and concentration is largely linear, meaning that sensitivity analysis and source

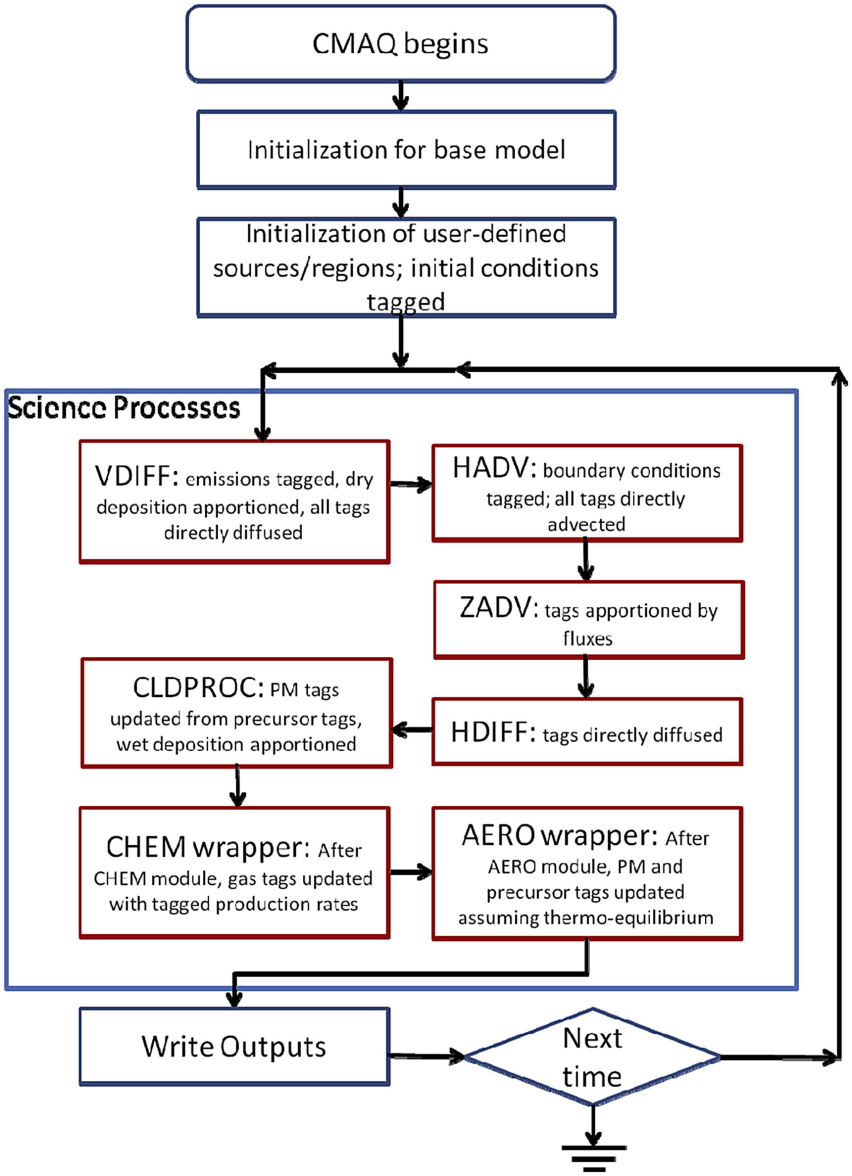

Figure 8: ISAM flow chart (Source: Kwok et al. [125]).

apportionment produce highly consistent results [101, 103, 134]. However, this relationship breaks down for secondary aerosols because their formation involves complex and often non-linear atmospheric reactions. Since mass-based source apportionment inherently tracks contributions proportionally, it is limited in its ability to fully capture the chemical feedbacks and competing pathways that occur when emissions of precursor gases are altered [101, 103, 134]. For this reason, source apportionment is often performed complementarily with sensitivity analysis to provide the most comprehensive understanding of both mass contribution and the chemical system's overall non-linear response to emission changes [104, 133, 135, 136, 137].

Chapter III

Contribution Assessment of Open Biomass Burning in Southeast Asia to $PM_{2.5}$ in Thailand

Contribution Assessment of Open Biomass Burning in Southeast Asia to $PM_{2.5}$ in Thailand

3

This chapter is based on the publication: ***Impact assessment of biomass burning in Southeast Asia to 2019 annual mean $PM_{2.5}$ concentration in Thailand using atmospheric chemical transport model****, published in E3S Web of Conferences, Volume 379, Article Number 01002, in April 2023.*

3.1 Introduction

Across Southeast Asian countries, the widespread use of open biomass burning (OBB) constitutes a common method for the disposal and management of agricultural residues [138, 139, 140, 141]. This method is widely adopted by cultivators, primarily because it offers an economical solution for rapidly clearing fields, controlling pests and crop diseases, and preparing land for subsequent planting cycles, which can also contribute to nutrient return to the soil [141, 142, 143, 144]. Despite these localized agricultural benefits, the combustion process releases substantial quantities of gaseous and particulate pollutants into the atmosphere, leading to significant degradation of ambient air quality and recognized risks to public health [145, 146, 147, 148, 149]. One of the primary pollutant generated from OBB is $PM_{2.5}$ [69, 75, 150]. Due to the small size of $PM_{2.5}$, these particles can remain suspended for extended periods of time and travel vast distances under favorable meteorological conditions. As a result, $PM_{2.5}$ originating from OBB contributes not only to local air quality issues, but also to regional pollution via transboundary transport [80, 140, 148, 149, 151, 152].

Numerous studies have confirmed that OBB serves as a dominant source of $PM_{2.5}$ in Thailand. Research utilizing receptor-modeling has consistently classified OBB as a major contributor to pollution in the capital city of Bangkok [74, 85, 88, 89] and as the primary source of particulate matter in the northern economic hub of Chiang Mai [82, 108, 110]. These studies also conclude that in the Northern Region, OBB is the major driver of $PM_{2.5}$ concentrations, particularly during the intense dry season haze episodes occurring from January to April. This conclusion for the Northern Region is further supported by radiocarbon analysis of $PM_{2.5}$ samples in Chiang Mai, which indicated that OBB was the principal source in both urban and rural settings [153]. Similarly, findings by Chansuebsri et al. [82] estimated that biomass burning can account for up to half of the $PM_{2.5}$ mass during these peak pollution periods in the north.

Despite these findings, the receptor modeling approaches used in such research possess inherent limitations, particularly regarding spatial and temporal resolution [106, 111]. Because these methods rely on physical sampling at specific locations, the results represent only the immediate vicinity and the specific time-frame of the collection period. Furthermore, due to the limited availability of sampling and

chemical analysis instruments, many of these studies are restricted to short-term sampling which does not adequately represent year-round contributions. For instance, in Chiang Mai, existing literature often focuses exclusively on haze and non-haze periods, leaving the true annual contribution of OBB largely unquantified.

Given these limitations, source-oriented models utilizing Chemical Transport Models (CTMs) are more suitable for assessing source contributions at high spatial and temporal resolutions [104, 106, 112]. While several studies have utilized this approach, existing research often lacks year-round assessments that specifically quantify the total contribution of Southeast Asian OBB to $PM_{2.5}$ levels in Thailand. Current literature typically focuses on broad regional trends. For instance, Hassan Bran et al. [77] estimated regional OBB contributions to $PM_{2.5}$ across Thailand using the WRF-Chem framework and found contributions ranging from 34.3% to 47.4%. Other modeling efforts maintain a more restricted scope. In the BMR, research has primarily assessed contributions within localized areas [86, 87], while in the Northern Region, studies focus almost exclusively on intense haze episodes [79, 80, 115]. Consequently, a comprehensive evaluation that quantifies the total annual contribution of OBB from across Southeast Asia to these critical urban and regional hubs remains absent from the literature.

3.2 Methodology

3.2.1 Study area

This study aims to investigate the contribution of OBB in the modeling domain to ambient $PM_{2.5}$ concentration in Thailand. The modeling domain was established to cover a wide geographical expanse of Asia, encompassing India, portions of China, Southeast Asia, and the southwestern Pacific region, as depicted in Figure 9. Two principal receptor areas within Thailand were selected: Bangkok and Chiang Mai. The specific locations of these two receptor sites are marked in Figure 9.

Bangkok, the capital of Thailand, was selected as a primary receptor site due to its status as the nation's most densely populated and economically vital urban center [154, 155]. As a result, the deterioration of air quality in this area carries significant consequences for both the well-being of its population and economic foundations. The concentrated population in the region faces a considerable threat from poor air quality, a critical vulnerability highlighted by a report by Pollution Control Department (PCD) [60] noted that Bangkok recorded $PM_{2.5}$ levels exceeding the national standard on more than 70 days.

Chiang Mai was chosen as the second key receptor area, as it serves as the primary urban center for the Northern Region of Thailand [156]. This region is a critical area of interest because of its persistent struggles with elevated $PM_{2.5}$ concentrations. The area's unique geography, characterized by mountainous terrain and basin-like topography, intensifies this problem by frequently trapping air pollutants. This topography results in a high susceptibility to severe pollution episodes [72, 73]. Similar to Bangkok, the PCD report [60] also indicated that Chiang Mai registered $PM_{2.5}$ concentrations in excess of the national standard for more than 70 days.

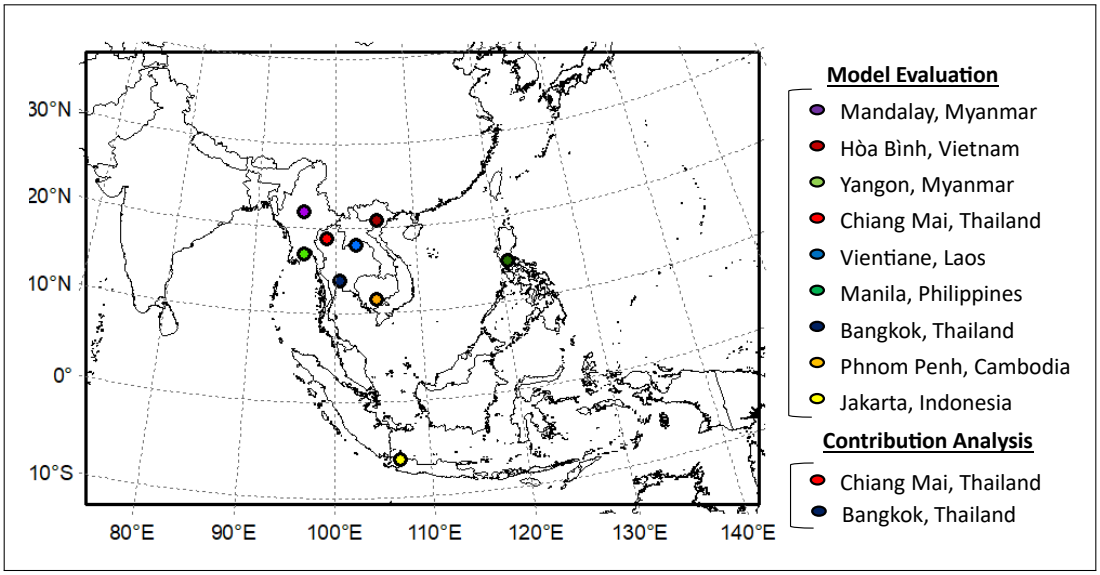

Figure 9: Modeling domain. The locations of monitoring stations (used for model evaluation) and receptor sites (used for contribution analysis) are marked by colored circles.

3.2.2 Simulation setup

The Community Multiscale Air Quality (CMAQ) model version 5.3.3 [157] was utilized to simulate the spatiotemporal variations of $PM_{2.5}$ across the domain in this study. The modeling domain was defined by a constant horizontal grid resolution of 45 × 45 km, comprising a total of 192 × 129 grid cells. The selected simulation period was the calendar year 2019, spanning January through December, with December 2018 served as spin-up period. The year 2019 was chosen to ensure a representative baseline, excluding the emission distortions observed in later years due to worldwide COVID-19 containment and lockdown measures [158, 159]. Furthermore, an intense episode of OBB in Mainland Southeast Asia was reported during the dry season of this year, making the assessment of its contribution particularly relevant to this study [160, 161, 162].

The necessary meteorological input fields were generated by the Weather Research and Forecasting (WRF) model version 4.3 [126], which served as the atmospheric driver for the CMAQ model. The WRF run employed the following physics and dynamics schemes: microphysical processes were handled by the Morrison double-moment scheme [163], radiative transfer for both shortwave and longwave components used the Rapid Radiative Transfer Model for Global Climate Models [164], surface fluxes were calculated using the MYNN surface layer scheme [165], the Noah Land Surface Model [166] described land-atmosphere interactions, vertical mixing within the boundary layer utilized the MYNN3 Planetary Boundary Layer (PBL) scheme [167], and convective processes were parameterized using the Grell 3D ensemble cumulus scheme [168]. Surface input data were based on the global multi-resolution terrain elevation data (GMTED) from 2010 [169] and moderate-resolution imaging spectroradiometer (MODIS) land use data [170]. Initial and boundary conditions for WRF were derived from the ECMWF Reanalysis

version 5 (ERA5) dataset [171]. Grid nudging was applied throughout the simulation period with nudging coefficients of $1.0 \times 10^{-4}\ s^{-1}$ for the wind components and $5.0 \times 10^{-4}\ s^{-1}$ for both temperature and the water vapor mixing ratio. Finally, the resulting hourly WRF outputs were reformatted into the required CMAQ input format using the Meteorology–Chemistry Interface Processor (MCIP) version 5.3.3.

The CMAQ simulation utilized the SAPRC07TC chemical mechanism developed by the State Air Pollution Research Center [172] for gas-phase chemistry, coupled with the AERO6 aerosol module, which incorporated aqueous chemistry processing. Large-scale atmospheric data required for the lateral boundary conditions were sourced from the output of the Whole Atmosphere Community Climate Model (WACCM) [173]. The full details of the model parameters for WRF and CMAQ are listed in Table 1.

To quantify the contribution from OBB, the brute force method was employed using two simulation runs: a base case which included all emissions, and an OBB0 case which included all emissions except OBB. The difference between the two resulting cases then represents the OBB contribution at each receptor site.

3.2.3 Emission inventories

The emission input for the CMAQ model utilized a combination of various emission inventories, as summarized in Table 2, to fully characterize atmospheric pollutant sources. For OBB emissions, the Fire Inventory from NCAR (FINN) version 1.5 [174] was chosen. This selection aligns with prior regional research [175] due to its superior spatial and temporal resolution (1 km, daily) over alternative global datasets. For instance, the Global Fire Emissions Database (GFED) [176] offers only monthly data at a 0.25° resolution, and the Global Fire Assimilation System (GFAS) [177] provides daily data at a coarser 0.1° resolution. Furthermore, FINN v1.5 demonstrated robust performance in accurately simulating $PM_{2.5}$ levels across Southeast Asia, outperforming the newer FINN version 2.5 [178].

Other emission sources included anthropogenic emissions from the Regional Emission Inventory in Asia (REAS) version 3.2 [179]. As the REAS dataset was current only up to 2015, these 2015 values were employed as representative input for the 2019 anthropogenic emissions. Emissions from marine and aviation traffic, which are not available in REAS, were taken from the Task Force for Hemispheric Transport of Air Pollution (HTAP) version 2.2 [180]. Natural biogenic emissions were derived from the Model of Emissions of Gases and Aerosols from Nature (MEGAN) version 2.04 [181]. Finally, volcanic SO_2 emissions were included based on research by Carn et al. [182]. These diverse inventories were subsequently processed using an in-house program to generate two distinct CMAQ-ready gridded inputs: one with all emissions combined for the base case and one with all emissions except OBB from FINN v1.5 for the OBB0 case. Figure 10 graphically illustrates the annual average emission intensity across the entire modeling domain for the base case and for the net OBB emissions, which are calculated as the difference between the base and OBB0 cases. In the simulation year, total $PM_{2.5}$ emissions from all sources amounted to 27.6 million tons across the entire domain, with 9.8 million tons originating from Southeast Asian countries. Of the total domain emissions,

Table 1: Model configuration settings used for the **WRF** and **CMAQ** models.

WRF Configuration	
Meteorology Model	**WRF v4.3**
Horizontal resolution	**45 × 45 km**
Vertical resolution	**30 vertical layers (Top pressure: 50 hPa)**
Projection	**Lambert Conformal Conic**
Microphysics	**Morrison 2-moment scheme**
Advection	**$5^{th}/3^{rd}$-order upwind-biased (horizontal/vertical)**
Longwave Radiation	**Rapid Radiative Transfer Model for General Circulation Models (RRTMG) scheme**
Shortwave Radiation	**RRTMG scheme**
Surface-layer option	**MYNN surface layer**
Land-surface	**Noah Land-Surface Model**
Planetary boundary layer scheme	**MYNN 3rd level TKE scheme**
Cumulus option	**Grell 3D ensemble scheme**
CMAQ Configuration	
Chemical Transport Model	**CMAQ v5.3.3**
Horizontal/vertical advection	**Piecewise Parabolic Method (PPM)/WRF-based scheme**
Horizontal/vertical diffusion	**Multiscale/Asymmetrical Convective Model Version 2 (ACM2)**
Gas-phase chemistry	**State Air Pollution Research Center Version 07tc (SAPRC07tc)**
Aerosol process	**AERO6**
Dry deposition	**M3DRY**
Wet deposition	**Regional Acid Deposition Model (RADM)**
Aqueous chemistry	**CMAQ's standard cloud chemistry treatment (AQCHEM)**

OBB accounted for 8.8 million tons. Within the Southeast Asian region specifically, OBB contributed 7.3 million tons, representing the vast majority of the domain's total biomass burning activity.

Table 2: Summary of Emission Inventories Used in the CMAQ Model.

Emission Inventory	Description
Fire Inventory from NCAR (FINN) version 1.5 [174]	Open biomass burning (OBB) emissions, including agricultural burning and forest fire.
Regional Emission Inventory in Asia (REAS) version 3.2 [179]	Anthropogenic emissions (Industrial, residential combustion, power generation, road transport, solvent use, agriculture, waste and manure management). The 2015 values were used as representative input for 2019.
Task Force for Hemispheric Transport of Air Pollution (HTAP) version 2.2 [180]	Marine and aviation traffic emissions.
Model of Emissions of Gases and Aerosols from Nature (MEGAN) version 2.04 [181]	Natural biogenic emissions.
Carn et al. [182]	Volcanic SO_2 emissions.

3.2.4 Observation data and model evaluation

To validate the CMAQ model's capability to replicate the spatiotemporal distribution of $PM_{2.5}$ concentrations, a comprehensive evaluation was conducted by comparing simulation outputs against ground-level measurements from air quality monitoring stations. For this validation process, observational data were sourced from the Acid Deposition Monitoring Network in East Asia (EANET) [183]. Ground measurement data from nine monitoring stations across seven countries were used. The locations of stations used for model evaluation are shown in Figure 9.

The statistical metrics used for the comparison were the Pearson correlation coefficient (r) and Normalized Mean Bias (NMB). These metrics are mathematically defined in equations 3.1 and 3.2 below:

$$r = \frac{\sum_{i=1}^{n}(O_i - \bar{O})(S_i - \bar{S})}{\sqrt{\sum_{i=1}^{n}(O_i - \bar{O})^2 \sum_{i=1}^{n}(S_i - \bar{S})^2}} \tag{3.1}$$

$$\text{NMB} = \frac{\sum_{i=1}^{n}(S_i - O_i)}{\sum_{i=1}^{n} O_i} \times 100\% \tag{3.2}$$

where the following are denoted:

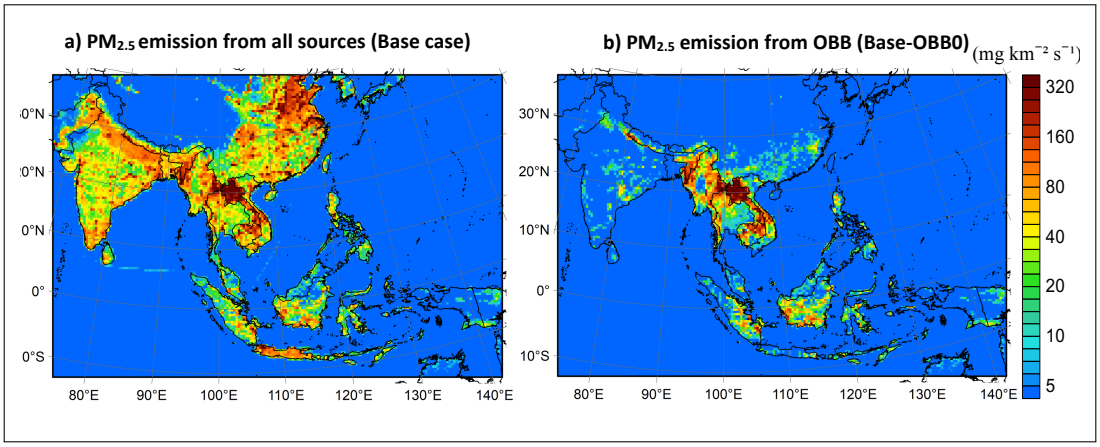

Figure 10: Average $PM_{2.5}$ emission intensities in the modeling domain: **(a)** Total $PM_{2.5}$ emissions from all sources and **(b)** $PM_{2.5}$ emissions solely from open biomass burning.

- O_i is the observed value for observation i;
- S_i is the simulated value for observation i;
- $\bar{O}$ is the mean of observed values;
- $\bar{S}$ is the mean of simulated values;
- n is the total number of observations.
- NMB are expressed as a percentage by multiplying the result by 100%.

3.3 Results and discussions

3.3.1 Model performance

The overall performance of the CMAQ model was statistically evaluated against annual mean $PM_{2.5}$ concentrations observed at EANET ground monitoring stations. As shown in Figure 11, the simulation demonstrated a strong linear relationship with observations, yielding a correlation coefficient (R) of 0.89 and NMB of 15%. This positive NMB suggests a consistent, slight overestimation by the model, which may be attributed to inherent uncertainties in local emission factors or meteorological inputs.

Figure 12 further illustrates the comparison between simulated and observed monthly mean $PM_{2.5}$ concentrations for Bangkok and Chiang Mai. The model effectively captures the distinct seasonal variations in both regions, particularly the intense burning episodes during the dry season, which are most pronounced in Chiang Mai. Collectively, the statistical performance metrics and the alignment of temporal profiles indicate the model's robustness in reproducing the spatial and temporal distribution of $PM_{2.5}$ across the domain, providing a reliable baseline for source contribution assessment.

For Bangkok, the simulated monthly mean $PM_{2.5}$ concentrations ranged from 8.4 to 42.3 $\mu g/m^3$. The calculated annual mean concentration was 26.2 $\mu g/m^3$, substantially exceeding the national air quality standard of 15 $\mu g/m^3$ [60]. The peak $PM_{2.5}$ concentration was simulated in January. In contrast, Chiang Mai exhibited significantly higher $PM_{2.5}$ levels, with monthly mean concentrations ranging widely from 2.3 to 114.7 $\mu g/m^3$. The annual mean for Chiang Mai was determined to be 34.9 $\mu g/m^3$, which surpasses the national standard more than two-fold. The peak concentration period for Chiang Mai was identified as March, aligning with the observed peak period for regional open biomass burning activity.

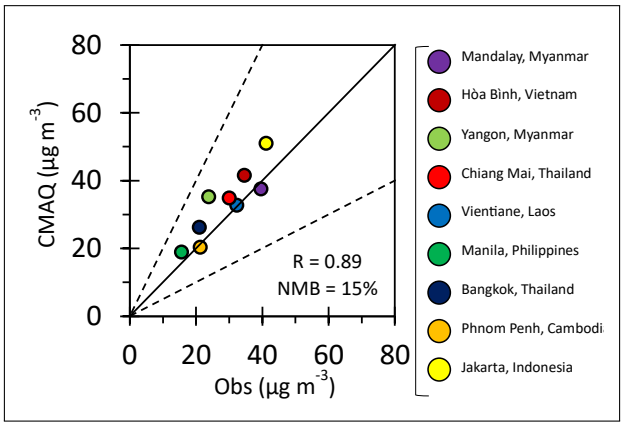

Figure 11: Comparison of the simulated (CMAQ) and observed $PM_{2.5}$ concentrations at selected ground-based monitoring stations

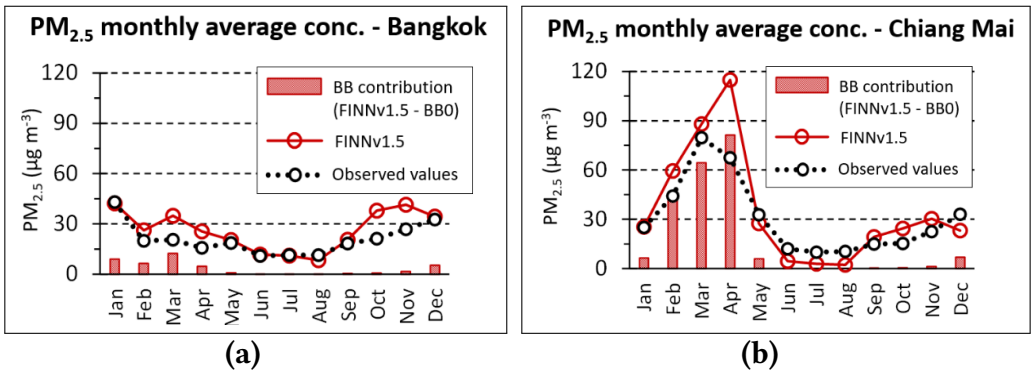

Figure 12: Comparison of observed (black line) and simulated (red line) monthly mean $PM_{2.5}$ concentrations at the target receptor sites. Red bars indicate the contribution from open biomass burning: (**a**) Bangkok and (**b**) Chiang Mai.

3.3.2 Contribution from open biomass burning

The spatial distribution of simulated annual mean $PM_{2.5}$ concentration is illustrated in Figure 13a, with the corresponding spatial contribution specifically from OBB illustrated in Figure 13b. Figure 13b clearly shows that the $PM_{2.5}$ burden from OBB is significantly more severe in the Northern Region of Thailand, as well as in bordering areas of Laos and Myanmar. Conversely, the central region, including the Bangkok

Metropolitan Region (BMR), is only mildly affected. Based on the simulation results from both the Base and OBB0 scenarios, the annual mean contribution percentages were quantified: OBB contributes 49.1% and 13.1% of the annual mean $PM_{2.5}$ concentration in Chiang Mai and Bangkok, respectively.

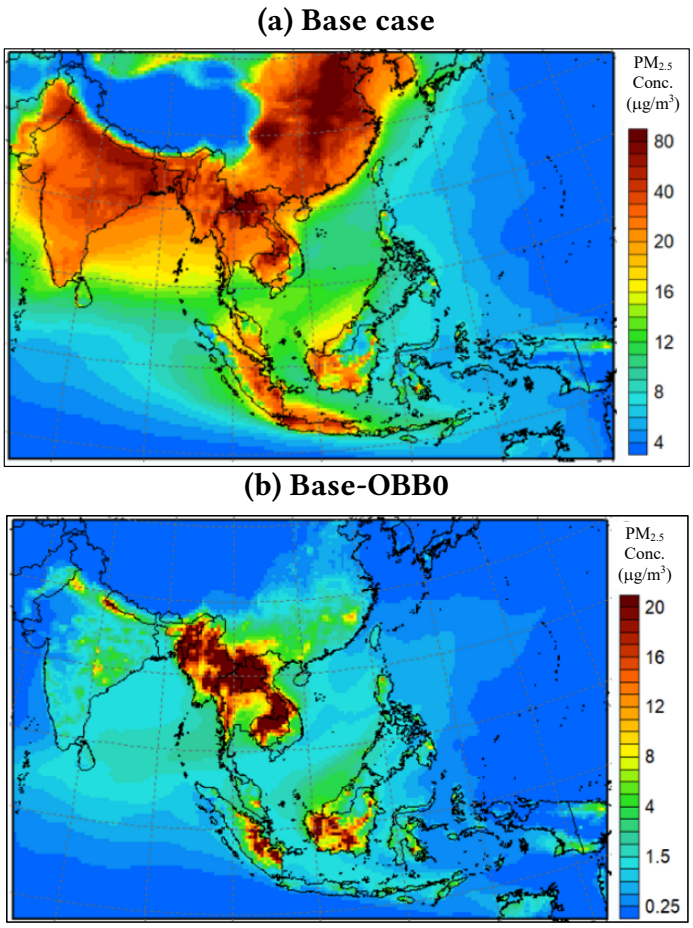

Figure 13: Spatial distribution of simulated $PM_{2.5}$ concentrations: **(a)** annual mean from base case and **(b)** annual mean from open biomass burning (base-OBB0).

The red bars in Figure 12 detail the monthly mean contribution from OBB. In Chiang Mai, the peak $PM_{2.5}$ concentration occurs in April, where OBB accounts for a major contribution of 70.7% to the monthly mean. In contrast, Bangkok's peak OBB contribution is observed earlier in March, contributing 35.5% of the monthly mean concentration. The substantially higher impact of OBB in Chiang Mai compared to Bangkok during these peak months is attributed to the combined effect of intensive local agricultural burning and cross-border burning activities. Due to its geographic proximity to the borders, Chiang Mai is more susceptible to transboundary transport than Bangkok. This conclusion is supported by the PCD report [94], which indicates that biomass burning activity in neighboring countries is highest during the dry season, as corroborated by satellite-observed hotspot increases.

3.4 Conclusion

This chapter successfully quantified the impact of regional open biomass burning (OBB) on annual and seasonal $PM_{2.5}$ concentrations in two distinct receptor areas in Thailand, Bangkok and Chiang Mai, for the year 2019. Utilizing the WRF-CMAQ model and the brute force sensitivity method across Base and OBB0 scenarios, the study established a comprehensive baseline for pollution levels and source contributions.

The model performance evaluation confirmed the CMAQ model's reliability in the region, exhibiting a strong correlation coefficient (R) of 0.89 against EANET observations and accurately capturing the characteristic seasonal pollution peaks. Simulation results indicated that the annual mean $PM_{2.5}$ concentration in Chiang Mai (34.9 $\mu g/m^3$) substantially exceeded the national standard, while Bangkok (26.2 $\mu g/m^3$) was also marginally above the threshold.

Quantifying the source impact revealed a profound regional variation in OBB influence. Annually, OBB was the dominant contributor in Chiang Mai, accounting for 49.1% of the mean $PM_{2.5}$ concentration, compared to only 13.1% in Bangkok. Seasonally, this impact intensified dramatically during the dry season, peaking at 70.7% of the monthly mean in Chiang Mai (April) and 35.5% in Bangkok (March). This severe vulnerability in Chiang Mai results from intensive local agricultural burning combined with substantial transboundary pollutant transport during the peak burning season.

The severe $PM_{2.5}$ levels and high OBB contribution in the Northern Region underscore the critical need for coordinated regional policy. Effective mitigation efforts must focus on collaborative strategies addressing both domestic and transboundary sources, particularly during the dry season. The results from this chapter leads to a more detailed contribution analysis addressed in the subsequent chapter.

Chapter IV

A Nation-by-Nation Contribution Assessment of Southeast Asian Open Biomass Burning to $PM_{2.5}$ in Thailand

4 A Nation-by-Nation Assessment of the Contribution of Southeast Asian Open Biomass Burning to $PM_{2.5}$ in Thailand

This chapter is based on the publication: ***A Nation-by-Nation Assessment of the Contribution of Southeast Asian Open Biomass Burning to $PM_{2.5}$ in Thailand Using the Community Multiscale Air Quality-Integrated Source Apportionment Method Model****, published in Atmosphere, Volume 15, Article Number 1358, in November 2024.*

4.1 Introduction

Continuing from the findings of Chapter 3, open biomass burning (OBB) remains a persistent and dominant source of $PM_{2.5}$ pollution in Thailand, particularly concentrated in the Upper Northern Region during the dry season which spans from January to April [60, 79, 84, 184, 185].

Given the small aerodynamic diameter of $PM_{2.5}$, OBB emissions can remain airborne for extended periods and travel vast distances under favorable meteorological conditions, a process resulting in significant regional air pollution through transboundary transport [80, 140, 148, 149, 151]. The critical question is whether domestic burning or transboundary flow represents the more significant pollutant burden. Previous studies have indicated a strong potential for transboundary sources to dominate. For instance, Amnuaylojaroen et al. [79] and Inlaung et al. [80] both suggested that biomass burning emissions originating from neighboring countries could contribute more substantially to Northern Thailand's $PM_{2.5}$ levels than domestic emissions.

Despite this evidence, the precise quantitative contribution between domestic and transboundary sources remains uncertain. More critically, the specific contributions of OBB from individual neighboring countries to $PM_{2.5}$ concentrations across different regions of Thailand have not been thoroughly investigataed. This knowledge gap is a major constraint on effective air quality governance, as mitigation policies—whether focused on local agricultural enforcement or multilateral regional cooperation—must be tailored based on the true origin of the pollution.

To address this scientific and policy challenge, this study aims to precisely assess the contribution of OBB to $PM_{2.5}$ in Thailand on a nation-by-nation basis using an advanced atmospheric chemical transport model, thereby providing the quantitative data necessary to inform targeted regional control strategies.

4.2 Methodology

4.2.1 Study area

The objective of this chapter is to precisely assess the contributions of OBB from five key source countries—Thailand, Laos, Myanmar, Cambodia, and Vietnam—to $PM_{2.5}$ levels in two major receptor areas within Thailand: the Upper Northern Region and the Bangkok Metropolitan Region (BMR). To accurately simulate the long-range transport and dispersion of $PM_{2.5}$, the modeling domain was established to encompass a wide geographical area, including all of Southeast Asia, India, portions of China, and the southwestern Pacific region, as illustrated in Figure 14a. The locations of the source countries, the Upper Northern Region, and the BMR are illustrated in Figure 14b–d, respectively.

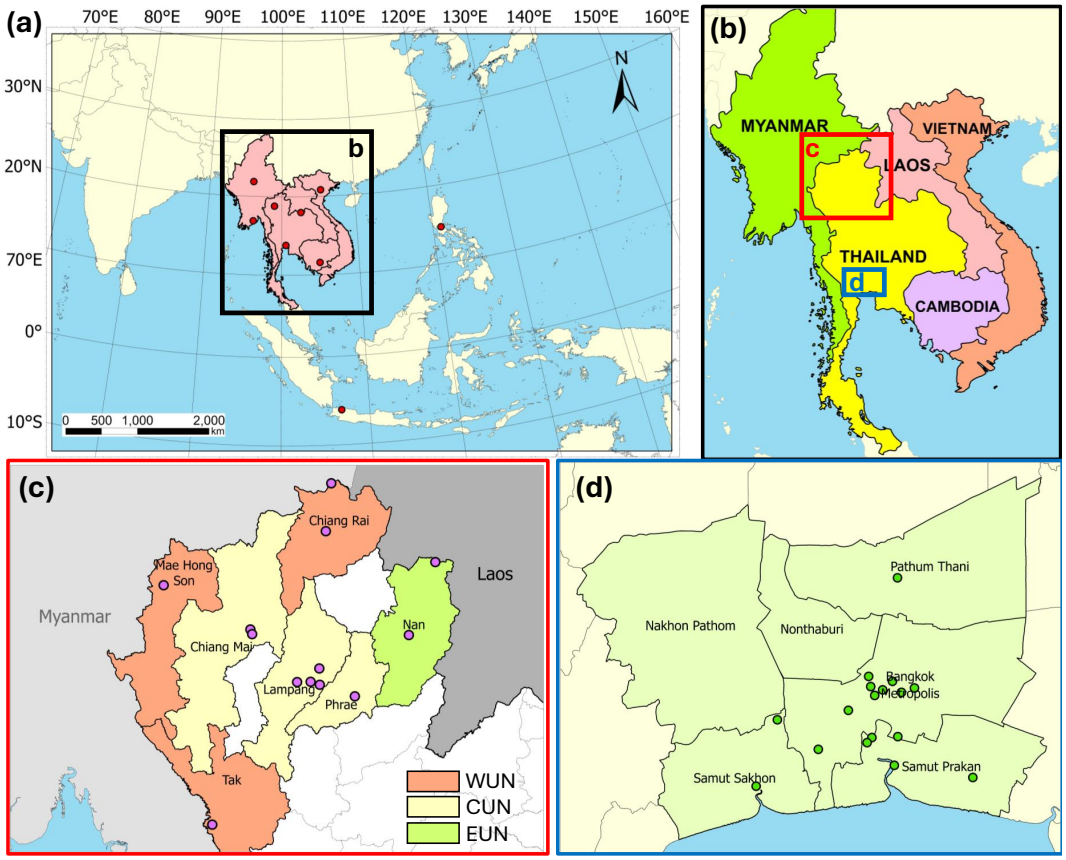

Figure 14: Study area: (**a**) Modeling domain. The locations of EANET monitoring stations used in the model evaluation are marked with red circles. (**b**) Target source countries. (**c**) Upper Northern Region of Thailand. The locations of PCD monitoring stations used in the model evaluation are shown in purple circles. (**d**) Bangkok Metropolitan Region, with the locations of PCD monitoring stations marked with green circles.

The Upper Northern Region was selected as receptor area for this study because of persistent $PM_{2.5}$ pollution issues described in Subsection 1.2.1 of Chapter 1. Because $PM_{2.5}$ pollution from transboundary plumes is expected to have a greater impact on border provinces [80], this study further subdivided the Upper Northern Region

into three distinct geographical units: the West Upper Northern (WUN), Central Upper Northern (CUN), and East Upper Northern (EUN) sub-areas. These divisions were established based on their proximity to international boundaries. Specifically, WUN includes Mae Hong Son, Tak, and Chiang Rai, which share borders with Myanmar. CUN comprises the inland provinces of Chiang Mai, Lampang, and Phrae, which mainly consist of urban areas and lack international borders. EUN, conversely, encompasses Nan, which is adjacent to Laos.

Tak province, although located in the Lower Northern Region, was also included in this study due to its documented high $PM_{2.5}$ levels, exceeding the national standard for over 70 days annually [60]. It is important to note that Lamphun was omitted from this analysis because of insufficient $PM_{2.5}$ observation data during the study period, which would have compromised the accuracy of the model validation and subsequent source apportionment results.

As for the BMR, it was included in this study because it is the economic center and most densely populated region in Thailand. As detailed in Subsection 1.2.2 of Chapter 1, this region faces significant air pollution challenges from a mix of sources. In this study, four of the six BMR provinces were selected for analysis: Bangkok (BKK), Samut Prakan (SMP), Samut Sakhon (SMS), and Pathum Thani (PT). The remaining two provinces, Nonthaburi and Nakhon Pathom, were excluded from the analysis due to insufficient observed data for model validation.

4.2.2 Model configuration

The Community Multiscale Air Quality (CMAQ) model, version 5.3.3 [157], was utilized to simulate the spatial and temporal fluctuations of $PM_{2.5}$ concentrations across the domain. The simulation period extended from January to December of the 2019 calendar year, following a one-month initial spin-up period. This selection of 2019 was deliberate, as it represented the most recent typical year of activity before the COVID-19 pandemic, thereby avoiding the significant and non-representative reductions in anthropogenic emissions caused by subsequent global lockdowns [158, 159].

The model configuration for both the CMAQ model and the Weather Research and Forecasting (WRF) model [126] was maintained consistently with the detailed settings provided in Subsection 3.2.2 of the previous chapter. The results from the WRF model served as the necessary meteorological field input for the CMAQ model. Similarly, the emission inventories utilized for this study align with those detailed in Subsection 3.2.3 of the previous chapter.

The sole major modification from the previous work involved the treatment of OBB emissions, which were sourced from the Fire Inventory from NCAR (FINN) version 1.5. To counteract the issue of substantial fire emissions being artificially confined to the surface layer, an operational adjustment was implemented. This was based on observations from an extensive set of preliminary model executions, where a clear pattern emerged of the model significantly overestimating $PM_{2.5}$ concentrations during periods of relatively shallow planetary boundary layer (PBL) heights. To mitigate this systematic bias, OBB smoke was vertically distributed in a uniform manner from the ground level up to the calculated height of the PBL.

Specifically, whenever the calculated PBL height fell below 0.5 km, OBB emissions were distributed uniformly up to a fixed minimum height of 0.5 km rather than the dynamically calculated height.

This approach is grounded in the physical principle that $PM_{2.5}$ from OBB behaves differently from other anthropogenic species due to the high thermal buoyancy associated with the combustion process [186, 187]. Unlike ground-level urban or industrial sources, moderate, landscape-scale fires, such as those from crop or grassland burning, generate a significant plume rise that injects pollutants directly into the turbulent PBL rather than at the surface [188, 189]. Within this convective layer, intense vertical mixing occurs at a timescale much faster than horizontal advection, rapidly distributing these aerosols throughout the column [190]. This mechanism is further supported by previous sensitivity studies demonstrating that $PM_{2.5}$ concentrations simulated by CMAQ remain largely identical when fire emissions are injected anywhere within the PBL [191, 192].

This operational adjustment was specifically designed to ensure physical consistency within the in-house emission processing framework used in this study. While iterative plume-rise schemes such as Briggs [193], Freitas et al. [187], and Sofiev et al. [194] offer high-resolution injection heights, they often require sub-grid fire information that may not be fully resolved at regional scales[195]. To address this, the current study employs a vertical distribution parameterization that prevents buoyant OBB emissions from being treated as simple surface releases during stable atmospheric conditions. This ensures that fire emissions are not unrealistically trapped within the shallow surface layer, which would otherwise lead to an overestimation of $PM_{2.5}$ concentrations. By enforcing a 0.5 km minimum distribution, the model captures the essential thermal injection characteristics of landscape-scale OBB plumes. This specific threshold was arrived at through iterative sensitivity analysis and aligns with established parameterization techniques used in various regional air quality studies [196, 197, 198, 199, 200, 201].

To enable source apportionment, the full emission inventory was divided into two distinct inputs for the model: OBB emissions only and all remaining non-OBB emissions. The annual average emission intensities across the entire modeling domain for both of these inputs are illustrated in Figure 15.

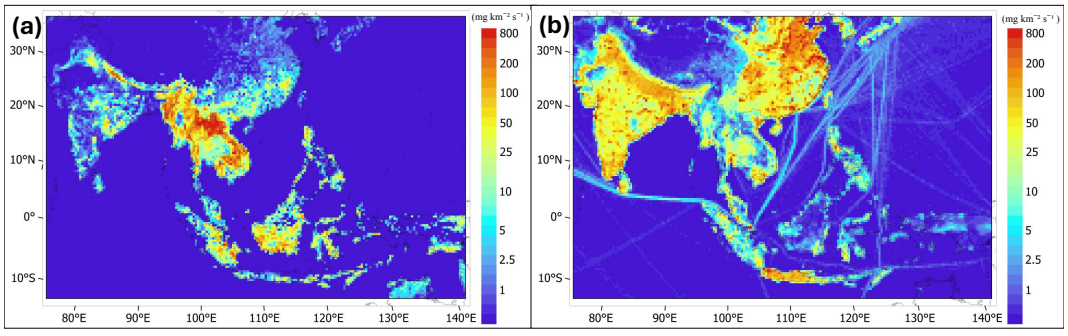

Figure 15: Average $PM_{2.5}$ emission intensities in the modeling domain: (**a**) emissions from open biomass burning and (**b**) emissions from other sources.

4.2.3 Source apportionment

To perform a nation-by-nation source apportionment, the Integrated Source Apportionment Method (ISAM) module [125], which is integrated into the CMAQ model package, was utilized. In this study, its purpose was to track $PM_{2.5}$ emissions resulting from OBB within each country of origin. To enable this detailed tracking, regional masks were systematically applied across the modeling domain, and a total of six identification tags were allocated: one domestic tag for Thailand (THA); transboundary tags for Laos (LAO), Myanmar (MYA), Cambodia (CAM), and Vietnam (VNM); and an external source tag (ETC) assigned to account for OBB emissions originating from areas outside of these five nations but within the modeling domain.

The total contribution attributed to OBB was quantified by dividing the aggregate sum of the $PM_{2.5}$ values tracked by the THA, LAO, MYA, CAM, VNM, and ETC tags by the total simulated $PM_{2.5}$ value. The remaining percentage of $PM_{2.5}$ was consequently designated as the contribution from non-OBB sources. The specific contributions from each individual source country were similarly determined by taking the value associated with that country's tag and dividing it by the overall simulated $PM_{2.5}$ concentration.

4.2.4 Observation data and model evaluation

The ability of the CMAQ model to accurately represent the temporal and spatial variations of $PM_{2.5}$ concentration in the modeling domain was verified by comparing its simulated values against observed values acquired from ground-based monitoring facilities.

Observed data from nine monitoring sites situated across seven Southeast Asian nations, as sourced from the Acid Deposition Monitoring Network in East Asia (EANET) [183] were used to evaluate the model. The evaluation of $PM_{2.5}$ within Thailand itself was further supported by observational data from 13 stations in the Upper Northern Region and 17 stations in the BMR. These domestic measurements were made available by the Pollution Control Department (PCD) through their official air quality website (http://air4thai.pcd.go.th/webV3/%23/History, accessed on 18 December 2023). The locations of all EANET and PCD stations used in model validation is marked in Figure 14.

Because the CMAQ output is structured as a gridded dataset with each cell providing a spatial average of $PM_{2.5}$ concentrations for its respective geographic grid, the comparison was conducted by aligning the predicted grid cell value with the observed measurement from the station residing in that specific grid. In instances where a simulation grid encompassed multiple monitoring stations, the collective average of the recorded observed values from those stations was calculated for the comparison. In addition to the Pearson correlation coefficient (r) and Normalized Mean Bias (NMB) defined in Chapter 3 (Equations 3.1 and 3.2), the Normalized Mean Error (NME) was also used in this chapter to evaluate the overall magnitude of the model error. Similar to NMB, NME is expressed as a percentage,

and its mathematical formulation is presented in Equation 4.1. The terms O_i, S_i, and n retain the same definition as previously established.

$$\text{NME} = \frac{\sum_{i=1}^{n} |S_i - O_i|}{\sum_{i=1}^{n} O_i} \times 100\% \tag{4.1}$$

4.3 Results and discussions

4.3.1 Model performance

For model evaluation, a comprehensive comparison was performed between the monthly average observed $PM_{2.5}$ concentrations and the corresponding simulated values across the BMR and the Upper Northern Region sub-areas: WUN, CUN, and EUN, as illustrated in Figure 16. The BMR registered monthly averages between 14.0 and 52.9 $\mu g/m^3$, yielding an annual average of 25.2 $\mu g/m^3$, which is marginally above the 25 $\mu g/m^3$ national ambient air quality standard. Concentrations in the BMR peaked in January. In sharp contrast, the sub-regions of the Upper Northern Region demonstrated markedly elevated $PM_{2.5}$ levels, with monthly figures spanning from 6.1 to 90.1 $\mu g/m^3$. The overall annual average for the entire Upper Northern Region stood at 31.0 $\mu g/m^3$, exceeding the national standard. Peak pollution for all three sub-areas in the Upper Northern Region uniformly occurred in March. WUN experienced the most intense pollution, recording an annual average of 33.1 $\mu g/m^3$ and a peak monthly concentration of 102.5 $\mu g/m^3$. CUN and EUN recorded similar annual averages (30.3 $\mu g/m^3$ and 29.6 $\mu g/m^3$, respectively), with their highest monthly concentrations in March at 66.8 $\mu g/m^3$ for CUN and 90.2 $\mu g/m^3$ for EUN.

The simulated $PM_{2.5}$ concentrations strongly supports the findings of previous research [80] on the impact of transboundary transport, particularly in regions adjacent to international borders. The highest pollution levels were concentrated in the border sub-regions: WUN (sharing a border with Myanmar) and EUN (sharing a border with Laos), highlighting the influence of cross-border pollutant plumes on local air quality. Conversely, areas geographically isolated from international borders and characterized by higher urbanization, specifically the BMR and the CUN region, generally exhibited lower $PM_{2.5}$ levels. This urban characteristic, which includes a reduced prevalence of OBB activities in densely populated centers like Chiang Mai and Lampang (CUN), helps account for the lower observed concentrations in these areas.

The statistical evaluation, detailed in Table 3 and visually represented in Figure 17, confirmed a robust agreement between the simulated and observed $PM_{2.5}$ concentrations. The correlation coefficients were high, registering 0.68 for the EANET international stations and 0.73 for the domestic PCD stations. These values underscore the model's significant capability to accurately reproduce the spatial and temporal distribution of $PM_{2.5}$ throughout the modeling domain.

Analysis of the bias metrics further affirmed the model's reliability. Normalized Mean Bias (NMB) values were 12% for EANET stations (indicating slight overestimation) and -8% for PCD stations (indicating slight underestimation).

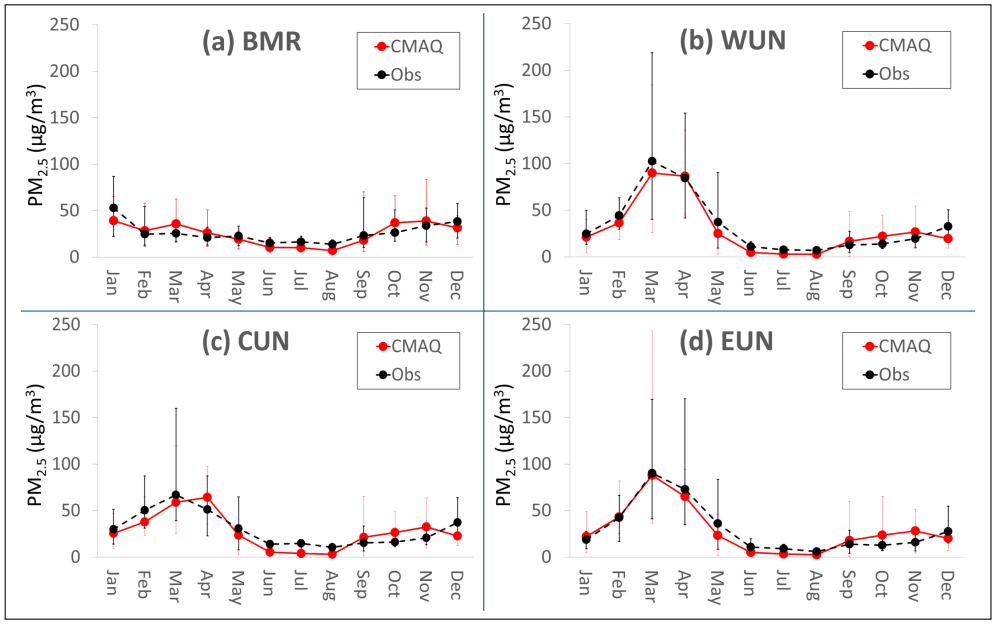

Figure 16: Time series of the observed (black line) and simulated (red line) monthly mean $PM_{2.5}$ concentrations in each target receptor area, with whiskers representing the range between minimum and maximum values: (**a**) BMR, (**b**) WUN, (**c**) CUN, and (**d**) EUN.

According to established benchmarking criteria [202], NMB values within ± 30% are considered acceptable. Similarly, the Normalized Mean Error (NME) values of 41% for EANET and 11% for PCD fall within the recognized acceptable performance range. Finally, the model successfully captured the distinct seasonal variations, particularly the intense pollution episodes during the dry season (Figure 16), a finding further reinforced by high regional correlation coefficients, including 0.78 for BMR, 0.97 for WUN, 0.86 for CUN, and 0.96 for EUN.

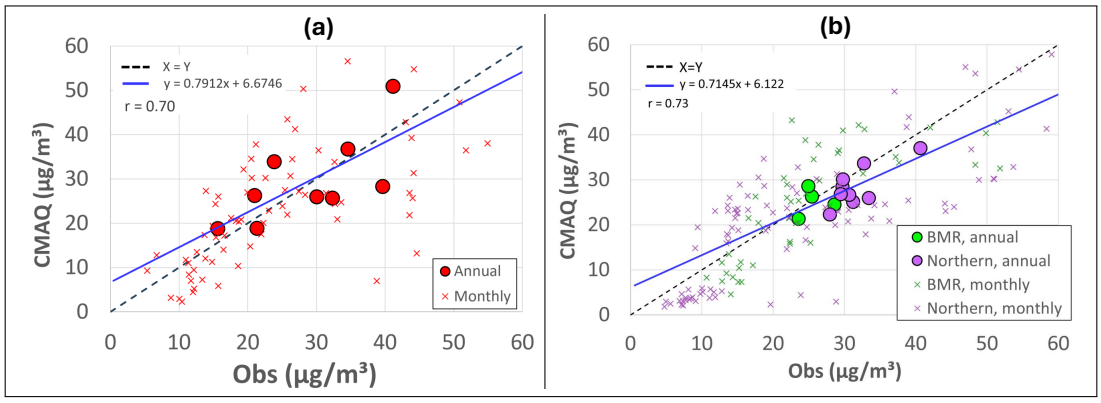

Figure 17: Comparison of the simulated and observed $PM_{2.5}$ concentrations: (**a**) EANET stations and (**b**) PCD stations.

Table 3: Statistical metrics for the evaluation of the CMAQ model's performance. Monthly mean values were used for calculation.

Monitoring Stations	Parameter (Unit)	Value
EANET	Mean CMAQ (μg/m³)	31.11
	Mean obs (μg/m³)	27.76
	r	0.68
	NMB (%)	12.0
	NME (%)	41.0
PCD (BMR+Upper Northern)	Mean CMAQ (μg/m³)	29.70
	Mean obs (μg/m³)	27.65
	r	0.73
	NMB (%)	−8.0
	NME (%)	11.0
PCD (BMR)	Mean CMAQ (μg/m³)	25.18
	Mean obs (μg/m³)	26.28
	r	0.78
	NMB (%)	−4.0
	NME (%)	26.0
PCD (WUN)	Mean CMAQ (μg/m³)	29.53
	Mean obs (μg/m³)	33.14
	r	0.97
	NMB (%)	−11.0
	NME (%)	22.0
PCD (CUN)	Mean CMAQ (μg/m³)	27.04
	Mean obs (μg/m³)	30.27
	r	0.86
	NMB (%)	−9.0
	NME (%)	32.0
PCD (EUN)	Mean CMAQ (μg/m³)	28.47
	Mean obs (μg/m³)	29.62
	r	0.96
	NMB (%)	−4.0
	NME (%)	21.0

4.3.2 Nation-by-nation contribution assessment

The spatial patterns of $PM_{2.5}$ concentrations, simulated by the model for both the annual average and the peak March–April burning season, are visually presented in Figure 18. This visualization distinctly reveals that $PM_{2.5}$ levels across Southeast Asia, particularly over Northern Thailand, Myanmar, and Laos, intensified dramatically during the March–April period compared to the overall annual average. In Thailand, the simulated annual average $PM_{2.5}$ concentration was 20.1 $\mu g/m^3$,

which escalated to 40.0 $\mu g/m^3$ during March and April, representing an approximate doubling of concentration. A direct comparison of these $PM_{2.5}$ concentration results with the OBB emission data presented in Figure 15 confirms that OBB is the primary underlying cause driving this dramatic increase in $PM_{2.5}$ concentrations. During this intense burning episode, the highest concentrations were observed in Laos, followed by Myanmar, and then Thailand, aligning precisely with the established regional emission intensities. These findings collectively emphasize the substantial and region-wide impact of OBB during the dry season's peak burning period, which significantly degrades air quality.

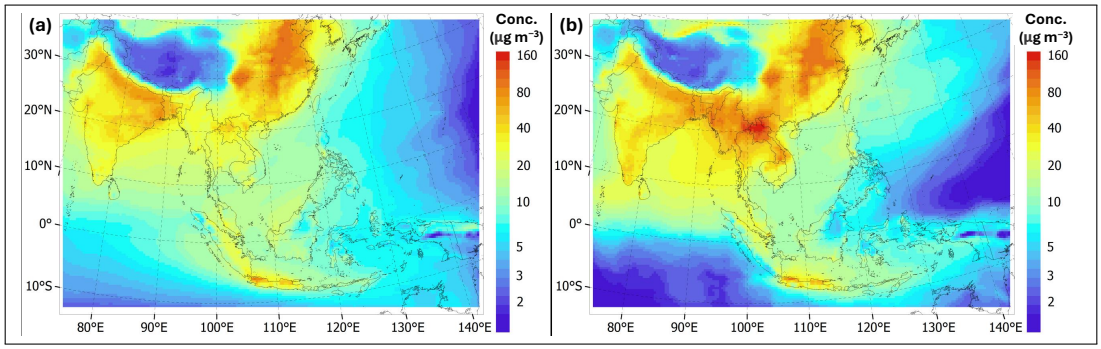

Figure 18: Spatial distribution of simulated $PM_{2.5}$ concentrations: (**a**) annual mean and (**b**) mean during the intensive burning period (March–April).

The spatial distribution of the annual contribution from OBB originating in each source country is illustrated in Figure 19, while the corresponding contributions specifically during the intense burning period of March to April are presented in Figure 20. A comparison between these two figures reveals that $PM_{2.5}$ levels attributable to OBB increased significantly across all target source countries during the March–April window relative to the annual mean. This direct comparison strongly supports the conclusion that the dramatic increase in $PM_{2.5}$ concentrations observed during this time is fundamentally driven by OBB, thus affirming its critical role in air quality degradation during the peak burning season.

The relative contributions of OBB from each source country, for both the annual average and the March-April intensive burning period, are visually presented in Figures 21 and 22, respectively. For the BMR, the annual source apportionment results show that OBB accounted for only 15.3% of the mean annual $PM_{2.5}$ concentration. This value is relatively low compared to contributions from other anthropogenic and natural emissions. This measured result presents a significant contrast to previous research [74, 89, 203], where OBB was frequently identified as a major contributor to $PM_{2.5}$ in the BMR with contributions ranging from 20% to 40%. The primary reason for the variation in results is likely the difference in the methodology employed. Prior studies relied on receptor modeling, which derives source composition from chemical fingerprints at specific monitoring stations. While offering accuracy for a specific site, this method is not well-suited to representing the contribution on a larger spatial scale, whereas the atmospheric chemical transport model utilized in this study offers source apportionment at higher spatial and temporal resolutions [104, 106, 111, 112].

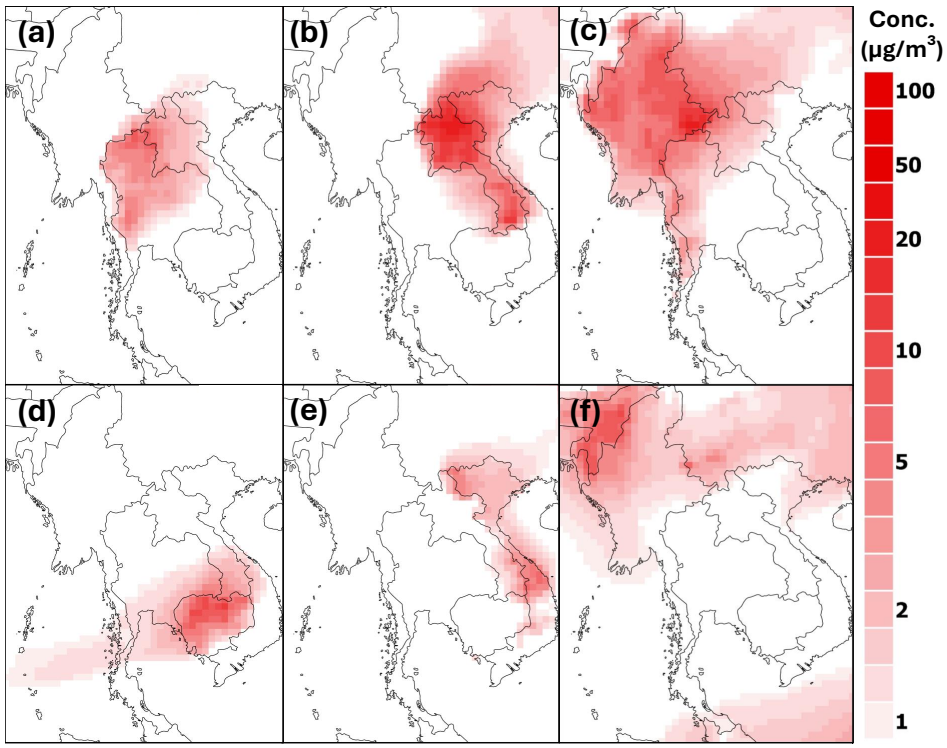

Figure 19: Average annual contribution of $PM_{2.5}$ concentrations due to OBB in each target source country: (**a**) Thailand, (**b**) Laos, (**c**) Myanmar, (**d**) Cambodia, (**e**) Vietnam, and (**f**) other countries.

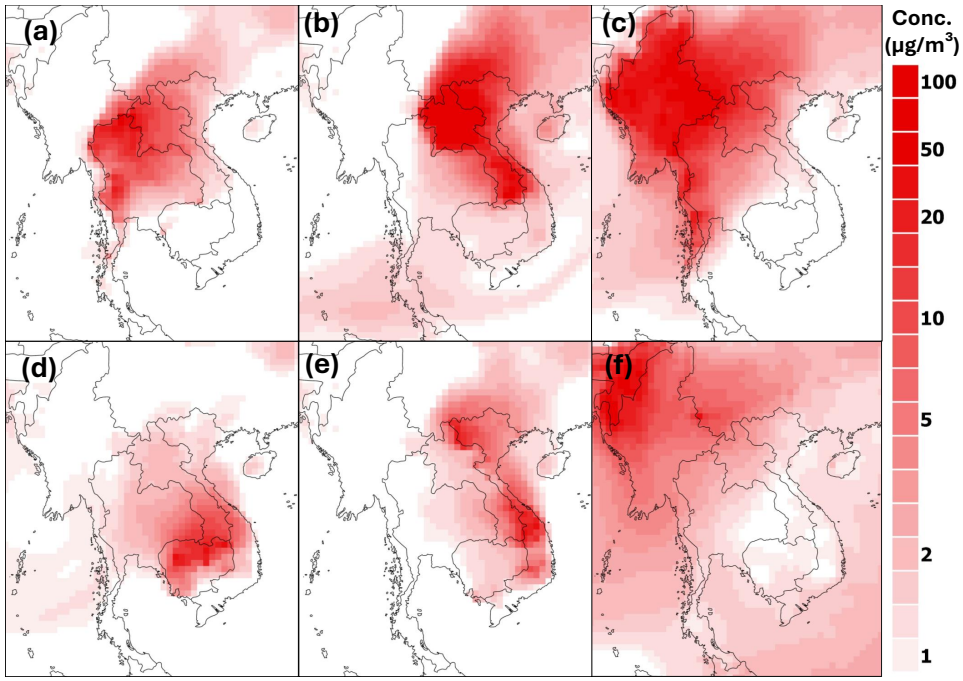

Figure 20: Spatial distribution of $PM_{2.5}$ from OBB in each target source country during March–April: (**a**) Thailand, (**b**) Laos, (**c**) Myanmar, (**d**) Cambodia, (**e**) Vietnam, and (**f**) other countries.

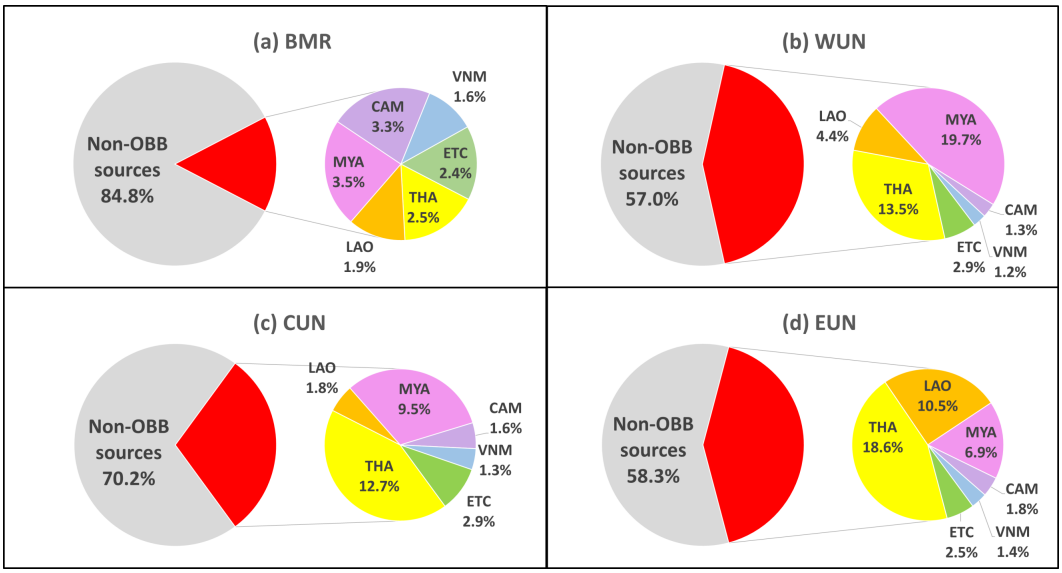

Figure 21: Annual nation-by-nation contributions from OBB to the $PM_{2.5}$ concentrations in each target receptor area: (**a**) BMR, (**b**) WUN, (**c**) CUN, and (**d**) EUN.

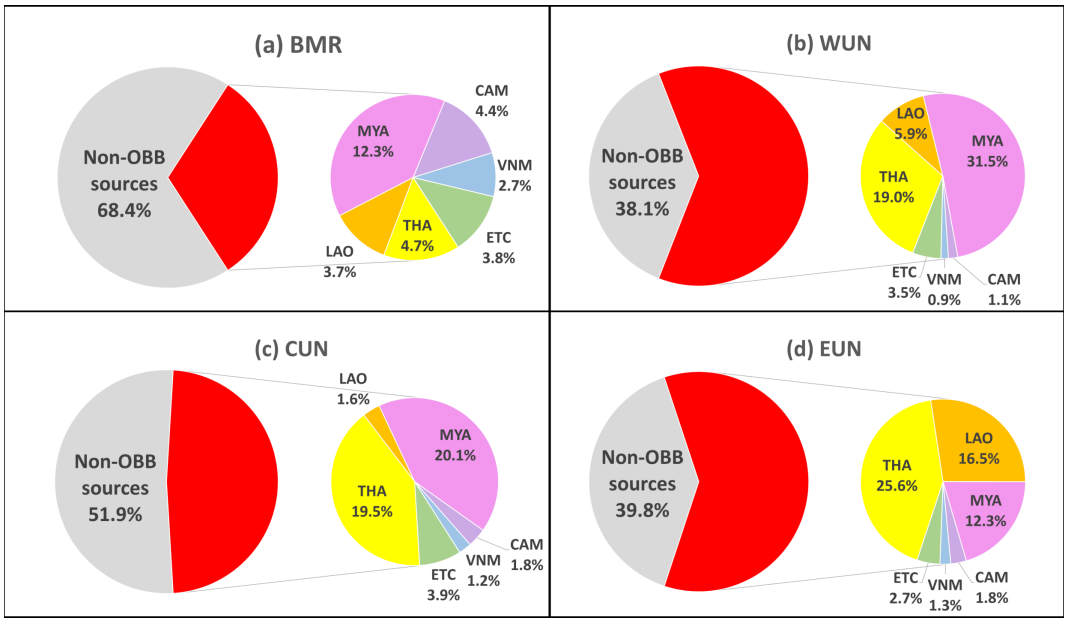

Figure 22: Nation-by-nation contributions from OBB to $PM_{2.5}$ concentrations from March to April in each target receptor area: (**a**) BMR, (**b**) WUN, (**c**) CUN, and (**d**) EUN.

Despite the moderate overall annual contribution of OBB, transboundary transport remained a recognizable contributor to $PM_{2.5}$ concentrations in the BMR, regardless of the distance from neighboring countries. Domestic OBB contributed only 2.5% to the annual $PM_{2.5}$ mean level, while external sources contributed 12.7%, led by Myanmar at 3.5%. However, during the intense burning season (March and April), the total OBB contribution to $PM_{2.5}$ concentrations drastically increased to 31.7%. During this peak period, domestic OBB accounted for 4.7%, while 27% was attributed to transboundary transport, with Myanmar once again being the largest

transboundary source at 12.3%. Although the overall effect remains lower than that observed in the Upper Northern Region, these results provide robust evidence of the persistent, major impact of transboundary transport on $PM_{2.5}$ concentrations in the BMR, particularly during March and April when burning activities intensify.

As for the Upper Northern Region, OBB was a significant factor for $PM_{2.5}$ levels. Annual OBB contributions were 43.0% in WUN, 29.9% in CUN, and 41.8% in EUN. These figures rose to 61.9%, 48.1%, and 60.2% during the March-April peak burning period. Myanmar contributed the most to $PM_{2.5}$ in WUN, accounting for 19.7% annually and 31.5% in the peak season. In CUN, Thailand was the top annual contributor at 12.7%. However, Myanmar became the largest source during peak months at 20.1%. Thailand remained the primary contributor to EUN in both annual (18.6%) and peak (25.6%) periods.

The findings showed that transboundary transport affected $PM_{2.5}$ in the Upper Northern Region more than domestic burning. Annual transboundary contributions were 29.5% in WUN, 17.1% in CUN, and 23.1% in EUN. In the peak season, these percentages increased to 42.4%, 28.6%, and 34.6% for WUN, CUN, and EUN. These results align with a prior study [80] that found similar transboundary contributions in WUN and EUN provinces. This study reported slightly lower percentages for CUN. This difference is likely due to variations in the modeling framework and emission inventories. WUN and EUN's proximity to international borders made them more susceptible to transboundary transport. In contrast, the centrally located CUN was mainly influenced by domestic sources. Although EUN is near Laos, the contribution from Laos (10.5%) was less than that from domestic burning (18.6%). Laos had high $PM_{2.5}$ emissions from OBB, but prevailing weather patterns dispersed this pollution eastward, away from Thailand's Upper Northern Region.

This study provided valuable insights but has limitations. First, the model's coarse spatial resolution might limit its accuracy in capturing $PM_{2.5}$ variations, especially in complex terrain. A finer resolution might offer a clearer picture of dispersion. Second, the study used older data as a proxy because an up-to-date emission inventory was unavailable. This means year-specific variations might be missing. These issues highlight the need for future work using improved spatial resolution and current emission data to better understand contributions from OBB and other sources.

4.4 Conclusion

This chapter successfully quantified the nation-by-nation contributions of open biomass burning (OBB) to $PM_{2.5}$ concentrations in Thailand's Upper Northern Region and the Bangkok Metropolitan Region (BMR) using the CMAQ-ISAM model. The model performance was validated against ground-based observations, showing strong correlations and an accurate capture of seasonal pollution peaks.

The findings revealed varied contribution profiles for each region. In the Upper Northern Region, OBB is the dominant $PM_{2.5}$ contributor, especially during the March-April peak, where it accounted for 61.9% in West Upper Northern (WUN), 48.1% in Central Upper Northern (CUN), and 60.2% in East Upper Northern (EUN).

A critical finding was that transboundary transport was a larger source than domestic burning in the border sub-regions of WUN and EUN, with Myanmar being the primary contributor to WUN. In contrast, the CUN was more affected by domestic sources annually, though influence from Myanmar's transboundary transport increased dramatically during the peak burning season.

For the BMR, OBB represented a smaller annual fraction at 15.3%. This result differs from some previous receptor-based studies, a variation attributed to the higher spatial and temporal resolution of the chemical transport model used here. However, OBB's impact on the BMR is still severe during the peak burning season, where its contribution rose to 31.7%. Transboundary transport was the reason behind this peak, contributing 27%, with Myanmar again identified as the largest single external source.

These results provide clear quantitative evidence for a transboundary and domestic $PM_{2.5}$ problem: domestic activities strongly influence the BMR and CUN, while transboundary pollution overwhelmingly impacts border regions like WUN and EUN. This distinction is crucial for policy, suggesting that effective air quality management requires a dual strategy of robust domestic controls and active multilateral cooperation, particularly with Myanmar. While this study provided valuable insights, its limitations, specifically the coarse spatial resolution and the use of older proxy emission data, highlight the need for future work. Subsequent research using improved resolution and current emission inventories is necessary to refine this understanding and better inform targeted abatement strategies.

Chapter V

Source Apportionment and Sensitivity Analyses of $PM_{2.5}$ and Its Species Over Thailand

5 Source Apportionment and Sensitivity Analyses of $PM_{2.5}$ and Its Species Over Thailand

This chapter is based on the publication: ***Comprehensive Source Apportionment and Sensitivity Analyses of $PM_{2.5}$ and Its Species Over Thailand Using the WRF-CMAQ Model****, under review for publication in Environmental Advances.*

5.1 Introduction

The analyses presented in Chapter 3 and Chapter 4 demonstrated that open biomass burning (OBB) constitutes a major source of $PM_{2.5}$ concentration in Thailand, particularly impacting the Upper Northern Region. However, air quality degradation is not solely attributable to OBB, as other emission sectors also substantially contribute to $PM_{2.5}$ pollution, especially in densely populated urban settings such as the Bangkok Metropolitan Region (BMR). Therefore, a thorough assessment of the source contribution is essential to provide policymakers with the scientific evidence necessary for crafting regionally specific pollution mitigation strategies.

As previously discussed in Section 2.2 of Chapter 2, the integration of source apportionment and sensitivity analysis techniques offers a complementary framework for establishing a clear understanding of the quantitative relationship between emission sources and ambient $PM_{2.5}$ concentrations within specific geographic areas. Source apportionment quantifies the proportional contribution of each emission source to the total pollutant mass, while sensitivity analysis captures the non-linear atmospheric chemical responses to emission reductions. Although there are some regional studies on this topic in the literature, a comprehensive analysis utilizing both source apportionment and sensitivity analysis applied to domestic emission sectors in Thailand remains a notable research gap. Therefore, this chapter is dedicated to conducting a thorough source contribution assessment by applying and comparing the results from both methods to seven domestic anthropogenic emission sectors across the distinct receptor regions of Thailand.

5.2 Methodology

5.2.1 Study area

In this chapter, $PM_{2.5}$ source contribution are assessed for four key receptor regions in Thailand: the Upper Northern Region, the BMR, Saraburi, and Khon Kaen. The rationale for selecting these areas, based on the significance of their pollution issues, is described in Subsections 1.2.1–1.2.4 of Chapter 1. Table 4 provides a detailed summary of these areas, including the selected provinces within each region and the abbreviations used in this study. Their locations are shown in Figure 4. For

the Saraburi region, two distinct subdistricts were designated as receptor areas: the heavily industrial Na Phra Lan subdistrict (SB-NPL) and the provincial urban center, Muang subdistrict (SB-M). These two sites are separated by a distance of approximately 20 km. The primary objective for selecting these two subdistricts is to specifically evaluate the transport and subsequent impact of industrial $PM_{2.5}$ emissions from SB-NPL on the air quality within the adjacent downtown area of SB-M.

Table 4: List of selected $PM_{2.5}$ receptor areas in this study, categorized by region.

Region	Province / Area	Abbreviation
Upper Northern Region	Chiang Rai	CR
	Chiang Mai	CM
	Nan	NAN
	Phrae	PH
	Mae Hong Son	MHS
	Lampang	LP
Bangkok Metropolitan Region (BMR)	Bangkok	BKK
	Samut Prakan	SMP
	Samut Sakhon	SMS
	Pathum Thani	PT
Northeastern Region	Khon Kaen	KK
Central Region	Saraburi - Na Phra Lan	SB-NPL
	Saraburi - Mueang	SB-M

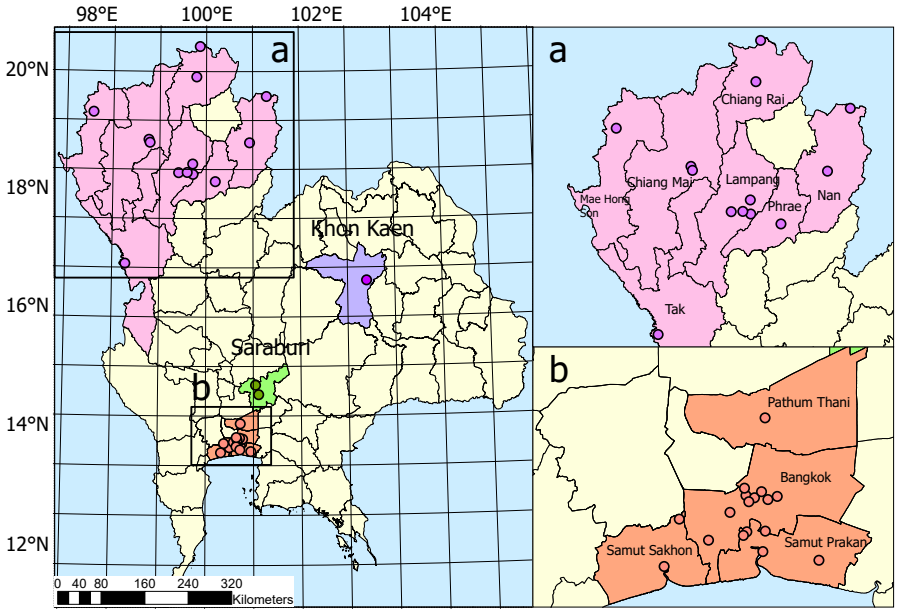

Figure 23: Study area. The locations of monitoring stations used in the model evaluation are marked with circles. (**a**) Upper Northern Region (**b**) BMR

5.2.2 Model configuration

To simulate the spatial and temporal variations of $PM_{2.5}$ concentrations throughout the modeling domain, this study employed the Community Multiscale Air Quality (CMAQ) model, version 5.3.3 [157]. The modeling assessment covered the entire 2019 calendar year, extending from January to December. This simulation was preceded by a one-month spin-up period to establish initial conditions. The year 2019 was deliberately chosen as the study period. It represents the most recent year of typical activity before the onset of the COVID-19 pandemic. This selection was critical to avoid the significant and non-representative reductions in anthropogenic emissions that resulted from the subsequent global lockdowns [158, 159].

The simulation framework for this chapter is largely based on the methodology established in Chapter 3. This applies to both the model setup and the emission inventories, which were detailed in Sections 3.2.2 and 3.2.3. Furthermore, this study incorporates the specific modification to the OBB emission inventory that was previously implemented in Chapter 4, as described in Section 4.2.2.

The only key difference from the previous analyses is the adoption of a nested domain configuration rather than a single domain, as illustrated in Figure 24. This domain structure includes a parent domain (d01) that is identical to the one employed in Chapters 3 and 4, defined with a 45×45 km horizontal grid resolution and 192×129 grid cells. Centered within this parent domain, a nested domain (d02) is introduced. This second domain utilizes a finer resolution of 15×15 km with 117×117 grid cells. The d02 domain is specifically designed to provide high-resolution coverage over Thailand, extending from the upper southern region to include portions of adjacent Laos and Myanmar.

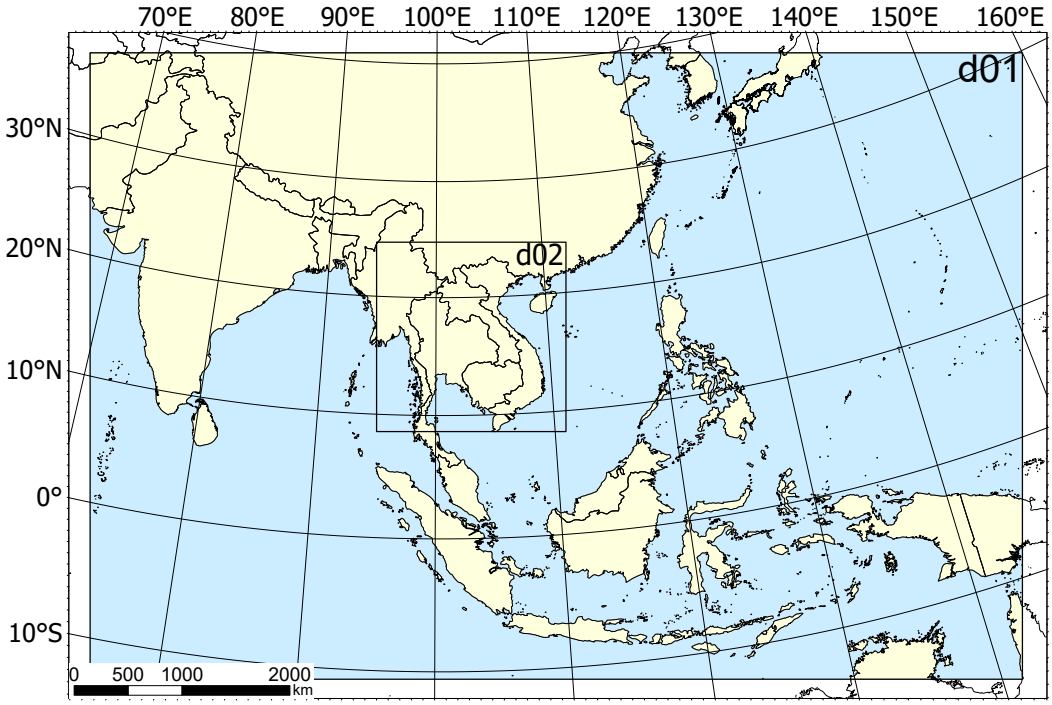

Figure 24: Modeling domains

5.2.3 Simulation setup

To achieve a comprehensive assessment of source contribution, this investigation applied both source apportionment and source sensitivity analyses. The study focused on seven distinct domestic emission sectors, which are detailed in Table 5. A separate category, designated "Other" (OTH), was established to account for all other unclassified sources. This OTH category includes, but is not limited to, natural emissions and the significant influence of transboundary transport originating from outside Thailand.

Table 5: Emission sectors for source apportionment and sensitivities in this study

Sector	Full Name	Description
OBB	Open biomass burning	Emissions from open biomass burning, including agricultural residue burning and forest fires.
RES	Residential	Emissions from residential fuel combustion, particularly from solid fuels like coal and biofuels used for heating and cooking.
IND	Industrial	Emissions from industrial fuel combustion and non-combustion processes, such as coke production and cement manufacturing.
POW	Power generation	Emissions from fuel combustion at power plants for electricity generation. Large plants are treated as distinct point sources.
ROAD	Road transport	Emissions from on-road vehicles, including hot exhaust, cold-start, and evaporative non-methane volatile organic compound (NMVOC) emissions.
OTT	Other transport	Emissions from marine transport and aviation
OTA	Other anthropogenic emissions	Emissions from other human-related activities, including agriculture, manure and waste management, solvent use, and ammonia from human physiological processes.
OTH	Other	Emissions from all remaining unclassified sources, including but not limited to transboundary transport and emissions from natural sources such as biogenic emission, wind-blown dust, and sea salt spray

Source apportionment was conducted using the Integrated Source Apportionment Method (ISAM) [125]. ISAM is a specialized tool integrated within the CMAQ model that employs a tagged species methodology [103]. These tags operate as passive tracers that are processed through the model's simulation of chemical reactions, transport, and deposition. This process allows for the

quantification of each tagged source's contribution to the total $PM_{2.5}$ concentration within every grid cell at each time step. For this dissertation, a region mask was applied to the emission inventory to isolate domestic sources, and individual tags were assigned to each of the seven emission sectors. A known constraint of the ISAM module in CMAQ version 5.3.3 is its inability to apportion secondary organic aerosols (SOA). Consequently, a post-processing adjustment was required to correctly account for SOA mass and ensure that the sum of all apportioned sectors matched the total simulated concentration.

For the source sensitivity analysis, the brute force method (BFM) was utilized. BFM is a well-established technique that assesses concentration changes by comparing a full-emission "base case" simulation against a series of "perturbed" simulations where emission inputs are systematically modified [101, 104, 112, 117]. The resulting difference in concentration between the base case and a perturbed case reveals the model's sensitivity to the altered emission source. In this study, the perturbation involved creating separate simulations where each domestic emission sector was zeroed-out individually. A critical aspect of atmospheric chemistry is its non-linear nature. Therefore, the sum of concentration changes from these individual sector-specific simulations does not typically equal the total concentration from the base case [112, 133]. The discrepancy is captured in a residual OTH term, which represents not only the contributions from unclassified transboundary and natural sources but also the complex, non-linear chemical interaction effects that arise from the simultaneous presence of all emission sectors.

During initial trial runs, an inconsistency was identified in the ISAM results where the sum of concentrations from all source-tagged species did not align with the total simulated $PM_{2.5}$ concentration, even after accounting for the un-apportioned SOA mass. To correct this, a ratio-based apportionment approach was adopted. First, the contribution ratio for each emission sector was determined by dividing the concentration of its specific tag by the total sum of concentrations from all tagged species. These calculated fractions were then applied to the total simulated non-SOA $PM_{2.5}$ concentration to ensure a properly balanced apportionment.

To validate the reliability of both the ISAM and BFM results, a comparative analysis was performed using primary carbonaceous species: elemental carbon (EC) and primary organic carbon (POC). These species are ideal for validation because they are directly emitted and exhibit largely linear behavior in the atmosphere [32, 204, 205]. As such, the results from the two methods for these species are expected to be highly consistent [103], a finding that has been confirmed in previous research [104].

5.2.4 Observation data and model evaluation

The performance of the CMAQ model in reproducing the spatiotemporal variations of $PM_{2.5}$ concentrations was validated by comparing simulation outputs with observed ground-level data. This observational dataset was gathered from a total of 24 monitoring stations across Thailand. The network consisted of 10 stations in the Upper Northern Region, 11 in the Bangkok Metropolitan Region (BMR), and one station each in Muang (Saraburi), Na Phra Lan (Saraburi), and Khon Kaen.

These data were sourced from the Pollution Control Department (PCD) through their official air quality data repository (http://air4thai.pcd.go.th/webV3/#/History, accessed on 18 December 2023). Figure 23 illustrates the specific geographical locations of all monitoring stations used in this evaluation.

To ensure the statistical validity of the observational data utilized for the simulation period, specific data completeness criteria were enforced. For a daily mean concentration to be calculated, more than 75% of the hourly data points for that day were required. Furthermore, for a monitoring station to be included in the annual evaluation, it must have met this daily completeness standard for more than 75% of the days during the year. This validation methodology aligns with approaches used in prior research [206, 207].

The model's performance was benchmarked using three primary statistical metrics: the Pearson correlation coefficient (r), Normalized Mean Bias (NMB), and Normalized Mean Error (NME). The evaluation criteria employed in this study were adopted from the benchmark established by Emery et al. [208]. This benchmark specifies that performance for total and speciated particulate matter should be evaluated at temporal scales not exceeding three months and spatial scales of 1000 km or less. As shown in Table 6, the benchmarks are categorized as "Goals" or "Criteria," which are derived from the statistical distribution of historical model performance. "Goals" indicate a high level of performance, reflecting values achieved by the top one-third of past modeling applications. "Criteria" are less stringent benchmarks, representing values met by two-thirds of previous applications, and serve as a general reference for acceptable model performance. Therefore, the model is considered acceptable if it satisfies at least the 'Criteria' threshold across all evaluated statistical metrics.

5.3 Results and discussions

5.3.1 Model performance

An evaluation of the model's performance in simulating $PM_{2.5}$ concentrations within the d02 domain was conducted across all four quarters of 2019. Figure 25 presents density scatter plots comparing simulated and observed daily mean concentrations for each quarter of the year. Figure 26 shows comparisons of simulated and observed monthly mean $PM_{2.5}$ concentrations in each target receptor area. The model effectively captured the temporal variation of $PM_{2.5}$ across all target receptor areas. This includes seasonal variation, particularly the elevated concentrations from January to April corresponding to intense agricultural burning episodes. However, $PM_{2.5}$ concentrations were slightly underestimated during this period, most notably in the Upper Northern Region where the impact of OBB is most pronounced.

A statistical summary, referencing the benchmark goals and criteria from Emery et al. [208], is detailed in Table 6. The R values for the first three quarters (Q1: 0.81, Q2: 0.82, Q3: 0.74) all surpassed the stringent goal of 0.70, which demonstrates a strong correspondence with observed temporal and spatial patterns. A notable decrease in the R value to 0.49 occurred in the fourth quarter (Q4). This

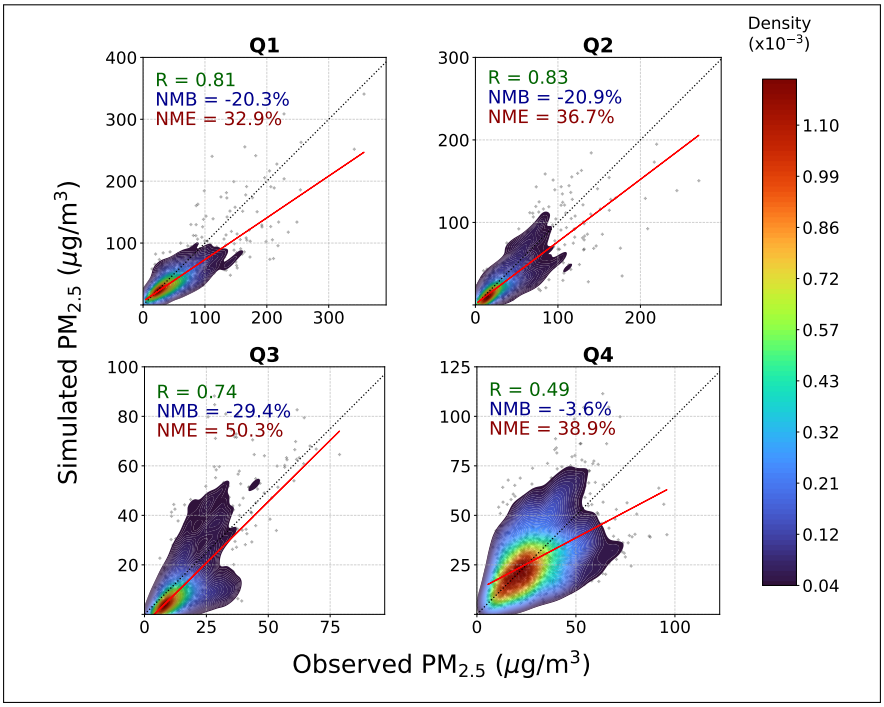

Figure 25: Density scatter plots of simulated versus observed hourly $PM_{2.5}$ concentrations for each quarter of 2019: Q1 (Jan-Mar), Q2 (Apr-Jun), Q3 (Jul-Sep), Q4 (Oct-Dec).

Table 6: Comparison of model performance metrics (R, NMB, NME) for simulated quarterly mean $PM_{2.5}$ concentrations against the benchmark criteria from Emery et al. (2017) [208].

Metric	Jan-Mar	Apr-Jun	Jul-Sep	Oct-Dec	Criteria	Goal
R	0.81	0.82	0.74	0.49	> 0.40	> 0.70
NMB	-20.3%	-20.9%	-29.4%	-3.6%	$< \pm 30\%$	$< \pm 10\%$
NME	32.9%	36.7%	50.3%	38.9%	$< 50\%$	$< 35\%$

value nonetheless satisfied the minimum benchmark criteria of > 0.40. Negative NMB values were recorded for all four quarters, which confirms the model's underestimation tendency, particularly during the peak burning season. All quarterly NMB figures (Q1: -20.3%, Q2: -20.9%, Q3: -29.4%, Q4: -3.6%) were within the established criteria of $< \pm 30\%$. The Q4 value of -3.6% was the only one to achieve the more rigorous goal of $< \pm 10\%$. The NME metric was generally within the $< 50\%$ benchmark criteria for the year. Specifically, Q1 (32.9%), Q2 (36.7%), and Q3 (38.9%) were all below this threshold. Q1 also achieved the stricter goal of $< 35\%$. The NME for Q3, at 50.3%, was the only metric to slightly miss the benchmark criteria.

Overall, the model demonstrated robust performance. It successfully met all established benchmark criteria for both R and NMB. Furthermore, the model satisfied the criteria for NME for all quarters, except for a single minor exceedance in Q3.

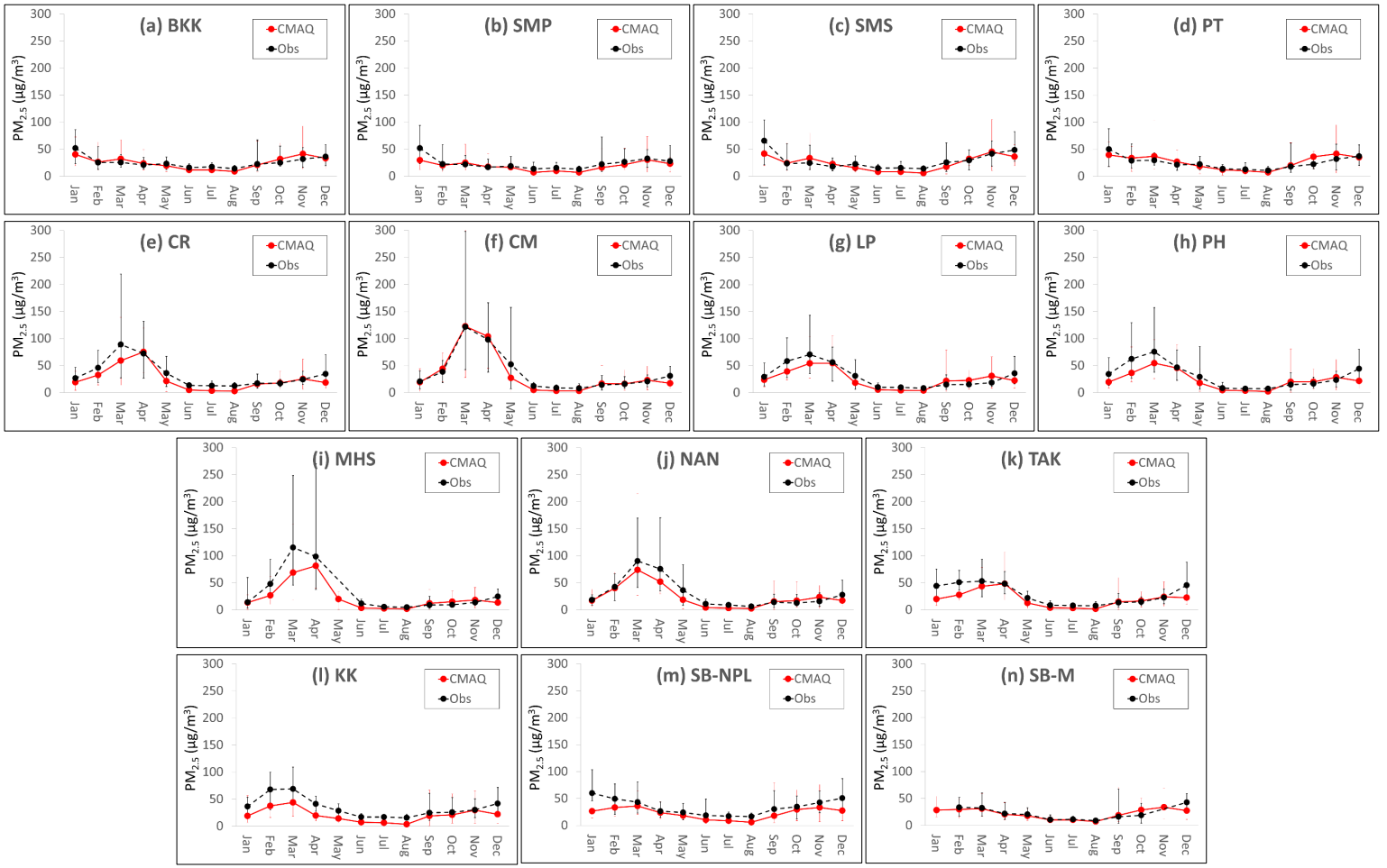

Figure 26: Comparison of observed (black line) and simulated (red line) monthly mean $PM_{2.5}$ concentrations at the target receptor sites. Whiskers indicate the monthly minimum-maximum range: (**a**) Bangkok, (**b**) Samut Prakan, (**c**) Samut Sakhon, (**d**) Pathum Thani, (**e**) Chiang Rai, (**f**) Chiang Mai, (**g**) Lampang, (**h**) Phrae, (**i**) Mae Hong Son, (**j**) Nan, (**k**) Tak, (**l**) Khon Kaen, (**m**) Saraburi - Na Phra Lan, and (**n**) Saraburi - Mueang.

5.3.2 Source apportionment and sensitivities of Total $PM_{2.5}$

Figure 27 illustrates the spatial distribution of annual mean $PM_{2.5}$ concentrations apportioned by ISAM to each domestic emission sector, with Figure 28 showing the contribution from OTH. A subsequent comparison between the ISAM source apportionment and the BFM sensitivity analysis is provided in Figure 29. This comparison evaluates the annual mean concentrations of total $PM_{2.5}$ and its key constituents: EC, POC, ammonium (NH_4^+), nitrate (NO_3^-), and sulfate (SO_4^{2-}). As the ISAM version used here cannot apportion SOA, the total simulated SOA concentration is manually integrated into the ISAM results, appearing as the light purple bar in Figure 29a. This ensures a direct comparison with the BFM results and is consistent with the post-processing procedure detailed in Section 5.2.3. To maintain the desired comparative structure, the BFM results for total $PM_{2.5}$ shown in Figure 29b were identically adjusted by subtracting the SOA concentration from total sum of sensitivities. Therefore, the sensitivities displayed for the domestic sectors in Figure 29b correspond exclusively to the non-SOA fraction of $PM_{2.5}$. The SOA formation sensitivities for each domestic sector, derived exclusively from the BFM calculation, are presented separately in Figure 30. Detailed numerical results for all source apportionment and sensitivity analyses discussed here are provided in Tables A.1 through A.7 in Appendix A.

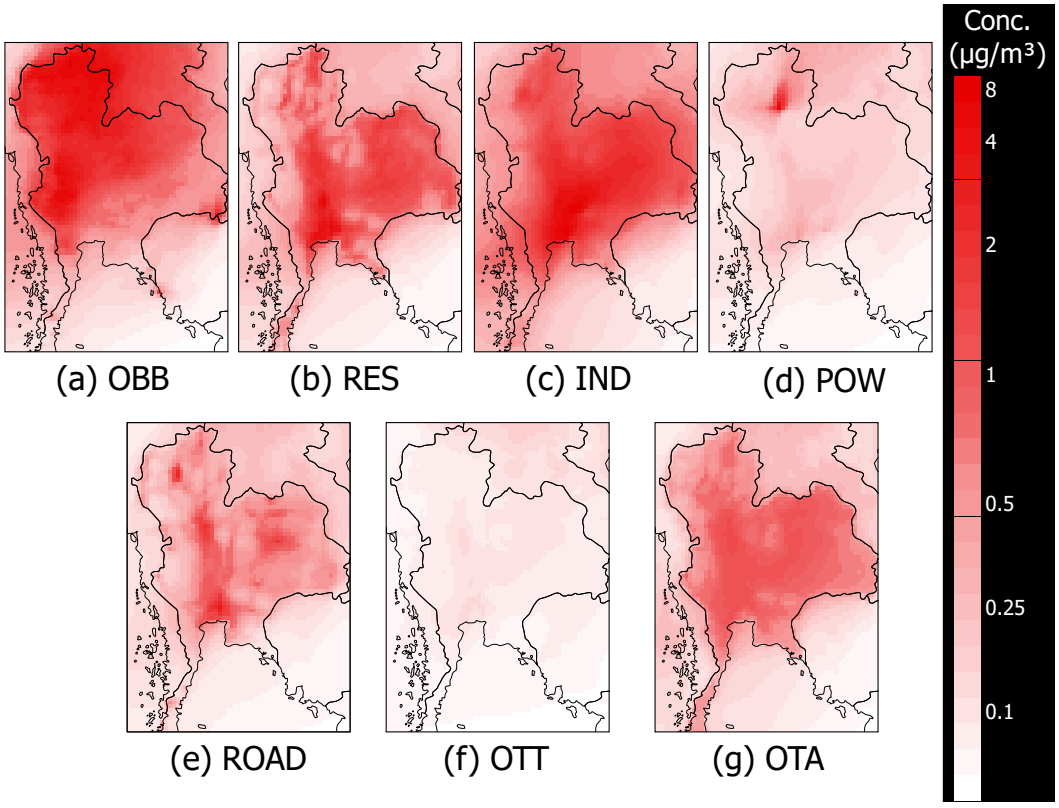

Figure 27: Spatial distribution of annual mean $PM_{2.5}$ contributions from domestic emission sectors in Thailand as estimated by ISAM: (**a**) Open Biomass Burning, (**b**) Residential, (**c**) Industrial, (**d**) Power Generation, (**e**) Road Transport, (**f**) Other Transport, and (**g**) Other Anthropogenic Sources.

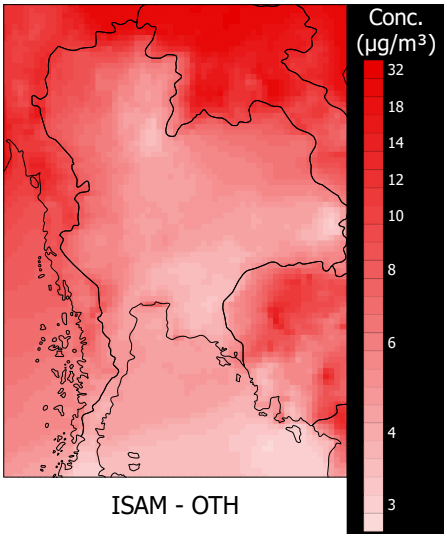

Figure 28: Spatial distribution of annual mean $PM_{2.5}$ contributions from other sources (including transboundary transport and natural emissions) in Thailand as estimated by ISAM.

Contribution from domestic emission sectors

A comparison of the source apportionment results from ISAM and the source sensitivity results from BFM, which are illustrated in Figure 29a, Figure 29b, and detailed in Table A.1, indicates that the findings from both methods are in close agreement. The results for sectors such as OBB, RES, and POW show a particularly strong alignment. This consistency is attributed to emissions from these sectors being dominated by combustion processes that emit a large fraction of their $PM_{2.5}$ as primary particulate matter [209, 210, 211, 212, 213]. This primary PM is not as affected by the complex and non-linear atmospheric processes that control the formation of secondary aerosols. This leads to more comparable outcomes between ISAM and BFM [32, 103, 134].

Despite the general agreement, minor inconsistencies are observable in the IND, ROAD, and OTA sectors. These differences arise from the non-linear responses in atmospheric chemistry that are characteristic of the BFM technique. In that method, the full removal of an emission sector changes the entire chemical composition of the atmosphere. For major sources that are rich in precursor gases like sulfur dioxide (SO_2) and nitrogen oxides (NO_x), this perturbation substantially alters the formation pathways of Secondary Inorganic Aerosols (SIA) [34, 103, 133, 214]. This alteration results in different contribution estimates between the two methods. For instance, in BKK, BFM calculates slightly higher contributions for IND (22.7% compared to 21.7%) and ROAD (6.1% compared to 5.8%). Conversely, in SB-M, BFM estimates a lower contribution for the OTA sector (1.6%) than ISAM does (3.8%). These non-linear impacts on SIA formation, which explain the observed differences, are discussed in greater detail in the subsequent section. Nonetheless, even with these small quantitative variations, both methods consistently identify the same sectors as the dominant contributors and show the same regional patterns.

The influence of the domestic emission sectors analyzed in this research



Figure 29: Source apportionment derived by ISAM and sensitivities derived by BFM of the simulated $PM_{2.5}$ and its species concentrations to all emission sectors in each target receptor area. Thick black lines denotes the simulated concentrations

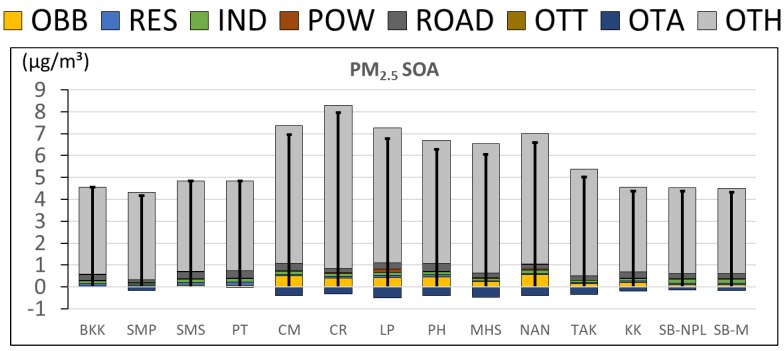

Figure 30: Source sensitivities to secondary organic aerosol (SOA) concentrations, derived by BFM in each target receptor region. Thick black lines indicate the simulated baseline concentrations.

demonstrates distinct variations across the different regions of Thailand. Although domestic anthropogenic sectors are significant contributors to the annual mean total $PM_{2.5}$ concentration, their cumulative impact is typically smaller than that of the OTH category at the majority of receptor locations. The total contribution from all domestic sources varies substantially by site. When factoring in their contributions to SOA (as shown in Figure 30), the combined domestic impact spans from 15.1% in Tak to a high of 50.1% in Bangkok according to ISAM results. BFM shows a comparable range, from 14.5% to 53.1%. In general, domestic sources are responsible for almost half of the total $PM_{2.5}$ in the urbanized BMR and Saraburi areas. In contrast, their influence is markedly less in the Upper Northern Region. Khon Kaen exhibits an intermediate profile. In Khon Kaen, the OTH contribution is dominant, yet the influence from domestic sectors is clearly more pronounced than in the northern provinces.

OBB is identified as the major domestic contributor to $PM_{2.5}$ within the Upper Northern Region. Its impact is greatest in provinces such as Nan, Phrae, and Chiang Mai, where it is responsible for 18.4% (ISAM) / 18.6% (BFM), 15.4% (ISAM) / 15.6% (BFM), and 16.3% (ISAM) / 16.3% (BFM) of the total $PM_{2.5}$, respectively. In sharp contrast, the influence of OBB is negligible in the highly urbanized BMR, contributing only 1.6-2.3% to the total $PM_{2.5}$. This distinct regional difference is consistent with the conclusions of the prior Chapter 3 and 4. A comparable profile is observed in the Saraburi region, where the OBB contribution is minimal, registering at 3.0% (ISAM) / 2.9% (BFM) in SB-NPL and 3.3% (ISAM) / 3.1% (BFM) in SB-M. Khon Kaen, however, displays a larger impact from OBB (6.8% ISAM, 7.1% BFM) than the BMR, although it remains less affected than the Upper Northern Region. This is plausibly a result of its geographical proximity to the North, where biomass burning activities are most concentrated.

The RES sector represents a significant contribution in densely populated urban centers, most notably the BMR and Saraburi, where it is consistently identified as the second-largest domestic source. This pattern is clearest in Bangkok and Pathum Thani, where RES emissions are responsible for 11.7% (ISAM and BFM) and 13.8% (ISAM and BFM) of total $PM_{2.5}$, respectively. This high contribution is probably driven by the extensive use of fuel for cooking within dense residential areas. Khon

Kaen exhibits a moderate contribution of 5.7% from this sector. Conversely, the contribution from the RES sector in the Upper Northern Region is comparatively small, generally falling within a range of 1.6% in Mae Hong Son to 3.4% in Phrae. A notable exception is Chiang Mai, the region's main urban center. It demonstrates a slightly higher contribution from RES (2.3% from ISAM, 2.0% from BFM) when compared to its more rural neighboring provinces, which reflects the influence of its greater population density.

The IND sector stands out as the predominant domestic source of $PM_{2.5}$ in the BMR and Saraburi. The most significant contributions are found at both sites in Saraburi, with contributions of 27.6%-28.3% (ISAM) and 28.8%-29.5% (BFM) of total $PM_{2.5}$ in both SB-NPL and SB-M. Given that the calculated concentrations from the IND sector by both methods are nearly identical, it can be inferred that emissions from the highly industrial Na Phra Lan subdistrict also affect the adjacent provincial center of Mueang. The BMR likewise shows a substantial industrial influence, with contributions in Bangkok reaching 21.7% (ISAM) and 22.7% (BFM). In Khon Kaen, the industrial sector's impact is also noteworthy, comprising 9.8% (ISAM) and 10.1% (BFM). In contrast, the impact from the industrial sector is considerably smaller in the Upper Northern Region, where contributions generally do not exceed 5.3%. Similar to other sectors associated with urban activity, Chiang Mai is distinct with a slightly higher contribution (4.3% from ISAM, 4.2% from BFM) relative to other northern locations, a finding that aligns with its status as the region's primary economic hub.

The contribution from the POW sector is distinctively notable in Lampang. In this province, it ranks as the second-largest domestic contributor to $PM_{2.5}$ after OBB and is responsible for a substantial 10.2% (ISAM) and 10.5% (BFM). This finding is a direct consequence of the Mae Moh power plant, which is the largest lignite-fired power plant in Thailand. Such a major local impact from a large-scale coal-fired power plant is in agreement with findings from other cities [212, 215]. In sharp contrast, contributions from the POW sector are negligible in all other study locations, including the BMR, Saraburi, and Khon Kaen, where it generally constitutes less than 1.5% of total $PM_{2.5}$. This finding is logical because coal is known to emit significantly higher levels of particulate matter than natural gas [216], the latter of which is the primary fuel for electricity generation in Thailand [217, 218].

The impact from the ROAD sector is most evident in the highly urbanized BMR, where high traffic density makes it the third-largest domestic contributor. In this region, its contributions range from 5.0–7.7% (ISAM) and 5.2–8.2% (BFM). While these results align with previous research [74, 88, 203], which also pinpointed road transport as a major contributor to $PM_{2.5}$ levels in the BMR, the contribution magnitude identified in this study is comparatively lower. This discrepancy is probably due to differences in research methodologies and modeling frameworks. The influence of road transport is also noteworthy in other regional centers, such as Khon Kaen (5.6% from ISAM, 6.8% from BFM) and Saraburi. In the Upper Northern Region, its impact is substantially smaller. Even the urban center of Chiang Mai shows a modest contribution (2.7% from ISAM, 2.8% from BFM), and more rural provinces often register below 2.5%. Concurrently, contributions from OTT, which

encompasses marine and aviation sources, were determined to be negligible at all receptor sites, with consistent estimates at 0.5% or less.

The contribution of the OTA sector is shaped by a complex combination of agricultural and urban activities. This category also includes sources that are concentrated in urban areas, such as waste management and solvent use. Consequently, a direct comparison that relies solely on agricultural land use area (data from Office of Agricultural Economics [219]) may be misleading. For example, the urbanized BMR has relatively small areas of agricultural land (350–800 km^2) but demonstrates a high OTA contribution, ranging from 2.8–3.6% (ISAM) and 1.6–3.2% (BFM). Conversely, the Upper Northern Region, which has a much larger agricultural land area (680–4,300 km^2), shows a comparatively lower OTA contribution, with values between 1.0–3.0% (ISAM) and 0.2–1.3% (BFM). The highest OTA contribution is observed in Khon Kaen (4.5% ISAM, 3.0% BFM), a location that combines the largest agricultural land use (approximately 6,200 km^2) with a major urban setting. A similarly high contribution is apparent in Saraburi, where significant agricultural land (approximately 1,700 km^2) combined with industrial activities leads to OTA contributions of 3.8–4.0% (ISAM) and 1.6–2.3% (BFM).

Contribution from transboundary and unclassified sources

Results from both ISAM and BFM (as shown in Figures 29a and 29b) indicate that the OTH category represents a significant source of annual mean $PM_{2.5}$ across all receptor locations. Based on the ISAM source apportionment, the largest contributions are observed in the Upper Northern Region (ranging from 39.8% to 62.7%). The contributions are also considerable in the BMR (31.6% to 48.7%), Saraburi (36.1% to 36.2%), and Khon Kaen (44.8%). Although the OTH category includes several unclassified sources detailed in Table 5, a precise quantification of its components is not an objective of the present study. Nevertheless, it is possible to qualitatively assess the primary sources within the OTH category for each target receptor area by examining relevant existing research.

Biogenic emissions originating from vegetation are major contributors to biogenic SOA formation, and this component is already factored in separately as part of the total SOA concentration. Additional natural sources, such as sea salt and wind-blown dust, have been quantified in prior research. Sea salt is responsible for as much as 10.5% in Bangkok, a site located near the coast [85]. It is anticipated, however, that the contribution from sea salt will be considerably smaller at other target receptor sites, given their inland locations. The contribution from wind-blown dust was calculated at an average of 3.2% for Thailand in 2017 [114]. In contrast, another study identified combined contributions from salt spray and dust at 18.5% in the Northern, 21% in the Northeastern, and 22.1% in the Central Region during 2019 [77]. Once these aforementioned sources are considered, the residual fraction of the OTH category is probably dominated by transboundary transport. This conclusion aligns with the findings in Chapter 4, which quantified the contributions from transboundary OBB as 12.7% in Bangkok and ranging from 17.1% to 29.5% in the Upper Northern Region. The substantial impact of transboundary pollution on the Upper Northern Region is supported

by numerous studies [79, 80, 85]. This pronounced influence from transboundary sources accounts for the larger OTH contributions observed in the Upper Northern Region. It also aligns with the spatial distribution of $PM_{2.5}$ from OTH, which indicates heightened concentrations near border areas as depicted in Figure 28.

The existing body of research indicates that the specific contributing sources within the OTH category differ significantly by region. In the Upper Northern Region, transboundary OBB emissions represent the primary factor, a consequence of the region's proximity to neighboring countries. This influence is also apparent in Khon Kaen, albeit to a lesser degree, and is minimal in both the BMR and Saraburi. In contrast, the OTH fractions within urban and industrial regions are defined by a complex mix of transboundary transport and wind-blown dust. An additional contribution from sea salt is also present in the BMR, owing to its coastal location. Consequently, achieving a more precise, source-specific quantification of the constituent parts of the OTH category remains an essential goal for future research.

5.3.3 Source apportionment and sensitivities of $PM_{2.5}$ species

Understanding the factors that create the distinct regional pollution profiles requires a detailed analysis of the chemical composition of $PM_{2.5}$. The subsequent sections will therefore investigate the source contributions to its primary chemical species. This includes primary carbonaceous aerosols (EC and POC), SOA, and SIA (ammonium, nitrate, and sulfate). By adopting this species-level analysis, it is possible to clearly distinguish between direct primary emissions and secondary pollutants that are formed through complex atmospheric chemistry. This approach will provide a more profound insight into the specific sources that contribute to $PM_{2.5}$ in each region.

Primary carbonaceous aerosols

As discussed in Section 5.2.3, the ISAM and BFM results for EC and POC were expected to be nearly identical. The findings, which are presented in Figures 29c to 29f and detailed in Tables A.2 and A.3, confirm this expectation. There is excellent agreement between the two methods for both EC and POC across all receptor sites. This strong consistency serves to validate the source apportionment and sensitivity results for all $PM_{2.5}$ components. Therefore, to maintain clarity and simplicity in the following discussion, only the ISAM results will be presented.

The contribution of EC to the total $PM_{2.5}$ mass varies considerably by region, revealing a distinct separation between urban and rural environments. In the BMR, EC makes up 7.1% to 9.2% of total $PM_{2.5}$. Its contribution is significantly lower in the Upper Northern Region, where it ranges from 3.6% to 4.7%. Khon Kaen and Saraburi show an intermediate profile, with EC fractions of 6.2% (KK), 5.3% (SB-NPL), and 5.1% (SB-M). This geographical distribution is a direct result of the different regional source profiles. For highly urbanized areas, the ROAD sector is the primary domestic source, accounting for 32.9% of EC in Bangkok and 35.6% in KK. The RES sector is also a major EC contributor in these populated areas,

responsible for 26.7% in BKK and up to 32.4% in Samut Sakhon. In Saraburi, the IND sector is the largest contributor, at 26.8% to 29.0%. IND is also a significant source in the BMR, providing 16.2% of EC in Bangkok. In contrast, domestic OBB's contribution is negligible in the BMR, at only 1.1% to 1.6% of EC. This impact is slightly higher in Khon Kaen (6.4%) and Saraburi (3.5% to 4.0%). This pattern differs from the Upper Northern Region, where domestic OBB is a major source of EC, contributing 19.4% in Chiang Mai. Nevertheless, the most dominant contributor to EC in the North is the OTH sector by a large margin. The OTH sector accounts for 47.0% in Chiang Mai and reaches a maximum of 76.3% in Chiang Rai. This high contribution is probably due to transboundary OBB plumes. This conclusion is supported by the POC to EC ratio. Both OBB and OTH sources in the Upper Northern Region exhibit high ratios, which have been reported to be associated with OBB origins [27, 28]. Conversely, urban areas display a lower ratio, indicating sources from high-temperature combustion, such as vehicle engines and residential coal burning [28, 29].

In a manner similar to EC, the fraction of POC in the annual mean total $PM_{2.5}$ concentrations also demonstrates a clear regional pattern. In the Upper Northern Region, POC represents a larger fraction, accounting for 26.0% of total $PM_{2.5}$ in Chiang Mai and reaching a high of 30.2% in Chiang Rai. In contrast, its contribution is lower in the BMR, where it ranges from 19.3% to 23.3%. It is lowest in the industrial Saraburi region, at approximately 15%. Khon Kaen again shows an intermediate contribution at 19.1%. The ISAM and BFM results for POC show a regional trend that is comparable to that of EC, where different sources are dominant in urban versus rural settings. In the Upper Northern Region, POC is governed by biomass burning. While the domestic OBB sector is a substantial contributor, responsible for 34.8% in Chiang Mai and 37.0% in Lampang, the OTH sector is the most significant source overall. The OTH contribution spans from 42.4% to 82.3% across the northern sites. This confirms that biomass burning from both domestic and transboundary sources is the principal driver of POC concentrations in the Upper Northern Region. Conversely, the POC contribution in the BMR and Saraburi is driven by urban and industrial activities. In Bangkok, the RES and IND sectors are the largest domestic contributors, as both are responsible for 28.2% of POC. In Saraburi, the IND sector is the major source, contributing 21.1% to 22.9%, with the RES sector following closely. To summarize, the source profiles of primary carbonaceous aerosols vary across the regions. The Upper Northern Region is dominated by OBB. The BMR is characterized by a combination of industrial, residential, and road transport emissions. Saraburi is primarily influenced by the industrial sector. Khon Kaen presents an intermediate profile that mixes influences from both urban and rural source types.

Secondary organic aerosols

As shown in Figures 29a and 29b, SOA is consistently identified as a dominant component of $PM_{2.5}$, second only to the OTH sector. Its contribution at the target receptor sites ranges from 18.4% to 27.1% of the total $PM_{2.5}$ concentration. The formation of SOA is governed by complex chemical reactions, which involve the

oxidation of both biogenic and anthropogenic precursors within the atmosphere. Given the established difficulty in definitively classifying all SOA formation pathways [36], the source sensitivity results from the BFM (as shown in Figure 30) are analyzed for the total SOA concentration. This analysis does not attempt to classify the specific biogenic or anthropogenic origins of the precursors.

The OTH sector is the predominant contributor to total SOA. It exhibits sensitivities that range from 85.1% in SMS and PT to as high as 97.6% in MHS. This significant contribution is expected, as the OTH category encompasses all natural biogenic volatile compound (BVOC) emissions, which are recognized as the primary precursors for a substantial fraction of SOA [220]. Additionally, transboundary OBB plumes originating from neighboring countries contribute a diverse array of volatile organic compounds (VOCs) that also function as SOA precursors [36]. These VOCs within the plumes can also elevate photochemical oxidant production, thereby accelerating the oxidation of BVOCs [221]. This influence is especially pronounced in the Upper Northern Region, where OTH sensitivities frequently surpass 90%. This finding is in agreement with previous research [222].

Regarding domestic emissions, the ROAD sector stands out as a significant anthropogenic source across all regions. It is ranked as a major domestic contributor, particularly in urban sites such as the BMR and Khon Kaen. This dominance is expected because vehicular emissions are known to be a major source of anthropogenic SOA precursors, especially in urban settings [223, 224, 225, 226, 227, 228]. The largest contributions are identified in the BMR, reaching 0.33 $\mu g/m^3$ (6.9%) in PT and 0.28 $\mu g/m^3$ (6.1%) in BKK. The ROAD sector is also prominent in Khon Kaen, contributing 0.27 $\mu g/m^3$ (6.3%). This urban influence aligns with previous research that focused on the BMR [229]. While the contribution is lower than in the BMR, the ROAD sector still contributes consistently across the Upper Northern Region, registering 0.18 $\mu g/m^3$ (2.3%) in CR and 0.21 $\mu g/m^3$ (3.2%) in NAN. The IND and RES sectors also demonstrate higher contributions in urbanized sites like the BMR and SB. The peak contributions for IND are observed in SB-M at 0.19 $\mu g/m^3$ (4.3%) and PT at 0.16 $\mu g/m^3$ (3.3%). Meanwhile, RES contributions peak in SMS at 0.14 $\mu g/m^3$ (2.9%) and PT at 0.14 $\mu g/m^3$ (2.8%). Conversely, OBB is the dominant domestic contributor to SOA in the Upper Northern Region. This sector's highest sensitivities are observed in NAN at 0.56 $\mu g/m^3$ (8.4%), followed by PH at 0.46 $\mu g/m^3$ (7.4%) and CM at 0.50 $\mu g/m^3$ (7.1%). OBB sensitivities are minimal in the highly urbanized BMR and SB areas, generally accounting for 0.05 $\mu g/m^3$ or less (2.0% or less) of the total SOA concentration. Khon Kaen shows a moderate impact with a 0.19 $\mu g/m^3$ (4.3%) contribution. The contribution from the POW sector is again observed only in Lampang, accounting for 0.14 $\mu g/m^3$ (2.1%), but it is otherwise a negligible source at all other receptor sites ($\leq$1.0%). The results also reveal negative sensitivities for the OTA sector at several receptor sites. This indicates that the removal of these emissions leads to an increase in the total SOA concentration. This phenomenon suggests that NO_x emissions, likely from fertilizer use and waste management, suppress SOA formation. NO_x can alter atmospheric oxidative pathways by scavenging key oxidants, such as O_3 and OH radicals, which are essential for oxidizing BVOCs to form biogenic SOA [35, 36].

Secondary inorganic aerosols

SIA represent a major fraction of the annual mean $PM_{2.5}$ concentration. They account for approximately 25–31% of $PM_{2.5}$ in urban and industrial areas and 18–32% in the Upper Northern Region. The analysis of SIA formation reveals the profound impact of non-linear atmospheric chemistry discussed in Subsection 1.1.1 of Chapter 1, which is the underlying cause for the inconsistencies between the ISAM and BFM results, as discussed previously in Section 5.3.2. The BFM approach, which perturbs the system by removing all emissions from a given sector, captures these complex interactions. This methodology can result in large, and sometimes negative, sensitivities that differ greatly from the linear source apportionment calculated by ISAM [103, 134].

The source analysis for ammonium, shown in Figure 29g-h and detailed in Table A.4, highlights the critical role of NH_3 availability and showcases the largest discrepancies between the two methods. By directly tracing tagged emissions, the ISAM results identify the OTA sector, which includes agricultural emissions, as the dominant domestic source of NH_3. This sector's contribution exceeds 50% in the BMR and Saraburi. In stark contrast, the BFM sensitivities for the OTA sector are drastically lower, typically registering below 15%. This major difference, where removing the largest domestic NH_3 source has a minimal effect on the final aerosol concentration, provides strong evidence that the atmosphere in these regions is in an "ammonia-rich" condition. In such a system, there is a surplus of NH_3. The formation of ammonium aerosol is therefore no longer limited by the NH_3 concentration but is instead limited by the availability of sulfate and nitrate for reaction [214, 230]. Consequently, removing a single domestic source (OTA) has little impact, as sufficient NH_3 remains from other sources, particularly the OTH sector, to complete the neutralization. The source profile differs in the Upper Northern Region, where the domestic OTA contribution is comparatively lower and ISAM identifies domestic OBB as a more significant NH_3 precursor source, with contributions reaching 10.5% in Nan. In the urban and industrial centers of the BMR, Saraburi, and Khon Kaen, the RES and IND sectors also contribute to ammonium formation, though their primary role is providing the acidic species for neutralization rather than being major NH_3 sources themselves.

Given this ammonia-rich environment, the formation of SIA is limited by the availability of acidic precursors, namely SO_2 and NO_x. Among the SIA components, sulfate exhibits the most linear behavior, with relatively good agreement between the ISAM and BFM results. Furthermore, a comparison of the SIA components reveals that sulfate is a far more abundant species than nitrate across all receptor sites. Its concentration is often an order of magnitude higher. For instance, the sulfate concentration in BKK (4.51 $\mu g/m^3$) is roughly nine times greater than that of nitrate (0.49 $\mu g/m^3$). This abundance confirms that sulfuric acid is the dominant acidic species available for neutralization and plays a primary role in SIA mass formation. The IND sector is the most significant domestic source of sulfate precursors in urban and industrial areas, contributing 22.6% (ISAM) and 23.5% (BFM) in BKK and reaching a high of 32.9% (ISAM) and 33.6% (BFM) in SB-M. The POW sector is also a notable contributor in LP, accounting for 11.7%

(ISAM) and 12.1% (BFM) due to the Mae Moh power plant. However, the OTH sector is overwhelmingly the largest contributor to sulfate across all sites, with its contribution ranging from 61.7% to 93.3%. This indicates that regional sulfate levels are predominantly controlled by transboundary transport. This finding is consistent with previous research identifying international shipping as a major source of sulfate in Bangkok [231]. Since the OTT sector in this study is confined to domestic transport, emissions from international vessels combusting high-sulfur fuel oil are instead accounted for in the OTH sector. This potentially explains the large contribution from OTH, although a more detailed source attribution study is required to further understand the sources of transboundary sulfate.

The source profile for nitrate is highly complex and clearly illustrates the non-linearities of SIA chemistry. The differences between the results from ISAM and BFM highlight the complex atmospheric reactions involved. The ISAM results reflect the direct contribution from each source to the $PM_{2.5}$ concentration, while the BFM's sensitivity analysis shows the non-linear response from the atmosphere to the complete removal of a source. In urban and industrial areas such as the BMR, SB-M, and KK, nitrate formation is driven by a complex mix of domestic NO_x sources. The ROAD sector is a major contributor, as evidenced by its ISAM contribution of 24.5% in SMS. Its BFM sensitivity, at 46.1%, is nearly double this linear contribution, indicating a significant non-linear influence on the overall system. The RES sector also consistently contributes to nitrate formation, accounting for 16.7% of total nitrate in BKK according to ISAM, while its BFM sensitivity is notably higher at 23.5%. Similarly, the IND sector exhibits a BFM sensitivity of 40.3% in SB-M, which is substantially higher than its moderate ISAM contribution of 22.0%. The POW sector displays a comparable pattern, with BFM sensitivities consistently exceeding their linear ISAM apportionments. For instance, in BKK, the BFM sensitivity is 15.4% compared to an ISAM contribution of 9.8%. The most dramatic non-linearity is observed in the OTA sector. While ISAM apportions its contribution at less than 4%, a chemically logical result given its low direct NO_x emissions, the BFM reveals a very high sensitivity, exceeding 60% in the BMR and 80% in SB-M.

In contrast, the source profile is different in the Upper Northern Region. Here, domestic OBB emerges as a significant source of NO_x precursors for nitrate, with BFM sensitivities reaching 45.3% in NAN and 41.2% in MHS. Conversely, its influence on nitrate formation is minimal in the BMR and SB-M, with BFM sensitivities around 5.2–5.5%, while a more moderate contribution of 13.4% is observed in KK. A key finding that highlights the non-linear chemistry is the strong negative sensitivity of the OTH sector in the BMR and SB-M, which reaches an extreme of -95.9% in SB-M. As the OTH sensitivity is calculated as a residual, this large negative value is a direct result of the sum of the individual domestic sector sensitivities being far greater than the total simulated nitrate concentration. This overestimation is driven by the exceptionally high sensitivities calculated for domestic sources like OTA and IND in the BFM simulations. This mathematical artifact highlights the highly non-linear nature of the chemical system, where nitrate formation is extremely sensitive to changes in domestic NH_3 and NO_x precursors. This effect is far less pronounced in the Upper Northern Region, where the OTH sensitivity for nitrate

is often positive. This indicates a different chemical regime, likely influenced more by transboundary NO_x from OBB than by industrial sulfate.

5.3.4 Implications for air pollution mitigation policies

The findings from the source apportionment and sensitivity analyses offer critical insights for planning effective air pollution mitigation policies in Thailand. The results clearly show that a uniform national strategy would be inadequate. This is due to the distinct regional pollution profiles that are driven by a complex mix of domestic and transboundary sources. The research highlights the necessity of a multi-faceted approach that is geographically customized, scientifically based on atmospheric chemistry, and incorporates international cooperation.

The most significant conclusion is the dominant impact of the OTH sector on $PM_{2.5}$ concentrations in all regions, an effect that is particularly pronounced in the Upper Northern Region. This implies that while regulating domestic emissions is important, achieving substantial air quality improvements will be challenging without also addressing transboundary transport. Consequently, a comprehensive strategy must give priority to diplomatic engagement and regional collaboration with neighboring countries to reduce transboundary OBB.

For controlling domestic emissions, a strategy targeted by region is necessary. In the Upper Northern Region, where OBB is the largest single domestic source, policies must concentrate on diminishing burning activities. Such measures could include providing economic incentives for farmers to use alternative residue management practices, strictly enforcing burn bans, and enhancing public education about the health impacts of smoke. In contrast, the urban and industrial areas of the BMR and Saraburi demand a focus on anthropogenic sources from the industrial, residential, and road transport sectors. Effective policies here might involve promoting cleaner fuels and technologies in industry, encouraging a shift to modern cookstoves in homes, and fostering fleet electrification to reduce vehicle emission along with investments in public transport.

The impact of the power generation sector, especially in Lampang, presents a unique case requiring its own specific policy. While a national policy exists to expand renewable energy and reduce natural gas consumption [232], the current strategy does not include a plan to replace the coal-fired power plants in the Upper Northern Region. Given the substantial local contribution of the Mae Mo lignite-fired power plant to $PM_{2.5}$ levels in Lampang, prioritizing fuel conversion or adopting cleaner technologies is critical for managing local air quality effectively.

Finally, the results related to secondary aerosols offer key insights on which precursors should be targeted for the greatest impact. The non-linearities identified by the BFM simulations, particularly for SIA, show that a proportional reduction in emissions will not result in a proportional decrease in $PM_{2.5}$ concentration. Because the atmosphere in urban and industrial areas appears to be in an ammonia-rich condition, policies aimed at controlling NH_3 from agriculture will likely have a limited impact on ammonium aerosol formation. Instead, mitigation efforts should focus on reducing the availability of acidic precursors. These are primarily SO_2 from industrial and power generation sectors, and NO_x from road transport and industrial

activities. The high sensitivities of the domestic sectors to nitrate formation, as revealed in the BFM results, provide a strong scientific foundation for aggressively targeting these sectors as a key part of an effective mitigation strategy.

5.4 Conclusion

A thorough source contribution assessment for Thailand's annual mean $PM_{2.5}$ concentrations in 2019 was undertaken using the WRF-CMAQ model. Two distinct methodologies were employed: the Integrated Source Apportionment Method (ISAM) for source apportionment and the brute force method (BFM) for evaluating source sensitivity. The analysis focused on seven primary anthropogenic emission sectors: Open Biomass Burning (OBB), Residential (RES), Industrial (IND), Power Generation (POW), Road Transport (ROAD), Other Transport (OTT), and Other Anthropogenic (OTA), with the latter encompassing sources such as agriculture and solvent use. All other emission sources, notably including transboundary transport and natural emissions, were aggregated into a single category designated as Other (OTH). The modeling framework demonstrated robust performance, as validated by statistical metrics that consistently satisfied established benchmark criteria.

The findings indicate that the OTH sector is the most significant contributor to annual mean $PM_{2.5}$ concentrations at all receptor locations. This contribution was most pronounced in the rural Upper Northern Region, where it reached a peak of 62.7%, an impact largely attributed to transboundary OBB plumes. The influence of the OTH sector was also substantial in key urban and industrial centers, including the Bangkok Metropolitan Region (BMR) (31.6%–48.7%), Saraburi (36.1%–36.2%), and Khon Kaen (44.8%). On the other hand, The contributions from domestic sources show considerable regional variation. In the Upper Northern Region, OBB is the dominant domestic source, with its impact being most significant in Nan (18.4%), Phrae (15.4%), and Chiang Mai (16.3%). Conversely, its influence is minimal in urban centers like the BMR and Saraburi (1.6%–3.3%). Khon Kaen presents an intermediate case, showing a greater OBB influence (6.8%–7.1%) than the central provinces but a much smaller one than the Upper Northern Region.

In contrast, the highly urbanized and industrial areas of the BMR and Saraburi are primarily affected by the IND, RES, and ROAD sectors. The IND sector is a major contributor in the BMR, accounting for 21.7% in Bangkok, followed by the RES sector at 11.7% and the ROAD sector at 5.0%–8.2%. In Saraburi, the IND sector is the most dominant source, responsible for 27.6%–29.5% of $PM_{2.5}$. The POW sector's contribution is negligible in most regions, with Lampang being a notable exception due to the Mae Moh lignite-fired power plant.

Furthermore, the BFM analysis of secondary inorganic aerosols (SIA) revealed that the urban atmosphere operates in an ammonia-rich regime. This finding implies that policies aimed at reducing ammonia from agriculture would have a limited impact on aerosol reduction. Instead, mitigation strategies must focus on controlling acidic precursors, particularly sulfur dioxide from the IND and POW sectors, as well as nitrogen oxides from the ROAD and IND sectors.

Chapter VI

Conclusions and Recommendations

6 Conclusions and Recommendations

6.1 Conclusions

Fine particulate matter ($PM_{2.5}$) is a significant global environmental problem and a primary public health hazard. This form of pollution is a major contributor to severe respiratory and cardiovascular diseases, with millions of premature deaths attributable to its exposure each year. Beyond its critical impacts on human health, $PM_{2.5}$ also degrades terrestrial and aquatic ecosystems and disrupts the global climate system by altering the planet's radiative balance. This issue constitutes a persistent and severe crisis in Thailand, where annual mean concentrations have consistently exceeded World Health Organization's guidelines. Consequently, this national pollution burden is directly associated with increased hospitalization rates and substantial economic damage, particularly from impacts on public health and tourism. This highlights the urgent need for effective pollution mitigation policies.

A robust understanding of the relationship between emission sources and ambient pollution levels is essential to plan effective pollution control policies. To establish this relationship for Thailand, this dissertation employed a chemical transport modeling framework, utilizing the Weather Research and Forecasting (WRF) model to generate meteorological fields and the Community Multiscale Air Quality (CMAQ) model to simulate $PM_{2.5}$ concentrations for the 2019 calendar year. This investigation applied two distinct, complementary methodologies to quantify source contributions. First, source sensitivity analysis was conducted using the brute force method (BFM), which assesses the atmosphere's response to emission perturbations and captures complex non-linear chemical feedbacks. Second, source apportionment was performed using the Integrated Source Apportionment Method (ISAM), a tagged species technique that tracks the proportional mass contribution of pollutants from their origin to a receptor.

Open biomass burning (OBB) is a widespread agricultural practice throughout Southeast Asia and has been widely reported as a major source of $PM_{2.5}$ pollution across the region. The findings from Chapter 3 provided an initial quantification of this total impact on Bangkok and Chiang Mai, utilizing the BFM approach. This analysis confirmed a stark regional disparity in the influence of OBB. In Chiang Mai, OBB was a dominant source, responsible for 49.1% of the annual mean $PM_{2.5}$ concentration. This impact intensified dramatically during the peak burning season, accounting for 70.7% of the monthly mean in April. In contrast, the annual impact on Bangkok was substantially lower at 13.1%. However, the influence from OBB on the capital remained significant during the dry season, peaking at 35.5% of the monthly mean in March, highlighting the critical role it plays as a seasonal contributor even in the central urban region.

Chapter 4 expanded this analysis by employing the ISAM module to perform a detailed nation-by-nation source apportionment of OBB, successfully differentiating

domestic impacts from transboundary transport from Myanmar, Laos, Cambodia, and Vietnam. This investigation revealed that transboundary pollution was the primary driver of the $PM_{2.5}$ fraction attributable to OBB in the BMR, contributing 12.7% annually compared to only 2.5% from domestic OBB. During the peak burning season, this transboundary contribution to the BMR rose to 27%, with Myanmar identified as the single largest external source. In the Upper Northern Region, a more complex contribution profile was observed. Annually, total transboundary transport was a larger contributor than domestic burning across all sub-regions: Western (WUN: 29.5% vs 13.5%), Central (CUN: 17.1% vs 12.7%), and Eastern (EUN: 23.1% vs 18.6%). This trend continued during the peak season, as total transboundary contributions again surpassed domestic ones, increasing significantly to 42.4% (WUN), 28.6% (CUN), and 34.6% (EUN). However, when identifying the single largest source during the peak, Myanmar was the dominant contributor in WUN and CUN, while domestic burning emerged as the largest individual contributor in EUN. Notably, Laos, despite having the highest OBB emissions in the region, had a minimal impact on the Upper Northern Region as prevailing winds dispersed the pollution eastward.

Finally, Chapter 5 provided a comprehensive source contribution analysis of seven domestic anthropogenic sectors: OBB, Residential (RES), Industrial (IND), Power Generation (POW), Road Transport (ROAD), Other Transport (OTT), and Other Anthropogenic (OTA). This study applied and compared both ISAM and BFM across four key receptor regions: the BMR, the Upper Northern Region, Khon Kaen, and Saraburi. The analysis revealed that the OTH category, which includes transboundary transport and natural emissions, was the most significant contributor to annual mean $PM_{2.5}$ concentrations at all receptor locations. Domestic contributions, in contrast, showed considerable regional variation. In the Upper Northern Region, OBB was confirmed as the dominant domestic source. Conversely, the highly urbanized and industrial areas of the BMR and Saraburi were primarily impacted by the IND, RES, and ROAD sectors. Furthermore, the BFM analysis of secondary inorganic aerosols demonstrated that urban atmospheres in Thailand operate in an ammonia-rich regime. This critical finding implies that effective mitigation strategies must prioritize the control of acidic precursors, specifically sulfur dioxide from the IND and POW sectors and nitrogen oxides from the ROAD and IND sectors. Such an approach is necessary, as the analysis indicates policies targeting ammonia reduction would likely have a limited impact on overall aerosol formation.

6.2 Limitations and recommendations

A significant limitation of this research is the inability to disaggregate the contributions of the OTH sector into specific constituent sources, based on the findings presented in Chapter 5. This constraint stems primarily from the computational limits of the high-performance computing resources available in the laboratory during this study. While the OTH sector was consistently identified in Chapter 5 as a major contributor to $PM_{2.5}$ concentrations across all study

regions in Thailand, increasing the number of tagged source sectors in the ISAM configuration would have raised the processing time and memory allocation beyond the capacity of the current hardware. Consequently, this technical limitation makes it challenging to develop highly targeted mitigation strategies based on the current results.

Therefore, a crucial direction for future research is a more detailed investigation to deconstruct this OTH sector by utilizing higher computational power. Future studies should prioritize the quantification of distinct contributions from various transboundary emission sectors, including OBB, industrial activities, and power generation. Such an investigation should also distinctly quantify the influence of natural sources, such as sea salt and wind-blown dust. In particular, the contribution of transboundary SO_2 emissions from sources like international shipping and regional industrial activities requires further examination. This is crucial given the finding in Chapter 5 that the OTH sector overwhelmingly dominates sulfate formation, and a more precise attribution is necessary to understand its significant influence.

Furthermore, a significant data-driven limitation is the lack of a comprehensive, official national emission inventory for Thailand. Current modeling efforts often rely on regional or global inventories, such as REAS, FINN, and HTAP. These datasets may not fully capture the localized nuances of Thailand's emission profiles, such as specific agricultural practices, seasonal variations in local industrial clusters, or small-scale biomass burning. The development of a high-resolution, bottom-up national inventory is essential for improving model performance and reducing uncertainties in contribution assessment.

Finally, a methodological limitation was identified in this study, as the version of ISAM employed cannot perform source apportionment for secondary organic aerosol (SOA). Consequently, if an updated modeling framework capable of apportioning SOA is used in the future, it would enable a complete and direct comparison with the BFM sensitivity results presented in this dissertation. Such a comparison would provide a more comprehensive understanding of SOA formation by distinguishing the linear contributions of various precursors from the complex non-linear sensitivities of the atmospheric system. This would, in turn, offer clearer scientific guidance for developing effective policies to mitigate anthropogenic SOA.

Appendices

A Sector-by-Sector Source Apportionment and Sensitivity Analyses Results

The following tables provide the complete results from the Integrated Source Apportionment Method (ISAM) and sensitivity analysis results from the brute force method (BFM), as discussed in Chapter 5. These results precisely quantify the contribution of each individual source sector: open biomass burning (OBB), residential (RES), industrial (IND), power generation (POW), road transport (ROAD), other transport (OTT), other anthropogenic sources (OTA), and other unclassified and transboundary sources (OTH). The quantification covers the contribution of these sectors to total $PM_{2.5}$ concentration and its constituents in each designated target receptor area, as displayed in Table 4. The constituents of $PM_{2.5}$ include Elemental Carbon (EC), Primary Organic Carbon (POC), Ammonium (NH_4^+), Nitrate (NO_3^-), Sulfate (SO_4^{2-}), and Secondary Organic Aerosol (SOA). For SOA, only BFM results are presented, since the specific version of the ISAM model used in this research does not support the apportionment of SOA.

Table A.1: Comparison of source contributions to Total $PM_{2.5}$ in each target receptor area. The values are shown as concentration in $\mu g/m^3$ with the percentage contribution in parentheses. For each cell, the top value represents the ISAM result (**bold**) and the bottom value represents the BFM result (*italic*).

	BKK	SMP	SMS	PT	CM	CR	LP
OBB	**0.39 (1.6%)** *0.36 (1.4%)*	**0.37 (2.0%)** *0.34 (1.8%)*	**0.51 (2.1%)** *0.47 (2.0%)*	**0.60 (2.3%)** *0.57 (2.1%)*	**4.55 (16.3%)** *4.53 (16.3%)*	**2.67 (7.5%)** *2.79 (7.8%)*	**2.87 (11.5%)** *2.89 (11.6%)*
RES	**2.90 (11.7%)** *2.90 (11.7%)*	**1.19 (6.3%)** *1.16 (6.2%)*	**3.26 (13.5%)** *3.35 (13.9%)*	**3.66 (13.8%)** *3.67 (13.8%)*	**0.63 (2.3%)** *0.55 (2.0%)*	**0.73 (2.1%)** *0.63 (1.8%)*	**0.70 (2.8%)** *0.64 (2.6%)*
IND	**5.38 (21.7%)** *5.62 (22.7%)*	**2.10 (11.2%)** *2.15 (11.5%)*	**4.07 (16.8%)** *4.34 (17.9%)*	**5.69 (21.4%)** *5.99 (22.6%)*	**1.19 (4.3%)** *1.16 (4.2%)*	**0.78 (2.2%)** *0.66 (1.8%)*	**1.02 (4.1%)** *1.00 (4.0%)*
POW	**0.32 (1.3%)** *0.33 (1.3%)*	**0.18 (1.0%)** *0.17 (0.9%)*	**0.27 (1.1%)** *0.32 (1.3%)*	**0.32 (1.2%)** *0.34 (1.3%)*	**0.22 (0.8%)** *0.17 (0.6%)*	**0.23 (0.7%)** *0.12 (0.3%)*	**2.55 (10.2%)** *2.61 (10.5%)*
ROAD	**1.44 (5.8%)** *1.50 (6.1%)*	**0.93 (5.0%)** *0.97 (5.2%)*	**1.27 (5.2%)** *1.55 (6.4%)*	**2.05 (7.7%)** *2.17 (8.2%)*	**0.75 (2.7%)** *0.78 (2.8%)*	**0.42 (1.2%)** *0.35 (1.0%)*	**0.36 (1.4%)** *0.44 (1.7%)*
OTT	**0.10 (0.4%)** *0.03 (0.1%)*	**0.10 (0.5%)** *0.03 (0.1%)*	**0.12 (0.5%)** *0.03 (0.1%)*	**0.11 (0.4%)** *0.04 (0.1%)*	**0.08 (0.3%)** *0.01 (0.0%)*	**0.13 (0.4%)** *0.00 (0.0%)*	**0.07 (0.3%)** *0.01 (0.0%)*
OTA	**0.69 (2.8%)** *0.40 (1.6%)*	**0.58 (3.1%)** *0.29 (1.6%)*	**0.88 (3.6%)** *0.78 (3.2%)*	**0.89 (3.3%)** *0.63 (2.4%)*	**0.50 (1.8%)** *0.19 (0.7%)*	**0.37 (1.0%)** *0.06 (0.2%)*	**0.69 (2.8%)** *0.33 (1.3%)*
OTH	**8.96 (36.2%)** *9.06 (36.6%)*	**9.11 (48.7%)** *9.44 (50.5%)*	**8.98 (37.1%)** *8.50 (35.1%)*	**8.40 (31.6%)** *8.31 (31.3%)*	**12.96 (46.5%)** *13.50 (48.5%)*	**22.34 (62.7%)** *23.05 (64.7%)*	**9.95 (39.8%)** *10.29 (41.2%)*
SOA	4.56 (18.4%)	4.17 (22.3%)	4.84 (20.0%)	4.84 (18.2%)	6.96 (25.0%)	7.95 (22.3%)	6.77 (27.1%)
Total	**24.74**	**18.72**	**24.20**	**26.54**	**27.85**	**35.63**	**24.98**

	PH	MHS	NAN	TAK	KK	SB-NPL	SB-M
OBB	**3.51 (15.4%)** *3.56 (15.6%)*	**2.88 (12.5%)** *2.76 (12.0%)*	**4.32 (18.4%)** *4.38 (18.6%)*	**1.00 (5.0%)** *0.97 (4.9%)*	**1.36 (6.8%)** *1.43 (7.1%)*	**0.68 (3.0%)** *0.65 (2.9%)*	**0.72 (3.3%)** *0.68 (3.1%)*
RES	**0.76 (3.4%)** *0.72 (3.2%)*	**0.37 (1.6%)** *0.30 (1.3%)*	**0.42 (1.8%)** *0.33 (1.4%)*	**0.48 (2.4%)** *0.45 (2.3%)*	**1.16 (5.7%)** *1.14 (5.7%)*	**1.30 (5.8%)** *1.26 (5.6%)*	**1.12 (5.1%)** *1.06 (4.8%)*
IND	**1.20 (5.3%)** *1.18 (5.2%)*	**0.32 (1.4%)** *0.29 (1.3%)*	**0.70 (3.0%)** *0.63 (2.7%)*	**0.55 (2.8%)** *0.57 (2.9%)*	**1.98 (9.8%)** *2.04 (10.1%)*	**6.23 (27.6%)** *6.51 (28.8%)*	**6.24 (28.3%)** *6.51 (29.5%)*
POW	**0.20 (0.9%)** *0.15 (0.7%)*	**0.15 (0.7%)** *0.12 (0.5%)*	**0.28 (1.2%)** *0.25 (1.1%)*	**0.11 (0.6%)** *0.07 (0.4%)*	**0.17 (0.8%)** *0.14 (0.7%)*	**0.22 (1.0%)** *0.21 (0.9%)*	**0.21 (1.0%)** *0.20 (0.9%)*
ROAD	**0.57 (2.5%)** *0.68 (3.0%)*	**0.39 (1.7%)** *0.37 (1.6%)*	**0.29 (1.2%)** *0.27 (1.2%)*	**0.39 (2.0%)** *0.47 (2.4%)*	**1.12 (5.6%)** *1.38 (6.8%)*	**0.63 (2.8%)** *0.75 (3.3%)*	**0.52 (2.4%)** *0.58 (2.6%)*
OTT	**0.08 (0.3%)** *0.01 (0.0%)*	**0.05 (0.2%)** *0.00 (0.0%)*	**0.08 (0.3%)** *0.00 (0.0%)*	**0.06 (0.3%)** *0.00 (0.0%)*	**0.09 (0.4%)** *0.01 (0.1%)*	**0.09 (0.4%)** *0.02 (0.1%)*	**0.08 (0.3%)** *0.02 (0.1%)*
OTA	**0.67 (3.0%)** *0.29 (1.3%)*	**0.29 (1.3%)** *0.07 (0.3%)*	**0.38 (1.6%)** *0.09 (0.4%)*	**0.55 (2.8%)** *0.19 (1.0%)*	**0.90 (4.5%)** *0.61 (3.0%)*	**0.91 (4.0%)** *0.53 (2.3%)*	**0.83 (3.8%)** *0.36 (1.6%)*
OTH	**9.46 (41.6%)** *9.87 (43.4%)*	**12.47 (54.3%)** *13.01 (56.6%)*	**10.47 (44.5%)** *10.97 (46.6%)*	**11.61 (58.7%)** *12.02 (60.8%)*	**9.03 (44.8%)** *9.03 (44.8%)*	**8.16 (36.1%)** *8.30 (36.7%)*	**7.98 (36.2%)** *8.29 (37.6%)*
SOA	6.28 (27.6%)	6.05 (26.3%)	6.59 (28.0%)	5.01 (25.4%)	4.36 (21.6%)	4.37 (19.4%)	4.33 (19.7%)
Total	**22.73**	**22.98**	**23.52**	**19.76**	**20.17**	**22.60**	**22.03**

Table A.2: Comparison of source contributions to $PM_{2.5}$ EC in each target receptor area. The values are shown as concentration in $\mu g/m^3$ with the percentage contribution in parentheses. For each cell, the top value represents the ISAM result (**bold**) and the bottom value represents the BFM result (*italic*).

	BKK	SMP	SMS	PT	CM	CR	LP
OBB	**0.02 (1.1%)**	**0.02 (1.6%)**	**0.03 (1.5%)**	**0.04 (1.5%)**	**0.25 (19.4%)**	**0.14 (8.7%)**	**0.15 (16.8%)**
	0.02 (1.1%)	*0.02 (1.6%)*	*0.03 (1.5%)*	*0.04 (1.4%)*	*0.25 (19.3%)*	*0.14 (8.6%)*	*0.15 (16.8%)*
RES	**0.54 (26.7%)**	**0.21 (15.8%)**	**0.59 (32.4%)**	**0.68 (28.1%)**	**0.10 (7.3%)**	**0.10 (6.4%)**	**0.10 (11.6%)**
	0.55 (27.0%)	*0.21 (15.9%)*	*0.60 (32.7%)*	*0.69 (28.3%)*	*0.10 (7.3%)*	*0.11 (6.7%)*	*0.10 (11.6%)*
IND	**0.33 (16.2%)**	**0.12 (9.1%)**	**0.24 (12.9%)**	**0.34 (13.9%)**	**0.06 (4.6%)**	**0.03 (1.9%)**	**0.05 (5.2%)**
	0.33 (16.3%)	*0.12 (8.9%)*	*0.23 (12.8%)*	*0.34 (13.9%)*	*0.06 (4.5%)*	*0.03 (1.8%)*	*0.05 (5.1%)*
POW	**0.01 (0.3%)**	**0.00 (0.1%)**	**0.00 (0.1%)**	**0.00 (0.2%)**	**0.00 (0.1%)**	**0.00 (0.1%)**	**0.04 (4.3%)**
	0.01 (0.3%)	*0.00 (0.2%)*	*0.00 (0.1%)*	*0.00 (0.2%)*	*0.00 (0.1%)*	*0.00 (0.1%)*	*0.04 (4.7%)*
ROAD	**0.67 (32.9%)**	**0.45 (34.2%)**	**0.54 (29.5%)**	**0.98 (40.2%)**	**0.28 (21.5%)**	**0.11 (6.5%)**	**0.12 (13.2%)**
	0.68 (33.3%)	*0.46 (34.9%)*	*0.54 (29.7%)*	*0.99 (40.6%)*	*0.28 (21.9%)*	*0.11 (6.6%)*	*0.12 (13.1%)*
OTT	**0.01 (0.3%)**	**0.01 (0.6%)**	**0.01 (0.3%)**	**0.01 (0.3%)**	**0.00 (0.1%)**	**0.00 (0.1%)**	**0.00 (0.1%)**
	0.01 (0.3%)	*0.01 (0.6%)*	*0.01 (0.3%)*	*0.01 (0.3%)*	*0.00 (0.1%)*	*0.00 (0.1%)*	*0.00 (0.1%)*
OTA	**0.00 (0.0%)**	**0.00 (0.0%)**	**0.00 (0.0%)**	**0.00 (0.0%)**	**0.00 (0.0%)**	**0.00 (0.0%)**	**0.00 (0.0%)**
	0.00 (0.0%)	*0.00 (0.0%)*	*0.00 (0.0%)*	*0.00 (0.0%)*	*0.00 (0.0%)*	*0.00 (0.0%)*	*0.00 (0.0%)*
OTH	**0.46 (22.5%)**	**0.51 (38.6%)**	**0.43 (23.4%)**	**0.38 (15.8%)**	**0.61 (47.0%)**	**1.24 (76.3%)**	**0.44 (48.8%)**
	0.44 (21.8%)	*0.50 (38.0%)*	*0.42 (22.8%)*	*0.37 (15.3%)*	*0.61 (46.7%)*	*1.23 (76.1%)*	*0.44 (48.6%)*
Total	**2.03**	**1.32**	**1.83**	**2.43**	**1.30**	**1.62**	**0.90**

	PH	MHS	NAN	TAK	KK	SB-NPL	SB-M
OBB	**0.19 (18.7%)**	**0.15 (15.8%)**	**0.24 (26.8%)**	**0.05 (6.2%)**	**0.08 (6.4%)**	**0.04 (3.5%)**	**0.04 (4.0%)**
	0.19 (18.7%)	*0.15 (15.6%)*	*0.23 (26.7%)*	*0.05 (5.8%)*	*0.08 (6.4%)*	*0.04 (3.6%)*	*0.05 (4.0%)*
RES	**0.12 (11.6%)**	**0.04 (4.6%)**	**0.05 (5.9%)**	**0.07 (7.8%)**	**0.19 (14.9%)**	**0.21 (17.5%)**	**0.18 (16.0%)**
	0.12 (11.6%)	*0.04 (4.7%)*	*0.05 (5.8%)*	*0.07 (8.0%)*	*0.18 (14.8%)*	*0.21 (17.4%)*	*0.18 (15.9%)*
IND	**0.06 (5.6%)**	**0.01 (1.2%)**	**0.03 (3.0%)**	**0.02 (2.6%)**	**0.10 (8.1%)**	**0.32 (26.8%)**	**0.32 (29.0%)**
	0.06 (5.6%)	*0.01 (1.1%)*	*0.03 (2.9%)*	*0.02 (2.5%)*	*0.10 (7.8%)*	*0.34 (28.1%)*	*0.34 (30.1%)*
POW	**0.00 (0.2%)**	**0.00 (0.1%)**	**0.00 (0.3%)**	**0.00 (0.1%)**	**0.00 (0.1%)**	**0.00 (0.1%)**	**0.00 (0.1%)**
	0.00 (0.1%)	*0.00 (0.1%)*	*0.00 (0.3%)*	*0.00 (0.1%)*	*0.00 (0.1%)*	*0.00 (0.2%)*	*0.00 (0.2%)*
ROAD	**0.23 (22.2%)**	**0.17 (18.3%)**	**0.09 (9.8%)**	**0.15 (17.2%)**	**0.44 (35.6%)**	**0.25 (20.9%)**	**0.20 (18.1%)**
	0.23 (22.6%)	*0.18 (18.7%)*	*0.09 (9.8%)*	*0.16 (18.2%)*	*0.46 (36.8%)*	*0.25 (20.9%)*	*0.20 (18.0%)*
OTT	**0.00 (0.2%)**	**0.00 (0.1%)**	**0.00 (0.1%)**	**0.00 (0.1%)**	**0.00 (0.2%)**	**0.00 (0.2%)**	**0.00 (0.2%)**
	0.00 (0.2%)	*0.00 (0.1%)*	*0.00 (0.1%)*	*0.00 (0.1%)*	*0.00 (0.2%)*	*0.00 (0.2%)*	*0.00 (0.2%)*
OTA	**0.00 (0.0%)**	**0.00 (0.0%)**	**0.00 (0.0%)**	**0.00 (0.0%)**	**0.00 (0.0%)**	**0.00 (0.0%)**	**0.00 (0.0%)**
	0.00 (0.0%)	*0.00 (0.0%)*	*0.00 (0.0%)*	*0.00 (0.0%)*	*0.00 (0.0%)*	*0.00 (0.0%)*	*0.00 (0.0%)*
OTH	**0.43 (41.5%)**	**0.57 (60.0%)**	**0.47 (54.1%)**	**0.58 (66.1%)**	**0.43 (34.7%)**	**0.37 (30.9%)**	**0.36 (32.5%)**
	0.42 (41.2%)	*0.57 (59.7%)*	*0.48 (54.4%)*	*0.57 (65.3%)*	*0.42 (33.8%)*	*0.36 (29.7%)*	*0.35 (31.6%)*
Total	**1.03**	**0.96**	**0.88**	**0.88**	**1.24**	**1.20**	**1.12**

Table A.3: Comparison of source contributions to $PM_{2.5}$ POC in each target receptor area. The values are shown as concentration in $\mu g/m^3$ with the percentage contribution in parentheses. For each cell, the top value represents the ISAM result (**bold**) and the bottom value represents the BFM result (*italic*).

	BKK	SMP	SMS	PT	CM	CR	LP
OBB	**0.16 (2.7%)** *0.16 (2.7%)*	**0.15 (4.3%)** *0.15 (4.3%)*	**0.21 (3.8%)** *0.20 (3.8%)*	**0.26 (4.2%)** *0.26 (4.2%)*	**2.52 (34.8%)** *2.52 (34.7%)*	**1.38 (12.8%)** *1.37 (12.7%)*	**1.65 (37.0%)** *1.66 (37.1%)*
RES	**1.63 (28.2%)** *1.66 (28.7%)*	**0.62 (17.3%)** *0.64 (17.6%)*	**1.78 (33.1%)** *1.83 (33.9%)*	**2.06 (33.3%)** *2.08 (33.8%)*	**0.28 (3.9%)** *0.29 (3.9%)*	**0.32 (3.0%)** *0.35 (3.2%)*	**0.31 (7.0%)** *0.32 (7.1%)*
IND	**1.63 (28.2%)** *1.66 (28.7%)*	**0.59 (16.4%)** *0.59 (16.5%)*	**1.12 (20.8%)** *1.13 (20.9%)*	**1.57 (25.5%)** *1.59 (25.7%)*	**0.29 (4.1%)** *0.30 (4.1%)*	**0.15 (1.4%)** *0.15 (1.3%)*	**0.23 (5.1%)** *0.23 (5.1%)*
POW	**0.01 (0.2%)** *0.01 (0.2%)*	**0.00 (0.1%)** *0.00 (0.1%)*	**0.01 (0.1%)** *0.01 (0.1%)*	**0.01 (0.2%)** *0.01 (0.2%)*	**0.00 (0.0%)** *0.00 (0.0%)*	**0.00 (0.0%)** *0.00 (0.0%)*	**0.00 (0.0%)** *0.00 (0.0%)*
ROAD	**0.30 (5.2%)** *0.30 (5.2%)*	**0.18 (5.0%)** *0.19 (5.1%)*	**0.23 (4.2%)** *0.23 (4.3%)*	**0.43 (7.0%)** *0.44 (7.1%)*	**0.14 (1.9%)** *0.15 (2.1%)*	**0.06 (0.5%)** *0.06 (0.6%)*	**0.05 (1.0%)** *0.05 (1.0%)*
OTT	**0.00 (0.1%)** *0.00 (0.1%)*	**0.01 (0.2%)** *0.01 (0.2%)*	**0.00 (0.1%)** *0.00 (0.1%)*	**0.00 (0.1%)** *0.00 (0.1%)*	**0.00 (0.0%)** *0.00 (0.0%)*	**0.00 (0.0%)** *0.00 (0.0%)*	**0.00 (0.0%)** *0.00 (0.0%)*
OTA	**0.00 (0.0%)** *0.00 (0.0%)*	**0.00 (0.0%)** *0.00 (0.0%)*	**0.00 (0.0%)** *0.00 (0.0%)*	**0.00 (0.0%)** *0.00 (0.0%)*	**0.00 (0.0%)** *0.00 (0.0%)*	**0.00 (0.0%)** *0.00 (0.0%)*	**0.00 (0.0%)** *0.00 (0.0%)*
OTH	**2.04 (35.4%)** *1.98 (34.3%)*	**2.05 (56.7%)** *2.03 (56.2%)*	**2.04 (37.8%)** *1.98 (36.8%)*	**1.84 (29.8%)** *1.79 (28.9%)*	**4.01 (55.3%)** *4.00 (55.1%)*	**8.86 (82.3%)** *8.85 (82.1%)*	**2.22 (49.8%)** *2.22 (49.6%)*
Total	**5.77**	**3.61**	**5.38**	**6.17**	**7.25**	**10.77**	**4.47**

	PH	MHS	NAN	TAK	KK	SB-NPL	SB-M
OBB	**2.00 (42.1%)** *2.01 (42.4%)*	**1.60 (28.2%)** *1.58 (27.8%)*	**2.35 (43.1%)** *2.35 (43.1%)*	**0.51 (14.3%)** *0.50 (14.0%)*	**0.66 (17.1%)** *0.67 (17.3%)*	**0.30 (8.5%)** *0.31 (8.7%)*	**0.33 (10.1%)** *0.34 (10.3%)*
RES	**0.35 (7.5%)** *0.36 (7.5%)*	**0.16 (2.8%)** *0.16 (2.9%)*	**0.16 (2.9%)** *0.16 (2.9%)*	**0.21 (5.8%)** *0.22 (6.2%)*	**0.55 (14.2%)** *0.55 (14.2%)*	**0.63 (18.0%)** *0.63 (17.9%)*	**0.54 (16.2%)** *0.54 (16.2%)*
IND	**0.29 (6.1%)** *0.29 (6.1%)*	**0.05 (1.0%)** *0.05 (0.9%)*	**0.13 (2.4%)** *0.13 (2.3%)*	**0.11 (3.1%)** *0.11 (3.1%)*	**0.46 (12.0%)** *0.46 (12.0%)*	**0.80 (22.9%)** *0.81 (23.2%)*	**0.70 (21.1%)** *0.71 (21.2%)*
POW	**0.00 (0.0%)** *0.00 (0.0%)*	**0.00 (0.0%)** *0.00 (0.0%)*	**0.00 (0.0%)** *0.00 (0.0%)*	**0.00 (0.0%)** *0.00 (0.0%)*	**0.00 (0.1%)** *0.00 (0.1%)*	**0.01 (0.1%)** *0.01 (0.2%)*	**0.00 (0.1%)** *0.01 (0.2%)*
ROAD	**0.09 (1.9%)** *0.09 (2.0%)*	**0.07 (1.2%)** *0.07 (1.2%)*	**0.03 (0.6%)** *0.03 (0.6%)*	**0.06 (1.7%)** *0.07 (1.8%)*	**0.21 (5.4%)** *0.23 (5.9%)*	**0.10 (2.9%)** *0.10 (2.8%)*	**0.08 (2.5%)** *0.08 (2.4%)*
OTT	**0.00 (0.0%)** *0.00 (0.0%)*	**0.00 (0.0%)** *0.00 (0.0%)*	**0.00 (0.0%)** *0.00 (0.0%)*	**0.00 (0.0%)** *0.00 (0.0%)*	**0.00 (0.0%)** *0.00 (0.0%)*	**0.00 (0.0%)** *0.00 (0.0%)*	**0.00 (0.0%)** *0.00 (0.0%)*
OTA	**0.00 (0.0%)** *0.00 (0.0%)*	**0.00 (0.0%)** *0.00 (0.0%)*	**0.00 (0.0%)** *0.00 (0.0%)*	**0.00 (0.0%)** *0.00 (0.0%)*	**0.00 (0.0%)** *0.00 (0.0%)*	**0.00 (0.0%)** *0.00 (0.0%)*	**0.00 (0.0%)** *0.00 (0.0%)*
OTH	**2.01 (42.4%)** *1.99 (41.9%)*	**3.81 (66.9%)** *3.82 (67.1%)*	**2.78 (51.0%)** *2.78 (51.0%)*	**2.70 (75.0%)** *2.69 (74.9%)*	**1.97 (51.1%)** *1.94 (50.4%)*	**1.66 (47.4%)** *1.65 (47.1%)*	**1.66 (50.0%)** *1.65 (49.6%)*
Total	**4.75**	**5.70**	**5.46**	**3.60**	**3.86**	**3.51**	**3.33**

Table A.4: Comparison of source contributions to $PM_{2.5}$ NH_4^+ in each target receptor area. The values are shown as concentration in $\mu g/m^3$ with the percentage contribution in parentheses. For each cell, the top value represents the ISAM result (**bold**) and the bottom value represents the BFM result (*italic*).

	BKK	SMP	SMS	PT	CM	CR	LP
OBB	**0.01 (0.5%)** *0.00 (0.1%)*	**0.01 (0.8%)** *0.00 (-0.1%)*	**0.01 (0.7%)** *0.01 (0.5%)*	**0.01 (1.0%)** *0.00 (0.1%)*	**0.12 (9.6%)** *-0.04 (-3.3%)*	**0.06 (4.9%)** *0.02 (1.5%)*	**0.08 (5.6%)** *-0.02 (-1.7%)*
RES	**0.10 (8.1%)** *0.09 (6.7%)*	**0.04 (3.8%)** *0.04 (3.6%)*	**0.11 (7.7%)** *0.13 (9.3%)*	**0.11 (8.0%)** *0.11 (8.0%)*	**0.03 (2.2%)** *0.02 (1.8%)*	**0.03 (2.4%)** *0.02 (1.6%)*	**0.03 (2.0%)** *0.03 (2.2%)*
IND	**0.15 (11.8%)** *0.20 (16.0%)*	**0.06 (5.5%)** *0.10 (9.3%)*	**0.11 (7.6%)** *0.22 (15.8%)*	**0.13 (9.3%)** *0.27 (18.9%)*	**0.05 (3.6%)** *0.08 (6.0%)*	**0.02 (1.6%)** *0.06 (4.4%)*	**0.03 (2.1%)** *0.08 (5.7%)*
POW	**0.04 (3.2%)** *0.05 (4.2%)*	**0.02 (1.6%)** *0.03 (2.6%)*	**0.03 (1.9%)** *0.06 (4.3%)*	**0.04 (2.5%)** *0.06 (4.3%)*	**0.01 (0.9%)** *0.02 (1.7%)*	**0.01 (0.5%)** *0.02 (1.2%)*	**0.04 (2.7%)** *0.07 (5.3%)*
ROAD	**0.02 (1.6%)** *0.07 (5.4%)*	**0.01 (1.2%)** *0.05 (4.2%)*	**0.01 (1.1%)** *0.14 (9.7%)*	**0.03 (1.8%)** *0.10 (7.1%)*	**0.02 (1.5%)** *0.04 (3.3%)*	**0.01 (0.5%)** *0.02 (1.7%)*	**0.00 (0.3%)** *0.04 (3.0%)*
OTT	**0.00 (0.0%)** *0.00 (0.3%)*	**0.00 (0.0%)** *0.00 (0.1%)*	**0.00 (0.0%)** *0.00 (0.3%)*	**0.00 (0.0%)** *0.00 (0.3%)*	**0.00 (0.0%)** *0.00 (0.1%)*	**0.00 (0.0%)** *0.00 (0.0%)*	**0.00 (0.0%)** *0.00 (0.1%)*
OTA	**0.64 (50.2%)** *0.10 (7.5%)*	**0.54 (49.2%)** *0.08 (7.1%)*	**0.82 (58.8%)** *0.19 (13.3%)*	**0.85 (60.3%)** *0.15 (10.8%)*	**0.44 (35.0%)** *0.06 (5.0%)*	**0.26 (20.5%)** *0.03 (2.0%)*	**0.64 (46.2%)** *0.12 (8.5%)*
OTH	**0.31 (24.6%)** *0.76 (59.9%)*	**0.41 (38.0%)** *0.80 (73.2%)*	**0.31 (22.2%)** *0.65 (46.9%)*	**0.24 (17.2%)** *0.71 (50.4%)*	**0.60 (47.1%)** *1.08 (85.4%)*	**0.89 (69.6%)** *1.12 (87.5%)*	**0.57 (41.1%)** *1.08 (77.1%)*
Total	**1.28**	**1.09**	**1.39**	**1.40**	**1.27**	**1.29**	**1.39**

	PH	MHS	NAN	TAK	KK	SB-NPL	SB-M
OBB	**0.09 (6.7%)** *-0.03 (-2.4%)*	**0.08 (7.2%)** *-0.03 (-3.0%)*	**0.12 (10.5%)** *-0.02 (-1.8%)*	**0.02 (1.6%)** *0.00 (-0.2%)*	**0.03 (1.9%)** *0.00 (0.3%)*	**0.02 (1.4%)** *0.00 (-0.2%)*	**0.02 (1.7%)** *-0.01 (-0.6%)*
RES	**0.03 (2.3%)** *0.03 (2.4%)*	**0.03 (2.3%)** *0.01 (0.9%)*	**0.02 (1.6%)** *0.01 (1.3%)*	**0.02 (1.2%)** *0.02 (1.4%)*	**0.03 (1.9%)** *0.06 (4.4%)*	**0.04 (2.8%)** *0.06 (4.1%)*	**0.03 (2.6%)** *0.04 (3.4%)*
IND	**0.03 (2.6%)** *0.09 (6.6%)*	**0.01 (1.1%)** *0.03 (2.8%)*	**0.02 (1.6%)** *0.06 (5.3%)*	**0.01 (0.8%)** *0.06 (4.0%)*	**0.04 (2.7%)** *0.15 (11.0%)*	**0.09 (6.6%)** *0.29 (21.3%)*	**0.08 (6.6%)** *0.27 (21.6%)*
POW	**0.01 (0.7%)** *0.02 (1.5%)*	**0.00 (0.4%)** *0.01 (1.2%)*	**0.01 (0.7%)** *0.03 (2.5%)*	**0.00 (0.3%)** *0.01 (0.7%)*	**0.01 (0.7%)** *0.03 (2.0%)*	**0.02 (1.5%)** *0.04 (2.8%)*	**0.02 (1.7%)** *0.04 (2.9%)*
ROAD	**0.01 (0.6%)** *0.05 (3.9%)*	**0.00 (0.3%)** *0.02 (1.7%)*	**0.00 (0.3%)** *0.02 (1.6%)*	**0.00 (0.3%)** *0.04 (2.7%)*	**0.01 (1.0%)** *0.11 (8.0%)*	**0.01 (0.4%)** *0.07 (4.8%)*	**0.00 (0.4%)** *0.05 (3.7%)*
OTT	**0.00 (0.0%)** *0.00 (0.1%)*	**0.00 (0.0%)** *0.00 (0.0%)*	**0.00 (0.0%)** *0.00 (0.0%)*	**0.00 (0.0%)** *0.00 (0.0%)*	**0.00 (0.0%)** *0.00 (0.1%)*	**0.00 (0.0%)** *0.00 (0.2%)*	**0.00 (0.0%)** *0.00 (0.2%)*
OTA	**0.63 (47.4%)** *0.09 (6.6%)*	**0.25 (21.7%)** *0.04 (3.8%)*	**0.32 (28.4%)** *0.05 (4.5%)*	**0.51 (34.6%)** *0.06 (4.0%)*	**0.88 (65.3%)** *0.16 (12.2%)*	**0.89 (65.7%)** *0.15 (11.2%)*	**0.82 (64.3%)** *0.11 (8.6%)*
OTH	**0.53 (39.7%)** *1.08 (81.4%)*	**0.77 (67.0%)** *1.06 (92.5%)*	**0.65 (56.8%)** *0.99 (86.5%)*	**0.91 (61.3%)** *1.29 (87.5%)*	**0.36 (26.5%)** *0.83 (62.0%)*	**0.29 (21.5%)** *0.76 (55.7%)*	**0.29 (22.7%)** *0.77 (60.2%)*
Total	**1.33**	**1.14**	**1.14**	**1.48**	**1.34**	**1.36**	**1.27**

Table A.5: Comparison of source contributions to $PM_{2.5}$ NO_3^- in each target receptor area. The values are shown as concentration in $\mu g/m^3$ with the percentage contribution in parentheses. For each cell, the top value represents the ISAM result (**bold**) and the bottom value represents the BFM result (*italic*).

	BKK	SMP	SMS	PT	CM	CR	LP
OBB	**0.02 (4.3%)** *0.02 (4.6%)*	**0.01 (4.6%)** *0.02 (5.5%)*	**0.04 (5.0%)** *0.05 (5.2%)*	**0.03 (4.8%)** *0.04 (5.3%)*	**0.07 (14.1%)** *0.16 (33.0%)*	**0.10 (9.0%)** *0.22 (19.9%)*	**0.03 (8.5%)** *0.07 (21.7%)*
RES	**0.08 (16.7%)** *0.12 (23.5%)*	**0.04 (14.0%)** *0.06 (18.4%)*	**0.16 (18.3%)** *0.24 (27.6%)*	**0.12 (16.8%)** *0.15 (21.7%)*	**0.04 (7.7%)** *0.03 (6.5%)*	**0.07 (6.3%)** *0.02 (2.0%)*	**0.03 (9.5%)** *0.05 (14.7%)*
IND	**0.06 (11.8%)** *0.16 (32.8%)*	**0.03 (9.1%)** *0.06 (20.9%)*	**0.10 (10.9%)** *0.22 (24.7%)*	**0.09 (12.9%)** *0.23 (32.8%)*	**0.03 (6.4%)** *0.02 (5.0%)*	**0.06 (5.7%)** *0.00 (-0.2%)*	**0.02 (6.8%)** *0.03 (9.2%)*
POW	**0.05 (9.8%)** *0.08 (15.4%)*	**0.03 (8.3%)** *0.04 (12.9%)*	**0.07 (8.2%)** *0.12 (13.3%)*	**0.06 (8.1%)** *0.09 (13.0%)*	**0.03 (5.6%)** *0.02 (3.1%)*	**0.06 (5.6%)** *0.01 (0.7%)*	**0.04 (12.6%)** *0.05 (15.4%)*
ROAD	**0.12 (25.3%)** *0.19 (37.9%)*	**0.08 (25.7%)** *0.12 (39.2%)*	**0.21 (24.5%)** *0.40 (46.1%)*	**0.19 (27.1%)** *0.25 (35.6%)*	**0.06 (13.1%)** *0.09 (19.0%)*	**0.08 (7.0%)** *0.04 (4.0%)*	**0.04 (13.6%)** *0.10 (32.0%)*
OTT	**0.03 (5.1%)** *0.01 (1.3%)*	**0.02 (7.2%)** *0.00 (-0.9%)*	**0.04 (5.0%)** *0.01 (1.3%)*	**0.03 (4.6%)** *0.01 (1.3%)*	**0.02 (4.5%)** *0.00 (0.2%)*	**0.06 (5.1%)** *0.00 (0.0%)*	**0.01 (3.9%)** *0.00 (0.4%)*
OTA	**0.02 (3.2%)** *0.30 (61.0%)*	**0.01 (3.3%)** *0.21 (70.0%)*	**0.03 (3.4%)** *0.60 (68.7%)*	**0.02 (3.1%)** *0.48 (67.4%)*	**0.02 (4.3%)** *0.12 (24.3%)*	**0.06 (5.1%)** *0.04 (3.3%)*	**0.01 (3.6%)** *0.19 (61.5%)*
OTH	**0.12 (23.9%)** *-0.38 (-76.5%)*	**0.08 (27.8%)** *-0.20 (-65.9%)*	**0.21 (24.6%)** *-0.76 (-86.8%)*	**0.16 (22.5%)** *-0.55 (-77.1%)*	**0.22 (44.2%)** *0.04 (9.0%)*	**0.63 (56.2%)** *0.78 (70.3%)*	**0.13 (41.5%)** *-0.17 (-54.9%)*
Total	**0.49**	**0.31**	**0.87**	**0.71**	**0.49**	**1.12**	**0.31**

	PH	MHS	NAN	TAK	KK	SB-NPL	SB-M
OBB	**0.04 (10.4%)** *0.10 (28.3%)*	**0.04 (19.4%)** *0.08 (41.2%)*	**0.06 (16.8%)** *0.17 (45.3%)*	**0.02 (6.5%)** *0.03 (10.8%)*	**0.04 (6.1%)** *0.09 (13.4%)*	**0.02 (5.3%)** *0.02 (5.5%)*	**0.02 (5.2%)** *0.02 (5.4%)*
RES	**0.03 (9.9%)** *0.05 (14.5%)*	**0.01 (4.6%)** *0.01 (3.0%)*	**0.02 (6.3%)** *0.01 (3.4%)*	**0.02 (8.1%)** *0.03 (10.0%)*	**0.08 (12.3%)** *0.11 (16.8%)*	**0.06 (12.7%)** *0.08 (19.0%)*	**0.03 (11.6%)** *0.05 (18.0%)*
IND	**0.02 (6.6%)** *0.03 (8.3%)*	**0.01 (4.3%)** *0.00 (1.6%)*	**0.02 (5.7%)** *-0.01 (-2.5%)*	**0.01 (4.6%)** *0.02 (6.0%)*	**0.05 (6.7%)** *0.07 (10.1%)*	**0.09 (20.5%)** *0.14 (32.6%)*	**0.07 (22.0%)** *0.12 (40.3%)*
POW	**0.02 (5.5%)** *0.02 (4.7%)*	**0.01 (4.2%)** *0.00 (1.3%)*	**0.02 (5.7%)** *0.01 (1.6%)*	**0.01 (4.0%)** *0.01 (2.9%)*	**0.03 (4.8%)** *0.03 (4.5%)*	**0.04 (8.1%)** *0.05 (11.1%)*	**0.03 (9.1%)** *0.04 (13.1%)*
ROAD	**0.06 (17.5%)** *0.14 (39.9%)*	**0.02 (9.9%)** *0.02 (10.3%)*	**0.03 (7.8%)** *0.03 (9.3%)*	**0.05 (17.7%)** *0.09 (33.2%)*	**0.15 (22.4%)** *0.31 (45.8%)*	**0.08 (17.7%)** *0.17 (38.3%)*	**0.05 (15.8%)** *0.11 (36.7%)*
OTT	**0.01 (4.1%)** *0.00 (0.4%)*	**0.01 (3.8%)** *0.00 (0.1%)*	**0.02 (4.8%)** *0.00 (0.1%)*	**0.01 (3.2%)** *0.00 (0.3%)*	**0.03 (3.8%)** *0.00 (0.5%)*	**0.02 (4.9%)** *0.01 (1.3%)*	**0.01 (4.9%)** *0.00 (1.6%)*
OTA	**0.01 (3.7%)** *0.20 (57.9%)*	**0.01 (3.7%)** *0.03 (16.2%)*	**0.02 (4.7%)** *0.04 (11.7%)*	**0.01 (3.0%)** *0.13 (46.3%)*	**0.02 (3.3%)** *0.45 (65.9%)*	**0.02 (3.6%)** *0.37 (82.5%)*	**0.01 (3.3%)** *0.24 (80.8%)*
OTH	**0.14 (42.4%)** *-0.18 (-54.1%)*	**0.09 (50.0%)** *0.05 (26.3%)*	**0.18 (48.2%)** *0.11 (31.0%)*	**0.15 (53.1%)** *-0.03 (-9.5%)*	**0.28 (40.7%)** *-0.39 (-56.8%)*	**0.12 (27.3%)** *-0.40 (-90.3%)*	**0.08 (28.0%)** *-0.29 (-95.9%)*
Total	**0.34**	**0.19**	**0.37**	**0.28**	**0.68**	**0.44**	**0.30**

Table A.6: Comparison of source contributions to $PM_{2.5}$ SO_4^{2-} in each target receptor area. The values are shown as concentration in $\mu g/m^3$ with the percentage contribution in parentheses. For each cell, the top value represents the ISAM result (**bold**) and the bottom value represents the BFM result (*italic*).

	BKK	SMP	SMS	PT	CM	CR	LP
OBB	**0.02 (0.5%)** *0.01 (0.2%)*	**0.02 (0.5%)** *0.01 (0.3%)*	**0.03 (0.6%)** *0.01 (0.3%)*	**0.03 (0.6%)** *0.01 (0.3%)*	**0.09 (2.1%)** *0.08 (1.9%)*	**0.06 (1.5%)** *0.06 (1.3%)*	**0.07 (1.5%)** *0.06 (1.3%)*
RES	**0.15 (3.4%)** *0.14 (3.0%)*	**0.07 (1.9%)** *0.06 (1.6%)*	**0.17 (4.0%)** *0.16 (3.6%)*	**0.19 (4.1%)** *0.18 (3.8%)*	**0.05 (1.1%)** *0.04 (0.9%)*	**0.05 (1.1%)** *0.04 (0.9%)*	**0.06 (1.2%)** *0.04 (1.0%)*
IND	**1.02 (22.6%)** *1.06 (23.5%)*	**0.45 (11.8%)** *0.45 (12.0%)*	**0.85 (19.6%)** *0.89 (20.5%)*	**1.16 (25.0%)** *1.21 (25.9%)*	**0.30 (7.2%)** *0.30 (7.1%)*	**0.22 (5.4%)** *0.22 (5.2%)*	**0.29 (6.1%)** *0.28 (5.9%)*
POW	**0.09 (2.1%)** *0.10 (2.1%)*	**0.05 (1.4%)** *0.05 (1.3%)*	**0.07 (1.6%)** *0.07 (1.7%)*	**0.09 (2.0%)** *0.10 (2.2%)*	**0.06 (1.5%)** *0.06 (1.4%)*	**0.05 (1.2%)** *0.05 (1.1%)*	**0.55 (11.7%)** *0.57 (12.1%)*
ROAD	**0.06 (1.3%)** *0.04 (0.9%)*	**0.04 (1.0%)** *0.03 (0.8%)*	**0.06 (1.3%)** *0.05 (1.2%)*	**0.07 (1.6%)** *0.07 (1.5%)*	**0.04 (1.0%)** *0.05 (1.1%)*	**0.03 (0.8%)** *0.03 (0.7%)*	**0.04 (0.8%)** *0.04 (0.8%)*
OTT	**0.02 (0.4%)** *0.00 (0.1%)*	**0.02 (0.4%)** *0.01 (0.2%)*	**0.02 (0.4%)** *0.00 (0.1%)*	**0.02 (0.4%)** *0.00 (0.1%)*	**0.01 (0.2%)** *0.00 (0.0%)*	**0.01 (0.2%)** *0.00 (0.0%)*	**0.01 (0.3%)** *0.00 (0.0%)*
OTA	**0.01 (0.2%)** *0.00 (0.1%)*	**0.01 (0.2%)** *0.01 (0.1%)*	**0.01 (0.3%)** *0.00 (0.0%)*	**0.01 (0.2%)** *0.00 (0.0%)*	**0.01 (0.2%)** *0.00 (0.1%)*	**0.01 (0.2%)** *0.00 (0.1%)*	**0.01 (0.3%)** *0.02 (0.4%)*
OTH	**3.13 (69.5%)** *3.16 (70.1%)*	**3.12 (82.7%)** *3.16 (83.7%)*	**3.12 (72.3%)** *3.13 (72.5%)*	**3.07 (66.0%)** *3.08 (66.1%)*	**3.62 (86.6%)** *3.66 (87.5%)*	**3.74 (89.5%)** *3.79 (90.6%)*	**3.67 (78.2%)** *3.68 (78.5%)*
Total	**4.51**	**3.78**	**4.32**	**4.65**	**4.18**	**4.18**	**4.69**

	PH	MHS	NAN	TAK	KK	SB-NPL	SB-M
OBB	**0.08 (1.9%)** *0.07 (1.7%)*	**0.05 (1.4%)** *0.04 (1.1%)*	**0.09 (2.5%)** *0.09 (2.4%)*	**0.04 (0.8%)** *0.03 (0.6%)*	**0.05 (1.2%)** *0.04 (1.0%)*	**0.03 (0.7%)** *0.02 (0.4%)*	**0.03 (0.6%)** *0.02 (0.4%)*
RES	**0.06 (1.4%)** *0.05 (1.1%)*	**0.03 (0.8%)** *0.02 (0.6%)*	**0.04 (1.0%)** *0.03 (0.8%)*	**0.04 (1.0%)** *0.03 (0.7%)*	**0.08 (2.0%)** *0.07 (1.7%)*	**0.10 (1.9%)** *0.08 (1.6%)*	**0.09 (1.8%)** *0.07 (1.5%)*
IND	**0.32 (7.6%)** *0.32 (7.6%)*	**0.11 (2.9%)** *0.11 (2.8%)*	**0.23 (6.2%)** *0.23 (6.1%)*	**0.18 (4.1%)** *0.18 (4.1%)*	**0.52 (13.1%)** *0.54 (13.4%)*	**1.59 (31.9%)** *1.63 (32.6%)*	**1.62 (32.9%)** *1.65 (33.6%)*
POW	**0.06 (1.4%)** *0.05 (1.2%)*	**0.05 (1.3%)** *0.05 (1.2%)*	**0.09 (2.4%)** *0.10 (2.5%)*	**0.03 (0.7%)** *0.02 (0.6%)*	**0.05 (1.3%)** *0.05 (1.3%)*	**0.07 (1.4%)** *0.07 (1.4%)*	**0.07 (1.5%)** *0.07 (1.5%)*
ROAD	**0.04 (0.8%)** *0.04 (0.9%)*	**0.04 (1.1%)** *0.04 (1.0%)*	**0.03 (0.8%)** *0.03 (0.7%)*	**0.03 (0.7%)** *0.04 (0.8%)*	**0.05 (1.3%)** *0.06 (1.4%)*	**0.04 (0.9%)** *0.05 (0.9%)*	**0.04 (0.8%)** *0.04 (0.8%)*
OTT	**0.01 (0.3%)** *0.00 (0.0%)*	**0.01 (0.2%)** *0.00 (0.0%)*	**0.01 (0.3%)** *0.00 (0.0%)*	**0.01 (0.3%)** *0.00 (0.0%)*	**0.01 (0.4%)** *0.00 (0.1%)*	**0.02 (0.3%)** *0.00 (0.1%)*	**0.02 (0.3%)** *0.00 (0.1%)*
OTA	**0.01 (0.3%)** *0.00 (0.0%)*	**0.01 (0.2%)** *0.00 (0.0%)*	**0.01 (0.3%)** *0.00 (0.0%)*	**0.01 (0.2%)** *0.00 (0.0%)*	**0.01 (0.3%)** *0.00 (0.1%)*	**0.01 (0.2%)** *0.01 (0.2%)*	**0.01 (0.2%)** *0.01 (0.2%)*
OTH	**3.61 (86.4%)** *3.65 (87.4%)*	**3.56 (92.1%)** *3.60 (93.3%)*	**3.28 (86.5%)** *3.32 (87.5%)*	**4.10 (92.2%)** *4.14 (93.1%)*	**3.22 (80.5%)** *3.25 (81.1%)*	**3.13 (62.7%)** *3.13 (62.7%)*	**3.03 (61.7%)** *3.04 (62.0%)*
Total	**4.18**	**3.86**	**3.79**	**4.45**	**4.00**	**5.00**	**4.91**

Table A.7: Source contributions from BFM to SOA in each target receptor area. The values are shown as concentration in $\mu g/m^3$ with the percentage contribution in parentheses.

	BKK	SMP	SMS	PT	CM	CR	LP
OBB	0.05 (1.0%)	0.04 (1.0%)	0.07 (1.4%)	0.07 (1.5%)	0.50 (7.1%)	0.41 (5.1%)	0.43 (6.3%)
RES	0.09 (2.0%)	0.05 (1.3%)	0.14 (2.9%)	0.14 (2.8%)	0.07 (1.0%)	0.08 (1.0%)	0.10 (1.5%)
IND	0.13 (2.9%)	0.08 (1.9%)	0.15 (3.0%)	0.16 (3.3%)	0.14 (2.0%)	0.14 (1.7%)	0.14 (2.0%)
POW	0.02 (0.4%)	0.01 (0.2%)	0.03 (0.7%)	0.03 (0.6%)	0.04 (0.6%)	0.04 (0.5%)	0.14 (2.1%)
ROAD	0.28 (6.1%)	0.15 (3.6%)	0.29 (5.9%)	0.33 (6.9%)	0.34 (4.8%)	0.18 (2.3%)	0.27 (4.1%)
OTT	0.00 (0.0%)	0.00 (0.0%)	0.00 (0.0%)	0.00 (0.1%)	0.00 (0.0%)	0.00 (0.0%)	0.00 (0.0%)
OTA	0.00 (0.1%)	-0.16 (-3.9%)	0.04 (0.9%)	-0.01 (-0.3%)	-0.41 (-5.8%)	-0.33 (-4.1%)	-0.49 (-7.2%)
OTH	3.99 (87.5%)	4.00 (95.9%)	4.12 (85.1%)	4.11 (85.1%)	6.28 (90.2%)	7.43 (93.5%)	6.16 (91.1%)
Total	**2.64**	**2.57**	**2.86**	**2.79**	**5.01**	**5.58**	**4.99**

	PH	MHS	NAN	TAK	KK	SB-NPL	SB-M
OBB	0.46 (7.4%)	0.24 (3.9%)	0.56 (8.4%)	0.14 (2.8%)	0.19 (4.3%)	0.09 (2.0%)	0.08 (2.0%)
RES	0.10 (1.5%)	0.02 (0.4%)	0.07 (1.0%)	0.06 (1.1%)	0.08 (1.9%)	0.09 (2.0%)	0.08 (1.9%)
IND	0.13 (2.1%)	0.11 (1.8%)	0.14 (2.1%)	0.09 (1.8%)	0.11 (2.5%)	0.18 (4.1%)	0.19 (4.3%)
POW	0.03 (0.5%)	0.06 (0.9%)	0.06 (1.0%)	0.02 (0.3%)	0.02 (0.5%)	0.02 (0.5%)	0.03 (0.6%)
ROAD	0.34 (5.4%)	0.20 (3.3%)	0.21 (3.2%)	0.21 (4.2%)	0.27 (6.3%)	0.24 (5.4%)	0.23 (5.3%)
OTT	0.00 (0.0%)	0.00 (0.0%)	0.00 (0.0%)	0.00 (0.0%)	0.00 (0.0%)	0.00 (0.0%)	0.00 (0.1%)
OTA	-0.41 (-6.5%)	-0.48 (-8.0%)	-0.41 (-6.2%)	-0.36 (-7.1%)	-0.19 (-4.3%)	-0.14 (-3.2%)	-0.16 (-3.8%)
OTH	5.62 (89.5%)	5.90 (97.6%)	5.96 (90.4%)	4.85 (96.8%)	3.87 (88.8%)	3.90 (89.2%)	3.88 (89.7%)
Total	**4.49**	**4.54**	**4.78**	**3.46**	**2.39**	**2.55**	**2.57**

Bibliography

[1] Ioannis Manisalidis, Elisavet Stavropoulou, Agathangelos Stavropoulos, and Eugenia Bezirtzoglou. **Environmental and Health Impacts of Air Pollution: A Review**. *Frontiers in Public Health* Volume 8 - 2020 (2020). ISSN: 2296-2565. DOI: 10.3389/fpubh.2020.00014 (see page 2).

[2] Getahun Mekuria. **Air Pollution: A Review of Its Impacts on Health and Ecosystems, and Analytical Techniques for Their Measurement and Modeling**. *Journal of Environmental Informatics Letters* 10 (2023), 115–131. DOI: 10.3808/jeil.202300116 (see page 2).

[3] Vivek Saxena. **Water Quality, Air Pollution, and Climate Change: Investigating the Environmental Impacts of Industrialization and Urbanization**. *Water, Air, & Soil Pollution* 236:2 (2025), 73. ISSN: 1573-2932. DOI: 10.1007/s11270-024-07702-4 (see page 2).

[4] Stephen Mosley, 143–169. In: *The Basic Environmental History*. Ed. by Mauro Agnoletti and Simone Neri Serneri. Cham: Springer International Publishing, 2014. ISBN: 978-3-319-09180-8. DOI: 10.1007/978-3-319-09180-8_5 (see page 2).

[5] Gillian Crane-Kramer and Jo Buckberry. **Changes in Health with the Rise of Industry**. *International Journal of Paleopathology* 40 (2023), 99–102. ISSN: 1879-9817. DOI: 10.1016/j.ijpp.2022.12.005 (see page 2).

[6] Xiaoyan Zhang, Lijian Han, Haiyan Wei, Xiaorui Tan, Weiqi Zhou, Weifen Li, and Yuguo Qian. **Linking Urbanization and Air Quality Together: A Review and a Perspective on the Future Sustainable Urban Development**. *Journal of Cleaner Production* 346 (2022), 130988. ISSN: 0959-6526. DOI: 10.1016/j.jclepro.2022.130988 (see page 2).

[7] Guangzhi Qi, Jiahang Che, and Zhibao Wang. **Differential Effects of Urbanization on Air Pollution: Evidences from Six Air Pollutants in Mainland China**. *Ecological Indicators* 146 (2023), 109924. ISSN: 1470-160X. DOI: 10.1016/j.ecolind.2023.109924 (see page 2).

[8] Johannes Lelieveld, John Evans, M Fnais, Despina Giannadaki, and Andrea Pozzer. **The Contribution of Outdoor Air Pollution Sources to Premature Mortality on a Global Scale**. *Nature* 525 (2015), 367–71. DOI: 10.1038/nature15371 (see page 2).

[9] Andrea Pozzer, Bettina Steffens, Yiannis Proestos, Sara Bacer, Aristeidis K. Georgoulias, Martin G. Schultz, and Jos Lelieveld. **Atmospheric Health Burden Across the Century and the Accelerating Impact of Temperature Compared to Pollution**. *Nature Communications* 15 (2024), 9379. DOI: 10.1038/s41467-024-53649-9 (see page 2).

[10] Raúl Ochoa-Hueso, Silvana Munzi, Rocío Alonso, María Arróniz-Crespo, Anna Avila, Victoria Bermejo, Roland Bobbink, Cristina Branquinho, Laura Concostrina-Zubiri, Cristina Cruz, Ricardo Cruz de Carvalho, Alessandra De Marco, Teresa Dias, David Elustondo, Susana Elvira, Belén Estébanez, Lina Fusaro, Giacomo Gerosa, Sheila Izquieta-Rojano, Mauro Lo Cascio, Riccardo Marzuoli, Paula Matos, Simone Mereu, José Merino, Lourdes Morillas, Alice Nunes, Elena Paoletti, Luca Paoli, Pedro Pinho, Isabel B. Rogers, Arthur Santos, Pierre Sicard, Carly J. Stevens, and Mark R. Theobald. **Ecological Impacts of Atmospheric Pollution and Interactions with Climate Change in Terrestrial Ecosystems of the Mediterranean Basin: Current Research and Future Directions**. *Environmental Pollution* 227 (2017), 194–206. ISSN: 0269-7491. DOI: 10.1016/j.envpol.2017.04.062 (see page 2).

[11] Alessandra De Marco, Chiara Proietti, Alessandro Anav, Luisella Ciancarella, Ilaria D'Elia, Silvano Fares, Maria Francesca Fornasier, Lina Fusaro, Maurizio Gualtieri, Fausto Manes, Aldo Marchetto, Mihaela Mircea, Elena Paoletti, Antonio Piersanti, Michela Rogora, Luca Salvati, Elisabetta Salvatori, Augusto Screpanti, Giovanni Vialetto, Marcello Vitale, and Cristina Leonardi. **Impacts of Air Pollution on Human and Ecosystem Health, and Implications for the National Emission Ceilings Directive: Insights from Italy**. *Environment International* 125 (2019), 320–333. ISSN: 0160-4120. DOI: 10.1016/j.envint.2019.01.064 (see page 2).

[12] T. Chen, Z. Li, R. A. Kahn, C. Zhao, D. Rosenfeld, J. Guo, W. Han, and D. Chen. **Potential Impact of Aerosols on Convective Clouds Revealed by Himawari-8 Observations over Different Terrain Types in Eastern China**. *Atmospheric Chemistry and Physics* 21:8 (2021), 6199–6220. DOI: 10.5194/acp-21-6199-2021 (see page 2).

[13] Friscilla Hermayurisca and Nutta Taneepanichskul. **Estimation of Premature Death Attributed to Short- and Long-term PM2.5 Exposure in Thailand**. *Environmental Monitoring and Assessment* 195 (2023), 1176. DOI: 10.1007/s10661-023-11807-4 (see page 2).

[14] Chul-Hee Lim, Jieun Ryu, Yuyoung Choi, Seong Woo Jeon, and Woo-Kyun Lee. **Understanding Global PM2.5 Concentrations and Their Drivers in Recent Decades (1998–2016)**. *Environment International* 144 (2020), 106011. ISSN: 0160-4120. DOI: 10.1016/j.envint.2020.106011 (see page 2).

[15] Jun Rentschler and Nina Leonova. **Global Air Pollution Exposure and Poverty**. *Nature Communications* 14 (2023), 4432. DOI: 10.1038/s41467-023-39797-4 (see page 2).

[16] World Health Organization. **WHO Global Air Quality Guidelines: Particulate Matter (PM2.5 and PM10), Ozone, Nitrogen Dioxide, Sulfur Dioxide and Carbon Monoxide**. World Health Organization, 2021, xxi, 273. URL: https://www.who.int/publications/i/item/9789240034228 (see page 2).

[17] Saurabh Sonwani and Anuradha Shukla. "Introduction to Airborne Particulate Matter: Source, Chemistry and Health." In: *Airborne Particulate Matter: Source, Chemistry and Health*. Ed. by Saurabh Sonwani and Anuradha Shukla. Singapore: Springer Nature Singapore, 2022, 1–7. ISBN: 978-981-16-5387-2. DOI: 10.1007/978-981-16-5387-2_1 (see page 2).

[18] M. Guevara. **Emissions of Primary Particulate Matter**. Ed. by R. M. Harrison, R. E. Hester, and Xavier Querol. The Royal Society of Chemistry, 2016. ISBN: 978-1-78262-491-2. DOI: 10.1039/9781782626589 (see pages 2, 3).

[19] United States Environmental Protection Agency (US EPA). *Particulate Matter (PM) Basics*. 2025. URL: https://www.epa.gov/pm-pollution/particulate-matter-pm-basics (see pages 2, 3).

[20] Kamonpan Fongsodsri, Supat Chamnanchanunt, Varunee Desakorn, Vipa Thanachartwet, Duangjai Sahassananda, Ponlapat Rojnuckarin, and Tsukuru Umemura. **Particulate Matter 2.5 and Hematological Disorders From Dust to Diseases: A Systematic Review of Available Evidence**. *Frontiers in Medicine* 8 (2021). ISSN: 2296-858X. DOI: 10.3389/fmed.2021.692008 (see pages 2, 4).

[21] Prakash Thangavel, Duckshin Park, and Young-Chul Lee. **Recent Insights into Particulate Matter (PM2.5)-Mediated Toxicity in Humans: An Overview**. *International Journal of Environmental Research and Public Health* 19:12 (2022). ISSN: 1660-4601. DOI: 10.3390/ijerph19127511 (see pages 2, 4).

[22] Wan Rozita Wan Mahiyuddin, Rohaida Ismail, Noraishah Mohammad Sham, Nurul Izzah Ahmad, and Nik Muhammad Nizam Nik Hassan. **Cardiovascular and Respiratory Health Effects of Fine Particulate Matters (PM2.5): A Review on Time Series Studies**. *Atmosphere* 14:5 (2023). ISSN: 2073-4433. DOI: 10.3390/atmos14050856 (see pages 2, 4).

[23] Saraswati. "Characterization of Primary and Secondary Airborne Particulates." In: *Airborne Particulate Matter: Source, Chemistry and Health*. Ed. by Saurabh Sonwani and Anuradha Shukla. Singapore: Springer Nature Singapore, 2022, 103–129. ISBN: 978-981-16-5387-2. DOI: 10.1007/978-981-16-5387-2_6 (see page 3).

[24] H. Andrew Gray and Glen R. Cass. **Source Contributions to Atmospheric Fine Carbon Particle Concentrations**. *Atmospheric Environment* 32:22 (1998), 3805–3825. ISSN: 1352-2310. DOI: 10.1016/S1352-2310(97)00446-9 (see page 3).

[25] Yamina Allouche, Marc Fadel, Amélie Ferté, Anthony Verdin, Frédéric Ledoux, and Dominique Courcot. **Phenomenology of the Composition of PM2.5 at an Urban Site in Northern France**. *Atmosphere* 15:5 (2024). ISSN: 2073-4433. DOI: 10.3390/atmos15050603 (see page 3).

[26] Deepika Bhattu. "Primary Organic Aerosols." In: *Air Pollution and Control*. Ed. by Nikhil Sharma, Avinash Kumar Agarwal, Peter Eastwood, Tarun Gupta, and Akhilendra P. Singh. Singapore: Springer Singapore, 2018, 109–117. ISBN: 978-981-10-7185-0. DOI: 10.1007/978-981-10-7185-0_7 (see page 3).

[27] Hélène Cachier, Marie-Pierre Brémond, and Patrick Buat-Ménard. **Carbonaceous Aerosols from Different Tropical Biomass Burning Sources**. *Nature* 340:6232 (1989), 371–373. ISSN: 1476-4687. DOI: 10.1038/340371a0 (see pages 3, 64).

[28] Hongmei Xu, Benjamin Guinot, Zhenxing Shen, Kin Fai Ho, Xinyi Niu, Shun Xiao, Ru-Jin Huang, and Junji Cao. **Characteristics of Organic and Elemental Carbon in PM2.5 and PM0.25 in Indoor and Outdoor Environments of a Middle School: Secondary Formation of Organic Carbon and Sources Identification**. *Atmosphere* 6:3 (2015), 361–379. ISSN: 2073-4433. DOI: 10.3390/atmos6030361 (see pages 3, 64).

[29] John G Watson, Judith C Chow, and James E Houck. **PM2.5 Chemical Source Profiles for Vehicle Exhaust, Vegetative Burning, Geological Material, and Coal Burning in Northwestern Colorado During 1995**. *Chemosphere* 43:8 (2001), 1141–1151. ISSN: 0045-6535. DOI: 10.1016/S0045-6535(00)00171-5 (see pages 3, 64).

[30] A. Samaké, A. Bonin, J.-L. Jaffrezo, P. Taberlet, S. Weber, G. Uzu, V. Jacob, S. Conil, and J. M. F. Martins. **High Levels of Primary Biogenic Organic Aerosols Are Driven by Only a Few Plant-Associated Microbial Taxa**. *Atmospheric Chemistry and Physics* 20:9 (2020), 5609–5628. DOI: 10.5194/acp-20-5609-2020 (see page 3).

[31] Heidi Bauer, Anne Kasper-Giebl, Franziska Zibuschka, Regina Hitzenberger, Günther F. Kraus, and Hans Puxbaum. **Determination of the Carbon Content of Airborne Fungal Spores**. *Analytical Chemistry* 74:1 (2002), 91–95. DOI: 10.1021/ac010331+ (see page 3).

[32] J.H. Seinfeld and S.N. Pandis. **Atmospheric Chemistry and Physics: From Air Pollution to Climate Change**. Wiley, 2016 (see pages 3, 4, 15, 53, 58).

[33] Guan-Yu Lin, Yu-Hsiang Cheng, and Racha Dejchanchaiwong. **Insight Into Secondary Inorganic Aerosol (SIA) Production Enhanced by Domestic Ozone Using a Machine Learning Technique**. *Atmospheric Environment* 316 (2024), 120194. ISSN: 1352-2310. DOI: 10.1016/j.atmosenv.2023.120194 (see page 3).

[34] Asif S. Ansari and Spyros N. Pandis. **Response of Inorganic PM to Precursor Concentrations**. *Environmental Science & Technology* 32:18 (1998), 2706–2714. DOI: 10.1021/es971130j (see pages 4, 58).

[35] Jesse H. Kroll, Nga L. Ng, Shane M. Murphy, Richard C. Flagan, and John H. Seinfeld. **Secondary Organic Aerosol Formation From Isoprene Photooxidation**. *Environmental Science & Technology* 40:6 (2006), 1869–1877. DOI: 10.1021/es0524301 (see pages 4, 65).

[36] Manish Shrivastava, Christopher D. Cappa, Jiwen Fan, Allen H. Goldstein, Alex B. Guenther, Jose L. Jimenez, Chongai Kuang, Alexander Laskin, Scot T. Martin, Nga Lee Ng, Tuukka Petaja, Jeffrey R. Pierce, Philip J. Rasch, Pontus Roldin, John H. Seinfeld, John Shilling, James N. Smith, Joel A. Thornton, Rainer Volkamer, Jian Wang, Douglas R. Worsnop, Rahul A. Zaveri, Alla Zelenyuk, and Qi Zhang. **Recent Advances in Understanding Secondary Organic Aerosol: Implications for Global Climate Forcing**. *Reviews of Geophysics* 55:2 (2017), 509–559. DOI: 10.1002/2016RG000540 (see pages 4, 65).

[37] Mithlesh Mahilang, Manas Kanti Deb, and Shamsh Pervez. **Biogenic Secondary Organic Aerosols: A Review on Formation Mechanism, Analytical Challenges and Environmental Impacts**. *Chemosphere* 262 (2021), 127771. ISSN: 0045-6535. DOI: 10.1016/j.chemosphere.2020.127771 (see page 4).

[38] M. Hallquist, J. C. Wenger, U. Baltensperger, Y. Rudich, D. Simpson, M. Claeys, J. Dommen, N. M. Donahue, C. George, A. H. Goldstein, J. F. Hamilton, H. Herrmann, T. Hoffmann, Y. Iinuma, M. Jang, M. E. Jenkin, J. L. Jimenez, A. Kiendler-Scharr, W. Maenhaut, G. McFiggans, Th. F. Mentel, A. Monod, A. S. H. Prévôt, J. H. Seinfeld, J. D. Surratt, R. Szmigielski, and J. Wildt. **The Formation, Properties and Impact of Secondary Organic Aerosol: Current and Emerging Issues**. *Atmospheric*

Chemistry and Physics 9:14 (2009), 5155–5236. DOI: 10.5194/acp-9-5155-2009 (see page 4).

[39] Chayakrit Krittanawong, Yusuf Kamran Qadeer, Richard B. Hayes, Zhen Wang, George D. Thurston, Salim Virani, and Carl J. Lavie. **PM2.5 and Cardiovascular Diseases: State-of-the-Art review**. *International Journal of Cardiology Cardiovascular Risk and Prevention* 19 (2023), 200217. ISSN: 2772-4875. DOI: 10.1016/j.ijcrp.2023.200217 (see page 4).

[40] Yu-Fei Xing, Yue-Hua Xu, Min-Hua Shi, and Yi-Xin Lian. **The Impact of PM2.5 on the Human Respiratory System**. *Journal of Thoracic Disease* 8:1 (2016). ISSN: 2077-6624. DOI: 10.3978/j.issn.2072-1439.2016.01.19. (see page 4).

[41] Sarawut Sangkham, Worradorn Phairuang, Samendra P. Sherchan, Nattapon Pansakun, Narongsuk Munkong, Kritsada Sarndhong, Md. Aminul Islam, and Pornpun Sakunkoo. **An Update on Adverse Health Effects from Exposure to PM2.5**. *Environmental Advances* 18 (2024), 100603. ISSN: 2666-7657. DOI: 10.1016/j.envadv.2024.100603 (see page 4).

[42] Shaowei Sang, Chong Chu, Tongchao Zhang, Hui Chen, and Xiaorong Yang. **The Global Burden of Disease Attributable to Ambient Fine Particulate Matter in 204 Countries and Territories, 1990–2019: A Systematic Analysis of the Global Burden of Disease Study 2019**. *Ecotoxicology and Environmental Safety* 238 (2022), 113588. ISSN: 0147-6513. DOI: 10.1016/j.ecoenv.2022.113588 (see page 4).

[43] Olivia V Sanderfoot and Tracey Holloway. **Air Pollution Impacts on Avian Species Via Inhalation Exposure and Associated Outcomes**. *Environmental Research Letters* 12:8 (2017), 083002. DOI: 10.1088/1748-9326/aa8051 (see pages 4, 5).

[44] D.A Grantz, J.H.B Garner, and D.W Johnson. **Ecological Effects of Particulate Matter**. *Environment International* 29:2 (2003). Future Directions in Air Quality Research : Ecological,Atmospheric,Regulatory/Policy/Economic, and Educational Issues, 213–239. ISSN: 0160-4120. DOI: 10.1016/S0160-4120(02)00181-2 (see page 5).

[45] Prabhat Kumar Rai. **Impacts of Particulate Matter Pollution on Plants: Implications for Environmental Biomonitoring**. *Ecotoxicology and Environmental Safety* 129 (2016), 120–136. ISSN: 0147-6513. DOI: 10.1016/j.ecoenv.2016.03.012 (see page 5).

[46] Wenting Wu and Yixin Zhang. **Effects of Particulate Matter (PM2.5) and Associated Acidity on Ecosystem Functioning: Response of Leaf Litter Breakdown**. *Environmental Science and Pollution Research* 25 (30 2018), 30720–30727. DOI: 10.1007/s11356-018-2922-1 (see page 5).

[47] Xuexi Tie, Ru-Jin Huang, Wenting Dai, Junji Cao, Xin Long, Xiaoli Su, Shuyu Zhao, Qiyuan Wang, and Guohui Li. **Effect of Heavy Haze and Aerosol Pollution on Rice and Wheat Productions in China**. *Scientific Reports* 6 (1 2016), 29612. DOI: 10.1038/srep29612 (see page 5).

[48] Vishal Verma, Roberto Rico-Martinez, Neel Kotra, Corey Rennolds, Jiumeng Liu, Terry W. Snell, and Rodney J. Weber. **Estimating the Toxicity of Ambient Fine Aerosols Using Freshwater Rotifer Brachionus Calyciflorus (Rotifera: Monogononta)**. *Environmental Pollution* 182 (2013), 379–384. ISSN: 0269-7491. DOI: 10.1016/j.envpol.2013.07.037 (see page 5).

[49] Yunli Zhao, Zhiqing Lin, Ruhan Jia, Guojun Li, Zhuge Xi, and Dayong Wang. **Transgenerational Effects of Traffic-Related Fine Particulate Matter (PM2.5) on Nematode Caenorhabditis Elegans**. *Journal of Hazardous Materials* 274 (2014), 106–114. ISSN: 0304-3894. DOI: 10.1016/j.jhazmat.2014.03.064 (see page 5).

[50] Danny Hartono, Billion Lioe, Yixin Zhang, Bailiang Li, and Jianzhen Yu. **Impacts of Particulate Matter (PM2.5) on the Behavior of Freshwater Snail Parafossarulus Striatulus**. *Scientific Reports* 7 (1 2017), 644. DOI: 10.1038/s41598-017-00449-5 (see page 5).

[51] Tamilselvan Gokul, Kamatchi Ramesh Kumar, Veeramani Veeramanikandan, Alagarsamy Arun, Paulraj Balaji, and Caterina Faggio. **Impact of Particulate Pollution on Aquatic Invertebrates**. *Environmental Toxicology and Pharmacology* 100 (2023), 104146. ISSN: 1382-6689. DOI: 10.1016/j.etap.2023.104146 (see page 5).

[52] Stephen Jarvis, Olivier Deschenes, Akshaya Jha, and Alan D. Radford. **The Impact of Air Pollution on Petcare Utilization**. *Proceedings of the National Academy of Sciences* 122:40 (2025), e2504553122. DOI: 10.1073/pnas.2504553122 (see page 5).

[53] Manuela Plutino, Elisa Bianchetto, Alessandra Durazzo, Massimo Lucarini, Luigi Lucini, and Ilaria Negri. **Rethinking the Connections Between Ecosystem Services, Pollinators, Pollution, and Health: Focus on Air Pollution and Its Impacts**. *International Journal of Environmental Research and Public Health* 19:5 (2022). ISSN: 1660-4601. DOI: 10.3390/ijerph19052997 (see page 5).

[54] Liwei Yang, Xiaoqing Gao, Zhenchao Li, and Dongyu Jia. **Quantitative Effects of Air Pollution on Regional Daily Global and Diffuse Solar Radiation Under Clear Sky Conditions**. *Energy Reports* 8 (2022), 1935–1948. ISSN: 2352-4847. DOI: 10.1016/j.egyr.2021.12.081 (see page 6).

[55] Zi-Ying Cai, Qing Yao, Su-Qin Han, and Jin-Le Liu. **The Influence of the Air Quality and Meteorological Field About Aerosol Direct Climate Effect on Tianjin**. *Zhongguo Huanjing Kexue/China Environmental Science* 37:3 (2017), 908–914. URL: https://www.scopus.com/inward/record.uri?eid=2-s2.0-85027973128&partnerID=40&md5=62db57f1767bbd9b48e8d9d521eba399 (see page 6).

[56] Liwei Yang, Xiaoqing Gao, Zhenchao Li, and Dongyu Jia. **Intra-Day Solar Irradiation Forecast Using Machine Learning With Satellite Data**. *Sustainable Energy, Grids and Networks* 36 (2023), 101212. ISSN: 2352-4677. DOI: 10.1016/j.segan.2023.101212 (see page 6).

[57] Ye Huang, Huizhong Shen, Han Chen, Rong Wang, Yanyan Zhang, Shu Su, Yuanchen Chen, Nan Lin, Shaojie Zhuo, Qirui Zhong, Xilong Wang, Junfeng Liu, Bengang Li, Wenxin Liu, and Shu Tao. **Quantification of Global Primary Emissions of PM2.5, PM10, and TSP From Combustion and Industrial Process Sources**. *Environmental Science & Technology* 48:23 (2014). PMID: 25347079, 13834–13843. DOI: 10.1021/es503696k (see page 6).

[58] Yi Li, Li Zhou, Hefan Liu, Song Liu, Miao Feng, Danlin Song, Qinwen Tan, Hongbin Jiang, Sophia Zuoqiu, and Fumo Yang. **Disparities in Precipitation Effects on PM2.5 Mass Concentrations and Chemical Compositions: Insights From Online Monitoring Data in Chengdu**. *Journal of Environmental Sciences* (2024). ISSN: 1001-0742. DOI: 10.1016/j.jes.2024.08.015 (see page 6).

[59] IPCC. **Climate Change 2023: Synthesis Report. Contribution of Working Groups I, II and III to the Sixth Assessment Report of the Intergovernmental Panel on Climate Change**. Synthesis Report. Geneva, Switzerland: Intergovernmental Panel on Climate Change, 2023, 35–115. DOI: 10.59327/IPCC/AR6-9789291691647 (see page 6).

[60] Pollution Control Department. **Thailand State of Pollution Report 2023**. Tech. rep. Pollution Control Department, Ministry of Resources and Environment, 2024. URL: https://www.pcd.go.th/publication/32171/ (see pages 6–9, 25, 31, 35, 37).

[61] Suhaimee Buya, Hideomi Gokon, Van-Nam Huynh, Hieu-Chi Dam, Sasiporn Usanavasin, Jessada Karnjana, and Nutta Taneepanichskul. **Spatiotemporal Association Between Monthly PM2.5 Levels and Cardiorespiratory Mortality in Thailand (2015–2019)**. *International Journal of Environmental Health Research* 0:0 (2025). PMID: 39862124, 1–12. DOI: 10.1080/09603123.2025.2458726 (see page 6).

[62] Piyanee Kasiravat and Thammasin Ingviya. **Effects of Fine Particulate Matter on Hospital Admission Due to Stroke in a Business City of Thailand**. *Chulalongkorn Medical Journal* 67:2 (2023). DOI: 10.56808/2673-060X.5447 (see page 6).

[63] Kannika Jarernwong, Shabbir H. Gheewala, and Sate Sampattagul. **Health Impact Related to Ambient Particulate Matter Exposure as a Spatial Health Risk Map Case Study in Chiang Mai, Thailand**. *Atmosphere* 14:2 (2023). ISSN: 2073-4433. DOI: 10.3390/atmos14020261 (see page 6).

[64] Nawapon Nakharutai, Patrinee Traisathit, Natthapat Thongsak, Titaporn Supasri, Pimwarat Srikummoon, Salinee Thumronglaohapun, Phonpat Hemwan, and Imjai Chitapanarux. **Impact of Residential Concentration of PM2.5 Analyzed as Time-Varying Covariate on the Survival Rate of Lung Cancer Patients: A 15-Year Hospital-Based Study in Upper Northern Thailand**. *International Journal of Environmental Research and Public Health* 19 (2022), 4521. DOI: 10.3390/ijerph19084521 (see page 6).

[65] Titaporn Supasri, Shabbir Gheewala, Ronald Macatangay, Anurak Chakpor, and Surat Sedpho. **Association Between Ambient Air Particulate Matter and Human Health Impacts in Northern Thailand**. *Scientific Reports* 13 (2023). DOI: 10.1038/s41598-023-39930-9 (see page 6).

[66] Napat Harnpornchai Pornchanok Praditthong and Paravee Maneejuk. **The Impact of Particulate Matter 2.5 on Tourist Arrival in Chiang Mai**. *Journal of Positive School Psychology* 6:11 (2022). URL: https://journalppw.com/index.php/jpsp/article/view/14866 (see page 6).

[67] Teerawat Namcome and Roengchai Tansuchat. **The Impact of Fine Particulate Matter (PM 2.5) Pollution on the Number of Foreign Tourists in Chiang Mai and Bangkok**. *Community and Social Development Journal* 22:3 (2021), 19–35. DOI: 10.14456/rcmrj.2021.247437 (see page 6).

[68] Phisek Srinamphon, Sainatee Chernbumroong, and Korrakot Yaibuathet Tippayawong. **The Effect of Small Particulate Matter on Tourism and Related SMEs in Chiang Mai, Thailand**. *Sustainability* 14:13 (2022). ISSN: 2071-1050. DOI: 10.3390/su14138147 (see page 6).

[69] Nguyen Ngoc Linh Thao, Sittichai Pimonsree, Kritana Prueksakorn, Pham Thi Bich Thao, and Patipat Vongruang. **Public Health and Economic Impact Assessment of PM2.5 From Open Biomass Burning Over Countries in Mainland Southeast Asia During the Smog Episode**. *Atmospheric Pollution Research* 13:6 (2022), 101418. ISSN: 1309-1042. DOI: 10.1016/j.apr.2022.101418 (see pages 6, 24).

[70] Gregor Kiesewetter, Zbigniew Klimont, Muye Ru, and Jessica Slater. **National Assessment of the Cost of Inaction of Tackling Air Pollution in Thailand**. Tech. rep. International Institute for Applied Systems Analysis and the United Nations Environment Programme, 2023. URL: https://pure.iiasa.ac.at/id/eprint/18826/1/Cost-of-Inaction-Thailand.pdf (see page 6).

[71] Steven Andrew Martin and Raymond James Ritchie. **Sourcing Thai Geography Literature for ASEAN and International Education**. *Singapore Journal of Tropical Geography* 41:1 (2020), 61–85. DOI: 10.1111/sjtg.12296 (see page 8).

[72] James Moran, Chirada NaSuwan, and Ora-Orn Poocharoen. **The Haze Problem in Northern Thailand and Policies to Combat It: A Review**. *Environmental Science & Policy* 97 (2019), 1–15. ISSN: 1462-9011. DOI: 10.1016/j.envsci.2019.03.016 (see pages 7, 25).

[73] Teerachai Amnuaylojaroen, Phonwilai Kaewkanchanawong, and Phatcharamon Panpeng. **Distribution and Meteorological Control of PM2.5 and Its Effect on Visibility in Northern Thailand**. *Atmosphere* 14:3 (2023). ISSN: 2073-4433. DOI: 10.3390/atmos14030538 (see pages 7, 25).

[74] Nguyen Thi Kim Oanh. **Final Report on the Study of Sources of Particulate Matter Less Than 2.5 Microns (PM2.5) and Secondary Pollutants (Secondary PM2.5) in Bangkok and Surrounding Areas**. Tech. rep. Submitted to Japan International Cooperation Agency (JICA) Research Institute. Bangkok, Thailand: Asian Institute of Technology (AIT), 2017. URL: https://www.jica.go.jp/Resource/jica-ri/publication/booksandreports/l75nbg00000kjwkk-att/Final%5C_report.pdf (see pages 8–10, 24, 43, 61).

[75] Shuai Yin, Xiufeng Wang, Xirui Zhang, Meng Guo, Moe Miura, and Yi Xiao. **Influence of Biomass Burning on Local Air Pollution in Mainland Southeast Asia From 2001 to 2016**. *Environmental Pollution* 254 (2019), 112949. ISSN: 0269-7491. DOI: 10.1016/j.envpol.2019.07.117 (see pages 8, 24).

[76] Jariya Kayee, Penjai Sompongchaiyakul, Nivedita Sanwlani, Sujaree Bureekul, Xianfeng Wang, and Reshmi Das. **Metal Concentrations and Source Apportionment of PM2.5 in Chiang Rai and Bangkok, Thailand during a Biomass Burning Season**. *ACS Earth and Space Chemistry* 4:7 (2020), 1213–1226. DOI: 10.1021/acsearthspacechem.0c00140 (see pages 8, 10).

[77] Sherin Hassan Bran, Ronald Macatangay, Chakrit Chotamonsak, Somporn Chantara, and Vanisa Surapipith. **Understanding the Seasonal Dynamics of Surface PM2.5 Mass Distribution and Source Contributions Over Thailand**. *Atmospheric Environment* 331 (2024), 120613. ISSN: 1352-2310. DOI: 10.1016/j.atmosenv.2024.120613 (see pages 8, 10, 25, 62).

[78] Karuna Jainontee, Prapat Pongkiatkul, Ying-Lin Wang, Roy J.F. Weng, Yi-Ting Lu, Ting-Shiuan Wang, and Wang-Kun Chen. **Strategy Design of PM2.5 Controlling for Northern Thailand**. *Aerosol and Air Quality Research* 23:6 (2023), 220432. ISSN: 2071-1409. DOI: 10.4209/aaqr.220432 (see page 8).

[79] Teerachai Amnuaylojaroen, Jirarat Inkom, Radshadaporn Janta, and Vanisa Surapipith. **Long Range Transport of Southeast Asian PM2.5 Pollution to Northern Thailand during High Biomass Burning Episodes**. *Sustainability* 12:23 (2020). ISSN: 2071-1050. DOI: 10.3390/su122310049 (see pages 8, 10, 25, 35, 63).

[80] Kevalin Inlaung, Chakrit Chotamonsak, Ronald Macatangay, and Vanisa Surapipith. **Assessment of Transboundary PM2.5 From Biomass Burning in Northern Thailand Using the WRF-Chem Model**. *Toxics* 12:7 (2024). ISSN: 2305-6304. DOI: 10.3390/toxics12070462 (see pages 8, 10, 24, 25, 35, 36, 40, 46, 63).

[81] Sarana Chansuebsri, Pavidarin Kraisitnitikul, Wan Wiriya, and Somporn Chantara. **Fresh and Aged PM2.5 and Their Ion Composition in Rural and Urban Atmospheres of Northern Thailand in Relation to Source Identification**. *Chemosphere* 286 (2022), 131803. ISSN: 0045-6535. DOI: 10.1016/j.chemosphere.2021.131803 (see page 8).

[82] Sarana Chansuebsri, Petr Kolar, Pavidarin Kraisitnitikul, Natthanit Kantarawilawan, Nuttipon Yabueng, Wan Wiriya, Duangduean Thepnuan, and Somporn Chantara. **Chemical Composition and Origins of PM2.5 in Chiang Mai (Thailand) by Integrated Source Apportionment and Potential Source Areas**. *Atmospheric Environment* 327 (2024), 120517. ISSN: 1352-2310. DOI: 10.1016/j.atmosenv.2024.120517 (see pages 8, 10, 24).

[83] Nanthapong Chantaraprachoom, Hikari Shimadera, Katsushige Uranishi, Luong Viet Mui, Tomohito Matsuo, and Akira Kondo. **A Nation-by-Nation Assessment of the Contribution of Southeast Asian Open Biomass Burning to PM2.5 in Thailand Using the Community Multiscale Air Quality-Integrated Source Apportionment Method Model**. *Atmosphere* 15:11 (2024). ISSN: 2073-4433. DOI: 10.3390/atmos15111358 (see page 9).

[84] Nanthapong Chantaraprachoom, Daichi Mochizuki, Hikari Shimadera, Mui Luong, Tomohito Matsuo, and Akira Kondo. **Impact Assessment of Biomass Burning in Southeast Asia to 2019 Annual Average PM2.5 Concentration in Thailand using Atmospheric Chemical Transport Model**. *E3S Web of Conferences* 379 (2023). DOI: 10.1051/e3sconf/202337901002 (see pages 9, 35).

[85] Chomsri ChooChuay, Siwatt Pongpiachan, Danai Tipmanee, Oramas Suttinun, Woranuch Deelaman, Qiyuan Wang, Li Xing, Guohui Li, Yongming Han, Jittree Palakun, and Junji Cao. **Impacts of PM2.5 Sources on Variations in Particulate Chemical Compounds in Ambient Air of Bangkok, Thailand**. *Atmospheric Pollution Research* 11:9 (2020), 1657–1667. ISSN: 1309-1042. DOI: 10.1016/j.apr.2020.06.030 (see pages 9, 10, 24, 62, 63).

[86] A.L. Savinda Heshani and Ekbordin Winijkul. **Numerical Simulations of the Effects of Green Infrastructure on PM2.5 Dispersion in an Urban Park in Bangkok, Thailand**. *Heliyon* 8:9 (2022), e10475. ISSN: 2405-8440. DOI: 10.1016/j.heliyon.2022.e10475 (see pages 9, 10, 25).

[87] Thammaluck Ratanavalachai and Win Trivitayanurak. **Application of a PM2.5 Dispersion Model in the Bangkok Central Business District for Air Quality Management**. *Frontiers in Environmental Science* 11 (2023). ISSN: 2296-665X. DOI: 10.3389/fenvs.2023.1237366 (see pages 9, 10, 25).

[88] Mushtaq Ahmad, Thanaphum Manjantrarat, Wachiraya Rattanawongsa, Phitchaya Muensri, Rattaporn Saenmuangchin, Annop Klamchuen, Sasitorn Aueviriyavit, Kanokwan Sukrak, Wiyong Kangwansupamonkon, and Sirima Panyametheekul. **Chemical Composition, Sources, and Health Risk Assessment of PM2.5 and PM10 in Urban Sites of Bangkok, Thailand**. *International Journal of Environmental Research and Public Health* 19:21 (2022). ISSN: 1660-4601. DOI: 10.3390/ijerph192114281 (see pages 9, 10, 24, 61).

[89] Daiju Narita, Nguyen Thi Kim Oanh, Keiichi Sato, Mingqun Huo, Didin Agustian Permadi, Nguyen Nhat Ha Chi, Tanatat Ratanajaratroj, and Ittipol Pawarmart. **Pollution Characteristics and Policy Actions on Fine Particulate Matter in a Growing Asian Economy: The Case of Bangkok Metropolitan Region**. *Atmosphere* 10:5 (2019). ISSN: 2073-4433. DOI: 10.3390/atmos10050227 (see pages 9, 10, 24, 43).

[90] Danny Marks. "Water Access and Resilience to Climate-Induced Droughts in the Thai Secondary City of Khon Kaen: Unequal and Unjust Vulnerability." In: *Urban Climate Resilience in Southeast Asia*. Ed. by Amrita G. Daniere and Matthias Garschagen. Cham: Springer International Publishing, 2019, 41–62. ISBN: 978-3-319-98968-6. DOI: 10.1007/978-3-319-98968-6_3 (see page 9).

[91] Tatchalerm Sudhipongpracha and Bharat Dahiya. **City Profile: Khon Kaen, Thailand**. *Environment and Urbanization ASIA* 10:2 (2019), 271–289. DOI: 10.1177/0975425319863931 (see page 9).

[92] Pornpun Sakunkoo, Theerachai Thonglua, Sarawut Sangkham, Chananya Jirapornkul, Yuparat Limmongkon, Sakda Daduang, Thanee Tessiri, Jetnapis Rayubkul, Sakesun Thongtip, Naowarat Maneenin, and Sittichai Pimonsree. **Human Health Risk Assessment of PM2.5-Bound Heavy Metal of Anthropogenic Sources in the Khon Kaen Province of Northeast Thailand**. *Heliyon* 8:6 (2022), e09572. ISSN: 2405-8440. DOI: 10.1016/j.heliyon.2022.e09572 (see page 9).

[93] Kornkawat Darunikorn, Chananya Jirapornkul, Yuparat Limmongkon, Rittirong Junggoth, Naowarat Maneenin, and Pornpun Sakunkoo. **PM 2.5 Levels in the Muang District of Khon Kaen Province by Ambient PM 2.5 Detectors With Real-Time Sensors**. *Environment Asia* 16:2 (2023), 109–117. DOI: 10.14456/ea.2023.25 (see page 9).

[94] Pollution Control Department. **Thailand State of Pollution Report 2019**. Tech. rep. Pollution Control Department, Ministry of Resources and Environment, 2020 (see pages 9, 32).

[95] Pornpun Sakunkoo, Pornsuda Manochai, David Koh, and Sarawut Sangkham. **Effects of PM 2.5 on the Incidence of Circulatory System Diseases in Muang District, Khon Kaen Province of Northeast Thailand**. *EnvironmentAsia* 15:1 (2022), 109–116. DOI: 10.14456/ea.2022.10 (see page 9).

[96] Chananya Jirapornkul, Kornkawat Darunikorn, Yuparat Limmongkon, Rittirong Junggoth, Naowarat Maneenin, Pornpun Sakunkoo, and Jetnapis Rayubkul. **Exploring the Link Between Ambient PM2.5 Concentrations and Respiratory Diseases in the Elderly: A Study in the Muang District of Khon Kaen, Thailand**. *Reviews on Environmental Health* 40:1 (2025), 175–183. DOI: 10.1515/reveh-2023-0138 (see page 9).

[97] Sirapong Sooktawee, Ratchatawan Ketwang, Aduldech Patpai, and Nirun Piemyai. **A Study on Determining the Potential Source Area of PM2.5 Using Bivariate Polar Plot Technique on Short-Term Monitoring Data in Bhan Phi District, Khonkhen Province, Thailand**. *Journal of Applied Research on Science and Technology (JARST)* 21:2 (2022), 66–78. DOI: 10.14456/jarst.2022.18 (see page 9).

[98] Tipawan Phetrawech and Sarawut Thepanondh. **Evaluation of Resuspension of Road Dust in a Cement Industrial Complex Area**. *GEOMATE Journal* 12:33 (2016), 96–103. DOI: 10.21660/2017.33.2628 (see page 9).

[99] Sirapong Sooktawee, Thongchai Kanabkaew, Suteera Boonyapitak, Aduldech Patpai, and Nirun Piemyai. **Characterising Particulate Matter Source Contributions in the Pollution Control Zone of Mining and Related Industries Using Bivariate Statistical Techniques**. *Scientific Reports* 10:21372 (2020). DOI: 10.1038/s41598-020-78445-5 (see pages 9, 10).

[100] Nguyen Thi Kim Oanh, Ohnmar May Tin Hlaing, and To Thi Hien. "Regional and Urban Air Quality in Mainland Southeast Asia Countries." In: *Handbook of Air Quality and Climate Change*. Ed. by Hajime Akimoto and Hiroshi Tanimoto. Singapore: Springer Nature Singapore, 2023, 507–531. ISBN: 978-981-15-2760-9. DOI: 10.1007/978-981-15-2760-9_69 (see page 9).

[101] Bonyoung Koo, Gary M. Wilson, Ralph E. Morris, Alan M. Dunker, and Greg Yarwood. **Comparison of Source Apportionment and Sensitivity Analysis in a Particulate Matter Air Quality Model**. *Environmental Science & Technology* 43:17 (2009), 6669–6675. DOI: 10.1021/es9008129 (see pages 10, 20–22, 53).

[102] Philip K. Hopke, Qili Dai, Linxuan Li, and Yinchang Feng. **Global Review of Recent Source Apportionments for Airborne Particulate Matter**. *Science of The Total Environment* 740 (2020), 140091. ISSN: 0048-9697. DOI: 10.1016/j.scitotenv.2020.140091 (see page 10).

[103] P. Thunis, A. Clappier, L. Tarrason, C. Cuvelier, A. Monteiro, E. Pisoni, J. Wesseling, C.A. Belis, G. Pirovano, S. Janssen, C. Guerreiro, and E. Peduzzi. **Source Apportionment to Support Air Quality Planning: Strengths and Weaknesses of Existing Approaches**. *Environment International* 130 (2019), 104825. ISSN: 0160-4120. DOI: 10.1016/j.envint.2019.05.019 (see pages 10, 21, 22, 52, 53, 58, 66).

[104] S. Chatani, H. Shimadera, S. Itahashi, and K. Yamaji. **Comprehensive Analyses of Source Sensitivities and Apportionments of $PM_{2.5}$ and Ozone over Japan via Multiple Numerical Techniques**. *Atmospheric Chemistry and Physics* 20:17 (2020), 10311–10329. DOI: 10.5194/acp-20-10311-2020 (see pages 10, 20, 22, 25, 43, 53).

[105] Philip K. Hopke. **Review of Receptor Modeling Methods for Source Apportionment**. *Journal of the Air & Waste Management Association* 66:3 (2016), 237–259. DOI: 10.1080/10962247.2016.1140693 (see page 10).

[106] Xiaole Zhang, Xiaoxiao Feng, Jie Tian, Yong Zhang, Zhiyu Li, Qiyuan Wang, Junji Cao, and Jing Wang. **Dynamic Harmonization of Source-Oriented and Receptor Models for Source Apportionment**. *Science of The Total Environment* 859 (2023), 160312. ISSN: 0048-9697. DOI: 10.1016/j.scitotenv.2022.160312 (see pages 10, 21, 24, 25, 43).

[107] Phatsarakorn Chaisongkaew, Racha Dejchanchaiwong, Muanfun Inerb, Napawan Mahasakpan, Nobchonnee Nim, Hisam Samae, Assoc.Prof.Dr. Panich Intra, John Morris, Thammasin Ingviya, Thanathip Limna, and Perapong Tekasakul. **Source Apportionment of PM2.5 in Thailand's Deep South by Principal Component Analysis and Impact of Transboundary Haze**. *Environmental Science and Pollution Research* 30 (2023), 1–17. DOI: 10.1007/s11356-023-28419-7 (see page 10).

[108] Supattarachai Saksakulkrai, Somporn Chantara, Pavidarin Kraisitnitikul, Deepchandra Srivastava, and Zongbo Shi. **Unveiling the Origins of Northern Thailand's Haze: Comprehensive Chemical Characterization and Source Apportionment of PM2.5 Using Targeted Molecular Markers**. *Journal of Environmental Sciences* 159 (2026), 635–648. ISSN: 1001-0742. DOI: 10.1016/j.jes.2025.04.040 (see pages 10, 24).

[109] Siwatt Pongpiachan, Sarunpron Khruengsai, Teerapong Sripahco, Radshadaporn Janta, Rungruang Janta, Jompob Waewsak, Danai Tipmanee, Saran Poshyachinda, and Patcharee Pripdeevech. **Identifying PM2.5-Bound Metal Pollution Sources in Southern Thailand Using Positive Matrix Factorization and Principal Component Analysis**. *Atmospheric Environment: X* 26 (2025), 100337. ISSN: 2590-1621. DOI: 10.1016/j.aeaoa.2025.100337 (see page 10).

[110] Pitakchon Ponsawansong, Tippawan Prapamontol, Kittipan Rerkasem, Somporn Chantara, Kraichat Tantrakarnapa, Sawaeng Kawichai, Guoxing Li, Cao Fang, Xiaochuan Pan, and Yanlin Zhang. **Sources of PM2.5 Oxidative Potential During Haze and Non-Haze Seasons in Chiang Mai, Thailand**. *Aerosol and Air Quality Research* 23:10 (2023), 230030. ISSN: 2071-1409. DOI: 10.4209/aaqr.230030 (see pages 10, 24).

[111] Sun-Kyoung Park, Amit Marmur, and Armistead G. Russell. **Environmental Risk Assessment: Comparison of Receptor and Air Quality Models for Source Apportionment**. *Human and Ecological Risk Assessment: An International Journal* 19:5 (2013), 1385–1403. DOI: 10.1080/10807039.2012.730475 (see pages 10, 24, 43).

[112] M. Mircea, G. Calori, G. Pirovano, and C. A. Belis. **European Guide on Air Pollution Source Apportionment for Particulate Matter with Source Oriented Models and Their Combined Use with Receptor Models**. Publications Office, 2020. DOI: 10.2760/470628 (see pages 10, 20, 21, 25, 43, 53).

[113] C. L. Reddington, L. Conibear, C. Knote, B. J. Silver, Y. J. Li, C. K. Chan, S. R. Arnold, and D. V. Spracklen. **Exploring the Impacts of Anthropogenic Emission Sectors on $PM_{2.5}$ and Human Health in South and East Asia**. *Atmospheric Chemistry and Physics* 19:18 (2019), 11887–11910. DOI: 10.5194/acp-19-11887-2019 (see page 10).

[114] Erin E. McDuffie, Randall V. Martin, Joseph V. Spadaro, Richard Burnett, Steven J. Smith, Patrick O'Rourke, Melanie S. Hammer, Aaron van Donkelaar, Liam Bindle, Viral Shah, Lyatt Jaeglé, Gan Luo, Fangqun Yu, Jamiu A. Adeniran, Jintai Lin, and Michael Brauer. **Source Sector and Fuel Contributions to Ambient PM2.5 and Attributable Mortality Across Multiple Spatial Scales**. *Nature Communications* 12:1 (2021), 3594. DOI: 10.1038/s41467-021-23853-y (see pages 10, 62).

[115] Worapop Thongsame, Daven K. Henze, Mary Barth, Gabriele Pfister, Rajesh Kumar, Ronald Macatangay, and Sherin Hassan Bran. **Source Attribution and Health Burden of PM2.5 in Mainland Thailand**. *GeoHealth* 9:9 (2025). e2024GH001315 2024GH001315, e2024GH001315. DOI: 10.1029/2024GH001315 (see pages 10, 25).

[116] ASEAN Secretariat. *ASEAN Agreement on Transboundary Haze Pollution*. Accessed: 2026-01-29. 2002. URL: https://asean.org/wp-content/uploads/2021/01/ASEANAgreementonTransboundaryHazePollution-1.pdf (see page 11).

[117] Daniel S. Cohan and Sergey L. Napelenok. **Air Quality Response Modeling for Decision Support**. *Atmosphere* 2:3 (2011), 407–425. ISSN: 2073-4433. DOI: 10.3390/atmos2030407 (see pages 15, 20, 21, 53).

[118] Z. Luo, Y. Han, K. Hua, Y. Zhang, J. Wu, X. Bi, Q. Dai, B. Liu, Y. Chen, X. Long, and Y. Feng. **The Effect of Emission Source Chemical Profiles on Simulated $PM_{2.5}$ Components: Sensitivity Analysis With the Community Multiscale Air Quality (CMAQ) Modeling System Version 5.0.2**. *Geoscientific Model Development* 16:22 (2023), 6757–6771. DOI: 10.5194/gmd-16-6757-2023 (see page 15).

[119] Deo Okure, Sarath K. Guttikunda, Richard Sserunjogi, Priscilla Adong, Sai Krishna Dammalapati, Dorothy Lsoto, Paul Green, Engineer Bainomugisha, and Jian Xie. **Integrated Air Quality Information for Kampala: Analysis of PM2.5, Emission Sources, Modelled Contributions, and Institutional Framework**. *Environ. Sci.: Atmos.* 5 (4 2025), 471–484. DOI: 10.1039/D4EA00081A (see page 15).

[120] Hyeon-Kook Kim, EunRyoung Kim, Chang-Keun Song, Jae-Ho Choi, Ganghan Kim, Myong-In Lee, Yujin J. Oak, Rokjin J. Park, Ilhan Ryoo, Seung-Muk Yi, Kyung-Mi Lee, Hyeok-Gi Cheo, and Kwon-Ho Jeon. **Comparative Evaluation of Surface-Level PM2.5 Modeling Across Northeast Asia: Relevance for Regulatory and Scientific Applications**. *Environmental Pollution* 377 (2025), 126428. ISSN: 0269-7491. DOI: 10.1016/j.envpol.2025.126428 (see page 15).

[121] Zhaoqi Gao and Xuehua Zhou. **A Review of the CAMx, CMAQ, WRF-Chem and NAQPMS Models: Application, Evaluation and Uncertainty Factors**. *Environmental Pollution* 343 (2024), 123183. ISSN: 0269-7491. DOI: 10.1016/j.envpol.2023.123183 (see page 15).

[122] Min-Woo Choi, Jae-Hyeong Lee, Ju-Wan Woo, Cheol-Hee Kim, and Sang-Hyun Lee. **Comparison of PM2.5 Chemical Components over East Asia Simulated by the WRF-Chem and WRF/CMAQ Models: On the Models' Prediction Inconsistency**. *Atmosphere* 10:10 (2019). ISSN: 2073-4433. DOI: 10.3390/atmos10100618 (see page 15).

[123] Fan Meng, Xiaohui Du, Wei Tang, Jing He, Yang Li, Xuesong Wang, Shaocai Yu, Xiao Tang, Jia Xing, Min Xie, Limin Zeng, and Huabin Dong. **Evaluation of Regional Atmospheric Models for Air Quality Simulations in the Winter Season in China**. *Atmosphere* 17:1 (2026). ISSN: 2073-4433. DOI: 10.3390/atmos17010001 (see page 15).

[124] Georg Grell and Alexander Baklanov. **Integrated Modeling for Forecasting Weather and Air Quality: A Call for Fully Coupled Approaches**. *Atmospheric Environment* 45:38 (2011). Modeling of Air Quality Impacts, Forecasting and Interactions with Climate., 6845–6851. ISSN: 1352-2310. DOI: 10.1016/j.atmosenv.2011.01.017 (see page 15).

[125] R.H.F. Kwok, S.L. Napelenok, and K.R. Baker. **Implementation and Evaluation of PM2.5 Source Contribution Analysis in a Photochemical Model**. *Atmospheric Environment* 80 (2013), 398–407. ISSN: 1352-2310. DOI: 10.1016/j.atmosenv.2013.08.017 (see pages 15, 21, 22, 39, 52).

[126] William C. Skamarock, Joseph B. Klemp, Jimy Dudhia, David O. Gill, Zhiquan Liu, Judith Berner, Wei Wang, Jordan G. Powers, Michael G. Duda, Dale Barker, and Xiang-yu Huang. **A Description of the Advanced Research WRF Model Version 4.3**. Tech. rep. National Center for Atmospheric Research, University Corporation for Atmospheric Research, 2021. DOI: 10.5065/1dfh-6p97 (see pages 16, 17, 26, 37).

[127] Z. I. Janjic. **A Nonhydrostatic Model Based on a New Approach**. *Meteorology and Atmospheric Physics* 82 (1 2003), 271–285. DOI: 10.1007/s00703-001-0587-6 (see page 16).

[128] S. Yu, R. Mathur, J. Pleim, G. Pouliot, D. Wong, B. Eder, K. Schere, R. Gilliam, and S. T. Rao. **Comparative Evaluation of the Impact of WRF/NMM and WRF/ARW Meteorology on CMAQ Simulations for $PM_{2.5}$ and Its Related Precursors During the 2006 TexAQS/GoMACCS Study**. *Atmospheric Chemistry and Physics* 12:9 (2012), 4091–4106. DOI: 10.5194/acp-12-4091-2012 (see page 16).

[129] Shaocai Yu, Rohit Mathur, Jonathan Pleim, George Pouliot, David Wong, Brian Eder, Kenneth Schere, Rob Gilliam, and S. Trivikrama Rao. **Comparative Evaluation of the Impact of WRF–NMM and WRF–ARW Meteorology on CMAQ Simulations for O3 and Related Species During the 2006 TexAQS/GoMACCS Campaign**. *Atmospheric Pollution Research* 3:2 (2012), 149–162. ISSN: 1309-1042. DOI: 10.5094/APR.2012.015 (see page 16).

[130] United States Environmental Protection Agency (US EPA). *CMAQ: The Community Multiscale Air Quality Modeling System*. Accessed: 2025-11-07. 2025. URL: https://www.epa.gov/cmaq (see pages 17, 19, 20).

[131] United States Environmental Protection Agency (US EPA). *CMAQv5.5 User's Guide*. Accessed: 2025-11-07. 2025. URL: https://github.com/USEPA/CMAQ/blob/main/DOCS/Users_Guide/README.md (see page 17).

[132] Francis S. Binkowski and Shawn J. Roselle. **Models-3 Community Multiscale Air Quality (CMAQ) Model Aerosol Component 1. Model Description**. *Journal of Geophysical Research: Atmospheres* 108:D6 (2003). DOI: 10.1029/2001JD001409 (see page 18).

[133] C. A. Belis, G. Pirovano, M. G. Villani, G. Calori, N. Pepe, and J. P. Putaud. **Comparison of Source Apportionment Approaches and Analysis of Non-Linearity in a Real Case Model Application**. *Geoscientific Model Development* 14:7 (2021), 4731–4750. DOI: 10.5194/gmd-14-4731-2021 (see pages 21, 22, 53, 58).

[134] A. Clappier, C. A. Belis, D. Pernigotti, and P. Thunis. **Source Apportionment and Sensitivity Analysis: Two Methodologies With Two Different Purposes**. *Geoscientific Model Development* 10:11 (2017), 4245–4256. DOI: 10.5194/gmd-10-4245-2017 (see pages 21, 22, 58, 66).

[135] Michael J. Burr and Yang Zhang. **Source Apportionment of Fine Particulate Matter Over the Eastern U.S. Part II: Source Apportionment Simulations Using CAMx/PSAT and Comparisons With CMAQ Source Sensitivity Simulations**. *Atmospheric Pollution Research* 2:3 (2011), 318–336. ISSN: 1309-1042. DOI: 10.5094/APR.2011.037 (see page 22).

[136] Zijun Li, Taotao Liu, Hong Zhang, Xinqi Wang, Jun Zhang, Zhiyong Qin, and Chengzhu Zhu. **Sensitivity Analysis of Ozone Formation and Source Apportionment of VOCs in a Typical Industrial City in the Yangtze River Delta Region During Summer**. *Atmospheric Pollution Research* 16:4 (2025), 102424. ISSN: 1309-1042. DOI: 10.1016/j.apr.2025.102424 (see page 22).

[137] Yujing Zhang, Yuncheng Zhao, Jie Li, Qizhong Wu, Hui Wang, Huiyun Du, Wenyi Yang, Zifa Wang, and Lili Zhu. **Modeling Ozone Source Apportionment and Performing Sensitivity Analysis in Summer on the North China Plain**. *Atmosphere* 11:9 (2020). ISSN: 2073-4433. DOI: 10.3390/atmos11090992 (see page 22).

[138] Krishna Vadrevu, Kristofer Lasko, Louis Giglio, Wilfrid Schroeder, Sumalika Biswas, and Chris Justice. **Trends in Vegetation Fires in South and Southeast Asian Countries**. *Scientific Reports* 9 (2019), 7422. DOI: 10.1038/s41598-019-43940-x (see page 24).

[139] Yoshio Inoue, Yoshiyuki Kiyono, Hidetoshi Asai, Yukihito Ochiai, Jiaguo Qi, Albert Olioso, Shiraiwa Tatsuhiko, Takeshi Horie, Kazuki Saito, and Linkham Dounagsavanh. **Assessing Land-Use and Carbon Stock in Slash-and-Burn Ecosystems in Tropical Mountain of Laos Based on Time-Series Satellite Images**. *International Journal of Applied Earth Observation and Geoinformation* 12 (2010), 287–297. DOI: 10.1016/j.jag.2010.04.004 (see page 24).

[140] Shuai Yin. **Biomass Burning Spatiotemporal Variations over South and Southeast Asia**. *Environment International* 145 (2020), 106153. ISSN: 0160-4120. DOI: 10.1016/j.envint.2020.106153 (see pages 24, 35).

[141] Nguyen Thi Oanh, Bich Thuy Ly, Danutawat Tipayarom, Bhai Manadhar, Prapat Pongkiatkul, Christopher Simpson, and L-J Liu. **Characterization of Particulate Matter Emission from Open Burning of Rice Straw**. *Atmospheric Environment* 45 (2011), 493–502. DOI: 10.1016/j.atmosenv.2010.09.023 (see page 24).

[142] Michael D. Hays, Philip M. Fine, Christopher D. Geron, Michael J. Kleeman, and Brian K. Gullett. **Open Burning of Agricultural Biomass: Physical and Chemical Properties of Particle-Phase Emissions**. *Atmospheric Environment* 39:36 (2005), 6747–6764. ISSN: 1352-2310. DOI: 10.1016/j.atmosenv.2005.07.072 (see page 24).

[143] George Nyamadzawo, Menas Wuta, Justice Nyamangara, Philip Nyamugafata, and Takesure Tendayi. **Burning, Biomass Removal and Tillage Effects on Soil Organic Carbon and Nutrients in Seasonal Wetlands (Dambos) of Chiota Smallholder Farming Area, Zimbabwe**. *Archives of Agronomy and Soil Science* 60:10 (2014), 1411–1427. DOI: 10.1080/03650340.2014.892583 (see page 24).

[144] Kristofor R. Brye. **Long-Term Effects of Aboveground Biomass Removal by Burning on Potential Nutrient Recycling**. *Crop Management* 11:1 (2012), 1–9. DOI: 10.1094/CM-2012-0822-01-RS (see page 24).

[145] H.-H. Lee, O. Iraqui, Y. Gu, S. H.-L. Yim, A. Chulakadabba, A. Y.-M. Tonks, Z. Yang, and C. Wang. **Impacts of Air Pollutants from Fire and Non-Fire Emissions on the Regional Air Quality in Southeast Asia**. *Atmospheric Chemistry and Physics* 18:9 (2018), 6141–6156. DOI: 10.5194/acp-18-6141-2018 (see page 24).

[146] Jianmin Chen, Chunlin Li, Zoran Ristovski, Andelija Milic, Yuantong Gu, Mohammad S. Islam, Shuxiao Wang, Jiming Hao, Hefeng Zhang, Congrong He, Hai Guo, Hongbo Fu, Branka Miljevic, Lidia Morawska, Phong Thai, Yun Fat LAM, Gavin Pereira, Aijun Ding, Xin Huang, and Umesh C. Dumka. **A Review of Biomass Burning: Emissions and Impacts on Air Quality, Health and Climate in China**. *Science of The Total Environment* 579 (2017), 1000–1034. ISSN: 0048-9697. DOI: 10.1016/j.scitotenv.2016.11.025 (see page 24).

[147] Nitaya Vajanapoom, Patcharee Kooncumchoo, and Thuan-Quoc Thach. **Acute Effects of Air Pollution on All-Cause mortality: A Natural Experiment from Haze Control Measures in Chiang Mai Province, Thailand**. *PeerJ* 8 (2020), e9207. DOI: 10.7717/peerj.9207 (see page 24).

[148] Shruti Pavagadhi, Raghu Betha, Shriram Venkatesan, Rajasekhar Balasubramanian, and Manoor Prakash Hande. **Physicochemical and Toxicological Characteristics of Urban Aerosols During a Recent Indonesian Biomass Burning Episode**. *Environmental Science and Pollution Research* 20 (2013), 2569–2578. DOI: 10.1007/s11356-012-1157-9 (see pages 24, 35).

[149] Jiraporn Chomanee, Kunchira Thongboon, Surajit Tekasakul, Masami Furuuchi, Racha Dejchanchaiwong, and Perapong Tekasakul. **Physicochemical and Toxicological Characteristics of Nanoparticles in Aerosols in Southern Thailand During Recent Haze Episodes in Lower Southeast Asia**. *Journal of Environmental Sciences* 94 (2020), 72–80. ISSN: 1001-0742. DOI: 10.1016/j.jes.2020.03.021 (see pages 24, 35).

[150] Scott Weichenthal, Ryan Kulka, Eric Lavigne, David Rijswijk, Michael Brauer, Paul Villeneuve, Dave Stieb, Lawrence Joseph, and Rick Burnett. **Biomass Burning as a Source of Ambient Fine Particulate Air Pollution and Acute Myocardial Infarction**. *Epidemiology* 28 (2017), 329–337. DOI: 10.1097/EDE.0000000000000636 (see page 24).

[151] Admir C. Targino, Patricia Krecl, Christer Johansson, Erik Swietlicki, Andreas Massling, Guilherme C. Coraiola, and Heikki Lihavainen. **Deterioration of Air Quality Across Sweden Due to Transboundary Agricultural Burning Emissions**. *Boreal Environment Research* 18 (2013), 19 (see pages 24, 35).

[152] Hiep Nguyen Duc, Ho Quoc Bang, Nguyen Hong Quan, and Ngo Xuan Quang. **Impact of Biomass Burnings in Southeast Asia on Air Quality and Pollutant Transport During the End of the 2019 Dry Season**. *Environmental Monitoring and Assessment* 193 (9 2021), 565. DOI: 10.1007/s10661-021-09259-9 (see page 24).

[153] Wenhuai Song, Yan-Lin Zhang, Yuxian Zhang, Fang Cao, Martin Rauber, Gary Salazar, Sawaeng Kawichai, Tippawan Prapamontol, and Sönke Szidat. **Is Biomass Burning Always a Dominant Contributor of Fine Aerosols in Upper Northern Thailand?** *Environment International* 168 (2022), 107466. ISSN: 0160-4120. DOI: 10.1016/j.envint.2022.107466 (see page 24).

[154] Shobhakar Dhakal and Ashish Shrestha. "Bangkok, Thailand." In: *Cities on a Finite Planet*. Routledge, 2016, 63–80 (see page 25).

[155] National Statistical Office. **Statistical Yearbook 2024**. Tech. rep. Statistical Forecasting Division, National Statistical Office, 2024. URL: https://www.nso.go.th/public/e-book/Statistical-Yearbook/SYB-2024/4/ (see page 25).

[156] Wiwat Pongruengkiat, Korrakot Y. Tippayawong, Pruk Aggarangsi, Preda Pichayapan, Tossapon Katongtung, and Nakorn Tippayawong. **Assessing Sustainability of Chiang Mai Urban Development**. *Discover Sustainability* 4:1 (2023), 54. ISSN: 2662-9984. DOI: 10.1007/s43621-023-00174-2 (see page 25).

[157] US EPA Office of Research and Development. *CMAQ*. Version 5.3.3. 2021. DOI: 10.5281/zenodo.5213949 (see pages 26, 37, 51).

[158] Lala Saha, Amit Kumar, Sanjeev Kumar, John Korstad, Sudhakar Srivastava, and Kuldeep Bauddh. **The Impact of the COVID-19 Lockdown on Global Air Quality: A Review**. *Environmental Sustainability* 5:1 (2022), 5–23. DOI: 10.1007/s42398-021-00213-6 (see pages 26, 37, 51).

[159] Abdullah Addas and Ahmad Maghrabi. **The Impact of COVID-19 Lockdowns on Air Quality—A Global Review**. *Sustainability* 13:18 (2021). ISSN: 2071-1050. DOI: 10.3390/su131810212 (see pages 26, 37, 51).

[160] Jiawei Li, Zhiwei Han, Jie Li, and Li Luo. **Impacts of Vertical Distribution of Southeast Asian Biomass Burning Emissions on Aerosol Distributions and Direct Radiative Effects Over East Asia**. *Atmospheric Environment* 318 (2024), 120211. ISSN: 1352-2310. DOI: 10.1016/j.atmosenv.2023.120211 (see page 26).

[161] Max G. Adam, Phuong T.M. Tran, Nanthi Bolan, and Rajasekhar Balasubramanian. **Biomass Burning-Derived Airborne Particulate Matter in Southeast Asia: A Critical Review**. *Journal of Hazardous Materials* 407 (2021), 124760. ISSN: 0304-3894. DOI: 10.1016/j.jhazmat.2020.124760 (see page 26).

[162] Hiep Duc Nguyen, Ho Quoc Bang, Nguyen Hong Quan, Ngo Xuan Quang, and Tran Anh Duong. **Effect of Biomass Burnings on Population Exposure and Health Impact at the End of 2019 Dry Season in Southeast Asia**. *Atmosphere* 15:11 (2024). ISSN: 2073-4433. DOI: 10.3390/atmos15111280 (see page 26).

[163] Hugh Morrison and Jason A. Milbrandt. **Parameterization of Cloud Microphysics Based on the Prediction of Bulk Ice Particle Properties. Part I: Scheme Description and Idealized Tests**. *Journal of the Atmospheric Sciences* 72:1 (2015), 287–311. DOI: 10.1175/JAS-D-14-0065.1 (see page 26).

[164] Michael J. Iacono, Jennifer S. Delamere, Eli J. Mlawer, Mark W. Shephard, Shepard A. Clough, and William D. Collins. **Radiative Forcing by Long-Lived Greenhouse Gases: Calculations with the AER Radiative Transfer Models**. *Journal of Geophysical Research: Atmospheres* 113:D13 (2008). DOI: 10.1029/2008JD009944 (see page 26).

[165] Joseph B. Olson, Tanya Smirnova, Jaymes S. Kenyon, David D. Turner, John M. Brown, Weizhong Zheng, and Benjamin W. Green. **A Description of the MYNN Surface-Layer Scheme**. Tech. rep. National Oceanic, Atmospheric Administration, Oceanic, and Atmospheric Research, Global Systems Laboratory, 2021. DOI: 10.25923/f6a8-bc75 (see page 26).

[166] Fei Chen and Jimy Dudhia. **Coupling an Advanced Land Surface–Hydrology Model with the Penn State–NCAR MM5 Modeling System. Part I: Model Implementation and Sensitivity**. *Monthly Weather Review* 129:4 (2001), 569–585. DOI: 10.1175/1520-0493(2001)129<0569:CAALSH>2.0.CO;2 (see page 26).

[167] Mikio Nakanishi and Hiroshi Niino. **Development of an Improved Turbulence Closure Model for the Atmospheric Boundary Layer**. *Journal of the Meteorological Society of Japan. Ser. II* 87:5 (2009), 895–912. DOI: 10.2151/jmsj.87.895 (see page 26).

[168] Georg A. Grell and Dezső Dévényi. **A Generalized Approach to Parameterizing Convection Combining Ensemble and Data Assimilation Techniques**. *Geophysical Research Letters* 29:14 (2002), 38-1-38–4. DOI: 10.1029/2002GL015311 (see page 26).

[169] Jeffrey J. Danielson and Dean B. Gesch. **Global Multi-Resolution Terrain Elevation Data 2010 (GMTED2010)**. Tech. rep. Earth Resources Observation and Science (EROS) Center, 2011. DOI: 10.3133/ofr20111073 (see page 26).

[170] Patrick D. Broxton, Xubin Zeng, Damien Sulla-Menashe, and Peter A. Troch. **A Global Land Cover Climatology Using MODIS Data**. *Journal of Applied Meteorology and Climatology* 53:6 (2014), 1593–1605. DOI: 10.1175/JAMC-D-13-0270.1 (see page 26).

[171] Hans Hersbach, Bill Bell, Paul Berrisford, Shoji Hirahara, András Horányi, Joaquín Muñoz-Sabater, Julien Nicolas, Carole Peubey, Raluca Radu, Dinand Schepers, Adrian Simmons, Cornel Soci, Saleh Abdalla, Xavier Abellan, Gianpaolo Balsamo, Peter Bechtold, Gionata Biavati, Jean Bidlot, Massimo Bonavita, Giovanna De Chiara, Per Dahlgren, Dick Dee, Michail Diamantakis, Rossana Dragani, Johannes Flemming, Richard Forbes, Manuel Fuentes, Alan Geer, Leo Haimberger, Sean Healy, Robin J. Hogan, Elías Hólm, Marta Janisková, Sarah Keeley, Patrick Laloyaux, Philippe Lopez, Cristina Lupu, Gabor Radnoti, Patricia de Rosnay, Iryna Rozum, Freja Vamborg, Sebastien Villaume, and Jean-Noël Thépaut. **The ERA5 Global Reanalysis**. *Quarterly Journal of the Royal Meteorological Society* 146:730 (2020), 1999–2049. DOI: 10.1002/qj.3803 (see page 27).

[172] William P.L. Carter. **Development of the SAPRC-07 Chemical Mechanism**. *Atmospheric Environment* 44:40 (2010). Atmospheric Chemical Mechanisms: Selected Papers from the 2008 Conference, 5324–5335. ISSN: 1352-2310. DOI: 10.1016/j.atmosenv.2010.01.026 (see page 27).

[173] Atmospheric Chemistry Observations and Modeling, National Center for Atmospheric Research, University Corporation for Atmospheric Research. *Whole Atmosphere Community Climate Model (WACCM) Model Output*. Boulder CO, 2020. DOI: 10.5065/G643-Z138 (see page 27).

[174] C. Wiedinmyer, S. K. Akagi, R. J. Yokelson, L. K. Emmons, J. A. Al-Saadi, J. J. Orlando, and A. J. Soja. **The Fire INventory from NCAR (FINN): a High Resolution Global Model to Estimate the Emissions from Open Burning**. *Geoscientific Model Development* 4:3 (2011), 625–641. DOI: 10.5194/gmd-4-625-2011 (see pages 27, 29).

[175] Katsushige Uranishi, Fumikazu Ikemori, Hikari Shimadera, Akira Kondo, and Seiji Sugata. **Impact of Field Biomass Burning on Local Pollution and Long-Range Transport of PM2.5 in Northeast Asia**. *Environmental Pollution* 244 (2019), 414–422. ISSN: 0269-7491. DOI: 10.1016/j.envpol.2018.09.061 (see page 27).

[176] Louis Giglio, James T. Randerson, and Guido R. van der Werf. **Analysis of Daily, Monthly, and Annual Burned Area Using the Fourth-Generation Global Fire Emissions Database (GFED4)**. *Journal of Geophysical Research: Biogeosciences* 118:1 (2013), 317–328. DOI: 10.1002/jgrg.20042 (see page 27).

[177] J. W. Kaiser, A. Heil, M. O. Andreae, A. Benedetti, N. Chubarova, L. Jones, J.-J. Morcrette, M. Razinger, M. G. Schultz, M. Suttie, and G. R. van der Werf. **Biomass Burning Emissions Estimated with a Global Fire Assimilation System Based on Observed Fire Radiative Power**. *Biogeosciences* 9:1 (2012), 527–554. DOI: 10.5194/bg-9-527-2012 (see page 27).

[178] Worapop Thongsame, Daven K. Henze, Rajesh Kumar, Mary Barth, and Gabriele Pfister. **Evaluation of WRF-Chem PM2.5 Simulations in Thailand with Different Anthropogenic and Biomass-Burning Emissions**. *Atmospheric Environment: X* 23 (2024), 100282. ISSN: 2590-1621. DOI: 10.1016/j.aeaoa.2024.100282 (see page 27).

[179] J. Kurokawa and T. Ohara. **Long-Term Historical Trends in Air Pollutant Emissions in Asia: Regional Emission Inventory in ASia (REAS) Version 3**. *Atmospheric Chemistry and Physics* 20:21 (2020), 12761–12793. DOI: 10.5194/acp-20-12761-2020 (see pages 27, 29).

[180] G. Janssens-Maenhout, M. Crippa, D. Guizzardi, F. Dentener, M. Muntean, G. Pouliot, T. Keating, Q. Zhang, J. Kurokawa, R. Wankmüller, H. Denier van der Gon, J. J. P. Kuenen, Z. Klimont, G. Frost, S. Darras, B. Koffi, and M. Li. **HTAP_v2.2: A Mosaic of Regional and Global Emission Grid Maps for 2008 and 2010 to Study Hemispheric Transport of Air Pollution**. *Atmospheric Chemistry and Physics* 15:19 (2015), 11411–11432. DOI: 10.5194/acp-15-11411-2015 (see pages 27, 29).

[181] A. Guenther, T. Karl, P. Harley, C. Wiedinmyer, P. I. Palmer, and C. Geron. **Estimates of Global Terrestrial Isoprene Emissions Using MEGAN (Model of Emissions of Gases and Aerosols from Nature)**. *Atmospheric Chemistry and Physics* 6:11 (2006), 3181–3210. DOI: 10.5194/acp-6-3181-2006 (see pages 27, 29).

[182] Simon Carn, Vitali Fioletov, Chris Mclinden, Coco Li, and Nickolay Krotkov. **A Decade of Global Volcanic SO2 Emissions Measured from Space**. *Scientific Reports* 7 (2017), 44095. DOI: 10.1038/srep44095 (see pages 27, 29).

[183] Acid Deposition Monitoring Network in East Asia (EANET). **Data Report 2019**. Tech. rep. Acid Deposition Monitoring Network in East Asia (EANET), 2020. URL: https://monitoring.eanet.asia/document/public/index (see pages 29, 39).

[184] Phuchiwan Suriyawong, Santi Chuetor, Hisam Samae, Suthida Piriyakarnsakul, Muhammad Amin, Masami Furuuchi, Mitsuhiko Hata, Muanfun Inerb, and Worradorn Phairuang. **Airborne Particulate Matter from Biomass Burning in Thailand: Recent Issues, Challenges, and Options**. *Heliyon* 9:3 (2023), e14261. ISSN: 2405-8440. DOI: 10.1016/j.heliyon.2023.e14261 (see page 35).

[185] Praphatsorn Punsompong, Shantanu Kumar Pani, Sheng-Hsiang Wang, and Thao Thi Bich Pham. **Assessment of Biomass-Burning Types and Transport Over Thailand and The Associated Health Risks**. *Atmospheric Environment* 247 (2021), 118176. ISSN: 1352-2310. DOI: 10.1016/j.atmosenv.2020.118176 (see page 35).

[186] Maria Val Martin, Ralph A. Kahn, Jennifer A. Logan, Ronan Paugam, Martin Wooster, and Charles Ichoku. **Space-Based Observational Constraints for 1-D Fire Smoke Plume-Rise Models**. *Journal of Geophysical Research: Atmospheres* 117:D22 (2012). DOI: 10.1029/2012JD018370 (see page 38).

[187] S. R. Freitas, K. M. Longo, R. Chatfield, D. Latham, M. A. F. Silva Dias, M. O. Andreae, E. Prins, J. C. Santos, R. Gielow, and J. A. Carvalho Jr. **Including the Sub-Grid Scale Plume Rise of Vegetation Fires in Low Resolution Atmospheric Transport Models**. *Atmospheric Chemistry and Physics* 7:13 (2007), 3385–3398. DOI: 10.5194/acp-7-3385-2007 (see page 38).

[188] Derek V. Mallia, Adam K. Kochanski, Shawn P. Urbanski, and John C. Lin. **Optimizing Smoke and Plume Rise Modeling Approaches at Local Scales**. *Atmosphere* 9:5 (2018). ISSN: 2073-4433. DOI: 10.3390/atmos9050166 (see page 38).

[189] R. Paugam, M. Wooster, S. Freitas, and M. Val Martin. **A Review of Approaches to Estimate Wildfire Plume Injection Height Within Large-Scale Atmospheric Chemical Transport Models**. *Atmospheric Chemistry and Physics* 16:2 (2016), 907–925. DOI: 10.5194/acp-16-907-2016 (see page 38).

[190] Roland B. Stull. **An Introduction to Boundary Layer Meteorology**. 1st ed. Vol. 13. Atmospheric and Oceanographic Sciences Library. Dordrecht, Netherlands: Springer Dordrecht, 1988. ISBN: 978-90-277-2768-8. DOI: 10.1007/978-94-009-3027-8 (see page 38).

[191] Fernando Garcia-Menendez, Yongtao Hu, and Mehmet T. Odman. **Simulating Smoke Transport from Wildland Fires with a Regional-Scale Air Quality Model: Sensitivity to Spatiotemporal Allocation of Fire Emissions**. *Science of The Total Environment* 493 (2014), 544–553. ISSN: 0048-9697. DOI: 10.1016/j.scitotenv.2014.05.108 (see page 38).

[192] Eun-Su Yang, Sundar A. Christopher, Shobha Kondragunta, and Xiaoyang Zhang. **Use of Hourly Geostationary Operational Environmental Satellite (GOES) Fire Emissions in a Community Multiscale Air Quality (CMAQ) model for Improving Surface Particulate Matter Predictions**. *Journal of Geophysical Research: Atmospheres* 116:D4 (2011). DOI: 10.1029/2010JD014482 (see page 38).

[193] Gary A. Briggs. **Plume Rise**. Tech. rep. Air Resources Atmospheric Turbulence and Diffusion Lab., Oak Ridge, Tenn., 1969. DOI: 10.2172/4743102 (see page 38).

[194] M. Sofiev, T. Ermakova, and R. Vankevich. **Evaluation of the Smoke-Injection Height from Wild-Land Fires Using Remote-Sensing Data**. *Atmospheric Chemistry and Physics* 12:4 (2012), 1995–2006. DOI: 10.5194/acp-12-1995-2012 (see page 38).

[195] Y. Li, D. Tong, S. Ma, S. R. Freitas, R. Ahmadov, M. Sofiev, X. Zhang, S. Kondragunta, R. Kahn, Y. Tang, B. Baker, P. Campbell, R. Saylor, G. Grell, and F. Li. **Impacts of Estimated Plume Rise on PM2.5 Exceedance Prediction During Extreme Wildfire Events: A Comparison of Three Schemes (Briggs, Freitas, and Sofiev)**. *Atmospheric Chemistry and Physics* 23:5 (2023), 3083–3101. DOI: 10.5194/acp-23-3083-2023 (see page 38).

[196] Isao Kanda, Roberto Basaldud, Miguel Magaña, Armando Retama, Ryushi Kubo, and Shinji Wakamatsu. **Comparison of Ozone Production Regimes between Two Mexican Cities: Guadalajara and Mexico City**. *Atmosphere* 7:7 (2016). ISSN: 2073-4433. DOI: 10.3390/atmos7070091 (see page 38).

[197] A. de Meij, C. Cuvelier, P. Thunis, E. Pisoni, and B. Bessagnet. **Sensitivity of Air Quality Model Responses to Emission Changes: Comparison of Results Based on Four EU Inventories Through FAIRMODE Benchmarking Methodology**. *Geoscientific Model Development* 17:2 (2024), 587–606. DOI: 10.5194/gmd-17-587-2024 (see page 38).

[198] Bertrand Bessagnet, Elissavet Bossioli, Arineh Cholakian, Marta García Vivanco, Kees Cuvelier, Mark R. Theobald, Victoria Gil, Laurent Menut, Alexander de Meij, Enrico Pisoni, and Philippe Thunis. **Impact of Air Quality Model Settings for the Evaluation of Emission Reduction Strategies to Curb Air Pollution**. *Environmental Research* 255 (2024), 119112. ISSN: 0013-9351. DOI: 10.1016/j.envres.2024.119112 (see page 38).

[199] Lishu Shi, Ansheng Zhu, Ling Huang, Elly Yaluk, Ying Gu, Yangjun Wang, Shunyao Wang, Andy Chan, and Li Li. **Impact of the Planetary Boundary Layer on Air Quality Simulations Over the Yangtze River Delta Region, China**. *Atmospheric Environment* 263 (2021), 118685. ISSN: 1352-2310. DOI: 10.1016/j.atmosenv.2021.118685 (see page 38).

[200] Anzel de Lange, Mogesh Naidoo, Rebecca M. Garland, and Liesl L. Dyson. **The sensitivity of simulated surface-level pollution concentrations to WRF-ARW-model PBL parameterisation schemes over the Highveld of South Africa**. *Atmospheric Research* 254 (2021), 105517. ISSN: 0169-8095. DOI: 10.1016/j.atmosres.2021.105517 (see page 38).

[201] Jikang Wang, Bihui Zhang, Hengde Zhang, and Mengyao Lv. **The Impacts of Three PBL Schemes on the Simulation of Boundary Layer Meteorological Factors and Air Pollutants in Northern China**. *IOP Conference Series: Earth and Environmental Science* 227 (2019), 052011. DOI: 10.1088/1755-1315/227/5/052011 (see page 38).

[202] L. Huang, Y. Zhu, H. Zhai, S. Xue, T. Zhu, Y. Shao, Z. Liu, C. Emery, G. Yarwood, Y. Wang, J. Fu, K. Zhang, and L. Li. **Recommendations on Benchmarks for Numerical Air Quality Model Applications in China – Part 1: $PM_{2.5}$ and Chemical Species**. *Atmospheric Chemistry and Physics* 21:4 (2021), 2725–2743. DOI: 10.5194/acp-21-2725-2021 (see page 41).

[203] Nares Chuersuwan, Subuntith Nimrat, Sukanda Lekphet, and Tida Kerdkumrai. **Levels and Major Sources of PM2.5 and PM10 in Bangkok Metropolitan Region**. *Environment international* 34 (2008), 671–7. DOI: 10.1016/j.envint.2007.12.018 (see pages 43, 61).

[204] Ha Young Yoo, Ki Ae Kim, Yong Pyo Kim, Chang Hoon Jung, Hye Jung Shin, Kwang Ju Moon, Seung Myung Park, and Ji Yi Lee. **Validation of SOC Estimation Using OC and EC Concentration in PM2.5 Measured at Seoul**. *Aerosol and Air Quality Research* 22:4 (2022), 210388. ISSN: 2071-1409. DOI: 10.4209/aaqr.210388 (see page 53).

[205] S. Wang, K. Liao, Z. Zhang, Y. Y. Cheng, Q. Wang, H. Chen, and J. Z. Yu. **Bayesian Inference-Based Estimation of Hourly Primary and Secondary Organic Carbon in Suburban Hong Kong: Multi-Temporal-Scale Variations and Evolution Characteristics During $PM_{2.5}$ Episodes**. *Atmospheric Chemistry and Physics* 24:10 (2024), 5803–5821. DOI: 10.5194/acp-24-5803-2024 (see page 53).

[206] Weiyi Wang, Daniela Fecht, Sean Beevers, and John Gulliver. **Predicting Daily Concentrations of Nitrogen Dioxide, Particulate Matter and Ozone at Fine Spatial Scale in Great Britain**. *Atmospheric Pollution Research* 13:8 (2022), 101506. ISSN: 1309-1042. DOI: 10.1016/j.apr.2022.101506 (see page 54).

[207] Sirapong Sooktawee, Suwimon Kanchanasuta, and Natthaya Bunplod. **Assessment of 24-H Moving Average PM2.5 Concentrations in Bangkok, Thailand Against WHO Guidelines**. *Sustainable Environment Research* 33:3 (2023). DOI: 10.1186/s42834-023-00165-y (see page 54).

[208] Christopher Emery, Zhen Liu, Armistead G. Russell, M. Talat Odman, Greg Yarwood, and Naresh Kumar. **Recommendations on Statistics and Benchmarks to Assess Photochemical Model Performance**. *Journal of the Air & Waste Management Association* 67:5 (2017). PMID: 27960634, 582–598. DOI: 10.1080/10962247.2016.1265027 (see pages 54, 55).

[209] S. Saarikoski, H. Timonen, K. Saarnio, M. Aurela, L. Järvi, P. Keronen, V.-M. Kerminen, and R. Hillamo. **Sources of Organic Carbon in Fine Particulate Matter in Northern European Urban Air**. *Atmospheric Chemistry and Physics* 8:20 (2008), 6281–6295. DOI: 10.5194/acp-8-6281-2008 (see page 58).

[210] T. C. Bond, S. J. Doherty, D. W. Fahey, P. M. Forster, T. Berntsen, B. J. DeAngelo, M. G. Flanner, S. Ghan, B. Kärcher, D. Koch, S. Kinne, Y. Kondo, P. K. Quinn, M. C. Sarofim, M. G. Schultz, M. Schulz, C. Venkataraman, H. Zhang, H. Zhang, N. Bellouin, S. K. Guttikunda, P. K. Hopke, M. Z. Jacobson, J. W. Kaiser, Z. Klimont, U. Lohmann, J. P. Schwarz, D. Shindell, T. Storelvmo, S. G. Warren, and C. S. Zender. **Bounding the Role of Black Carbon in the Climate System: A Scientific Assessment**. *Journal of Geophysical Research: Atmospheres* 118:11 (2013), 5380–5552. DOI: 10.1002/jgrd.50171 (see page 58).

[211] M. O. Andreae. **Emission of Trace Gases and Aerosols From Biomass Burning – An Updated Assessment**. *Atmospheric Chemistry and Physics* 19:13 (2019), 8523–8546. DOI: 10.5194/acp-19-8523-2019 (see page 58).

[212] Xi Chen, Ting Yang, Zifa Wang, Yufang Hao, Litao He, and Huanhuan Sun. **Investigating the Impacts of Coal-Fired Power Plants on Ambient PM2.5 by a Combination of a Chemical Transport Model and Receptor Model**. *Science of The Total Environment* 727 (2020), 138407. ISSN: 0048-9697. DOI: 10.1016/j.scitotenv.2020.138407 (see pages 58, 61).

[213] Suzana Sopčić, Ranka Godec, Ivana Jakovljević, and Ivan Bešlić. **The Influence of Biomass Burning on the Organic Content of Urban Aerosols**. *Biomass* 5:1 (2025). ISSN: 2673-8783. DOI: 10.3390/biomass5010001 (see page 58).

[214] Bin Cheng and Lingjuan Wang-Li. **Responses of Secondary Inorganic PM2.5 to Precursor Gases in an Ammonia Abundant Area in North Carolina**. *Aerosol and Air Quality Research* 19:5 (2019), 1126–1138. ISSN: 2071-1409. DOI: 10.4209/aaqr.2018.10.0384 (see pages 58, 66).

[215] Chang-You Tsai, Tu-Fu Chen, and Ken-Hui Chang. **Role of an Ultra-Large Coal-Fired Power Plant in PM2.5 Pollution in Taiwan**. *Atmosphere* 15:1 (2024). ISSN: 2073-4433. DOI: 10.3390/atmos15010056 (see page 61).

[216] Hyo-Jin Kim, Ju-Hee Kim, and Seung-Hoon Yoo. **Do People Place More Value on Natural Gas Than Coal for Power Generation to Abate Particulate Matter Emissions? Evidence From South Korea**. *Sustainability* 10:6 (2018). ISSN: 2071-1050. DOI: 10.3390/su10061740 (see page 61).

[217] Electricity Generating Authority of Thailand (EGAT). **Annual Report 2019**. Tech. rep. Accessed: 2025-09-15. Electricity Generating Authority of Thailand (EGAT), 2019. URL: https://www.egat.co.th/home/en/wp-content/uploads/2021/12/annual-report-2019-en.pdf (see page 61).

[218] Energy Policy and Planning Office. *Electricity Statistic*. Accessed: 2025-09-15. 2025. URL: https://www.eppo.go.th/index.php/en/en-energystatistics/electricity-statistic (see page 61).

[219] Office of Agricultural Economics. **Agricultural Statistics of Thailand 2023**. Tech. rep. Office of Agricultural Economics, Ministry of Agriculture and Cooperatives, 2023. URL: https://www.agrithai.org/wp-content/uploads/2024/03/statistic2566.pdf (see page 62).

[220] Y.-Q. Zhang, D.-H. Chen, X. Ding, J. Li, T. Zhang, J.-Q. Wang, Q. Cheng, H. Jiang, W. Song, Y.-B. Ou, P.-L. Ye, G. Zhang, and X.-M. Wang. **Impact of Anthropogenic Emissions on Biogenic Secondary Organic Aerosol: Observation in the Pearl River Delta, Southern China**. *Atmospheric Chemistry and Physics* 19:22 (2019), 14403–14415. DOI: 10.5194/acp-19-14403-2019 (see page 65).

[221] Bo Zhu, Xiao-Feng Huang, Shi-Yong Xia, Li-Liang Lin, Yong Cheng, and Ling-Yan He. **Biomass-Burning Emissions Could Significantly Enhance the Atmospheric Oxidizing Capacity in Continental Air Pollution**. *Environmental Pollution* 285 (2021), 117523. ISSN: 0269-7491. DOI: 10.1016/j.envpol.2021.117523 (see page 65).

[222] Wenhuai Song, Yihang Hong, Yuxian Zhang, Fang Cao, Martin Rauber, Teetawat Santijitpakdee, Sawaeng Kawichai, Tippawan Prapamontol, Sönke Szidat, and Yan-Lin Zhang. **Biomass Burning Greatly Enhances the Concentration of Fine Carbonaceous Aerosols at an Urban Area in Upper Northern Thailand: Evidence From the Radiocarbon-Based Source Apportionment on Size-Resolved Aerosols**. *Journal of Geophysical Research: Atmospheres* 129:10 (2024), e2023JD040692. DOI: 10.1029/2023JD040692 (see page 65).

[223] Drew R. Gentner, Shantanu H. Jathar, Timothy D. Gordon, Roya Bahreini, Douglas A. Day, Imad El Haddad, Patrick L. Hayes, Simone M. Pieber, Stephen M. Platt, Joost de Gouw, Allen H. Goldstein, Robert A. Harley, Jose L. Jimenez, André S. H. Prévôt, and Allen L. Robinson. **Review of Urban Secondary Organic Aerosol Formation From Gasoline and Diesel Motor Vehicle Emissions**. *Environmental Science & Technology* 51:3 (2017), 1074–1093. DOI: 10.1021/acs.est.6b04509 (see page 65).

[224] Rui Tan, Song Guo, Sihua Lu, Hui List Wang, Wenfei Zhu, Ying Yu, Rongzhi Tang, Ruizhe Shen, Kai Song, Daqi Lv, Wenbin Zhang, Zhou Zhang, Shijin Shuai, Shuangde Li, Yunfa Chen, and Yan Ding. **Characteristics and Secondary Organic Aerosol Formation of Volatile Organic Compounds From Vehicle and Cooking Emissions**. *Atmosphere* 14:5 (2023). ISSN: 2073-4433. DOI: 10.3390/atmos14050806 (see page 65).

[225] Hao Huang, Hui Hu, Jinjie Zhang, and Xiaoyong Liu. **Characteristics of Volatile Organic Compounds From Vehicle Emissions Through On–Road Test in Wuhan, China**. *Environmental Research* 188 (2020), 109802. ISSN: 0013-9351. DOI: 10.1016/j.envres.2020.109802 (see page 65).

[226] Haixu Zhang, Chunrong Chen, Weijia Yan, Nana Wu, Yu Bo, Qiang Zhang, and Kebin He. **Characteristics and Sources of Non-Methane VOCs and Their Roles in SOA Formation During Autumn in a Central Chinese city**. *Science of The Total Environment* 782 (2021), 146802. ISSN: 0048-9697. DOI: 10.1016/j.scitotenv.2021.146802 (see page 65).

[227] Jianghao Li, Shunxi Deng, Guanghua Li, Zhenzhen Lu, Hui Song, Jian Gao, Zhigang Sun, and Ke Xu. **VOCs Characteristics and Their Ozone and SOA Formation Potentials in Autumn and Winter at Weinan, China**. *Environmental Research* 203 (2022), 111821. ISSN: 0013-9351. DOI: 10.1016/j.envres.2021.111821 (see page 65).

[228] Yajun Wu, Jianfei Peng, Xiaoguo Wang, Peiji Liu, Yan Liu, Fuyang Zhang, Jinsheng Zhang, Bin Sun, Jingqiao Zhang, Kai Song, Pengfei Song, Lin Wu, Ting Wang, Song Guo, and Hongjun Mao. **Emissions and Potential Tracer Screening of Semivolatile/Intermediate-Volatility Organic Compounds From Urban Vehicle Fleets**. *npj Climate and Atmospheric Science* 8:1 (2025), 186. ISSN: 2397-3722. DOI: 10.1038/s41612-025-01078-w (see page 65).

[229] Peemapat Jookjantra, Sarawut Thepanondh, Jutarat Keawboonchu, Vanitchaya Kultan, and Wanna Laowagul. **Formation Potential and Source Contribution of Secondary Organic Aerosol From Volatile Organic Compounds**. *Journal of Environmental Quality* 51:5 (2022), 1016–1034. DOI: 10.1002/jeq2.20381 (see page 65).

[230] Lingjuan Wang-Li. **Insights to the Formation of Secondary Inorganic PM2.5: Current Knowledge and Future Needs**. *International Journal of Agricultural and Biological Engineering* 8 (2015), 1–13. DOI: 10.3965/j.ijabe.20150802.1810 (see page 66).

[231] Hsiang-He Lee, Oussama Iraqui, and Chien Wang. **The Impact of Future Fuel Consumption on Regional Air Quality in Southeast Asia**. *Scientific Reports* 9:1 (2019), 2648. ISSN: 2045-2322. DOI: 10.1038/s41598-019-39131-3 (see page 67).

[232] Energy Policy and Planning Office. **Thailand Power Development Plan 2015-2036**. Tech. rep. Energy Policy and Planning Office, Ministry of Energy, 2015. URL: https://www.eppo.go.th/images/POLICY/ENG/PDP2015_Eng.pdf (see page 68).